JOHANNES GUTENBERG
UNIVERSITÄT MAINZ

Hierarchical superhydrophobic composite membrane for enhanced distillation with excellent fouling resistance

Dissertation
zur Erlangung des Grades
"Doktor der Naturwissenschaften"
im Promotionsfach Chemie

der Johannes Gutenberg- Universität
in Mainz

vorgelegt von
Prexa Shah
geboren in Ahmedabad (India)
Mainz, 2023

Declaration of Authenticity

I, Prexa Shah declare that this thesis and the work presented in it are my own and have been generated by me as the result of my own original research under the supervision of Prof. Dr. Hans-Jürgen Butt and Dr. Michael Kappl.

Quotations from other authors and any ideas borrowed and/or passages paraphrased from the works of other authors are clearly marked within the text and acknowledged in the bibliographical references.

Mainz, June-2023

Prexa Shah

Zusammenfassung

Angesichts der ständig wachsenden Bevölkerung, des Klimawandels, der landwirtschaftlichen und industriellen Nutzung ist das Problem des Mangels an sauberem Wasser ein ständiges Thema. Die Meerwasserentsalzung ist zu einer wichtigen Quelle für sauberes Wasser in trockenen Küstenregionen geworden. Daher müssen energieeffiziente Entsalzungslösungen entwickelt werden, um die begrenzte Energieversorgung nicht übermäßig zu belasten. In den letzten Jahrzehnten wurden weltweit Entsalzungskapazitäten aufgebaut, um die Wasserknappheit an Orten zu lindern, an denen Angebot und Nachfrage aus dem Gleichgewicht geraten sind. Die bestehende Entsalzungsindustrie basiert fast vollständig auf nicht nachhaltigen, industriellen Verfahren, die nicht auf die Wasserknappheit in ländlichen Gebieten ausgerichtet sind. Eines der dringendsten Anliegen bei der Lösung langfristiger Wasserknappheit ist die Entwicklung kleiner, autarker und umweltverträglicher Entsalzungstechnologien.

Die Membrandestillation (MD) hat als hybride thermische/membranbasierte Entsalzungstechnik, die Abwärme oder Sonnenwärme für Entsalzungsanwendungen in kleinem Maßstab sowie für die Behandlung von Solen mit hohem Salzgehalt nutzen kann, großes Interesse geweckt. Das jüngste Interesse an dieser Technologie ist auf ihre einzigartigen Eigenschaften zurückzuführen, wie z. B. die niedrige Betriebstemperatur, die die Nutzung von Ab- oder Sonnenwärme als Energiequelle ermöglicht, die ultimative Zurückweisung von nicht flüchtigen Bestandteilen und der niedrige Betriebsdruck, der den Einsatz von kostengünstigen, korrosionsfreien Kunststoffmodulen ermöglicht. Die größten Hindernisse, die die Leistung von MD-Systemen beeinträchtigen, sind die potenziellen Probleme der Membranverschmutzung und -benetzung. Das wesentliche Ziel ist es daher, die Destillationsrate zu erhöhen und gleichzeitig die Membranbenetzung und -verschmutzung zu minimieren.

Das erste mögliche Problem ist die Membranverschmutzung, die auftritt, wenn Substanzen oder Mikroorganismen an die hydrophobe Membranoberfläche binden und die Membranporen verstopfen, was zu einer drastischen Verringerung des Wasserdampftransports führt. Die Membranbenetzung ist die zweithäufigste Ursache für das Versagen des MD-Betriebs. Wenn eine hydrophobe Membran in einem MD-Prozess zur

Entsalzung von Salzwasser verwendet wird, das amphiphile Moleküle wie Tenside und andere amphiphile organische Stoffe enthält, lagern sich diese an der hydrophoben Membranporenoberfläche an, machen die Membranporen schließlich hydrophil. Die Benetzung der Membranporen führt dazu, dass das Sole direkt in den Destillatstrom eindringt und die Salzabscheiderate drastisch reduziert wird.

Hydrophobe Membranen sind bei der Membrandestillation zur Gewinnung von sauberem Wasser von entscheidender Bedeutung, doch sind sie anfällig für Benetzung und Verschmutzung. Die vorliegende Studie befasst sich mit den Herausforderungen, die mit dem Membranen in der MD verbunden sind, sowie mit verschiedenen Ansätzen zur Vermeidung dieses Problems. Um dieses grundlegende Hindernis zu beseitigen, haben wir ein fluorfreies Nanofilament-Netzwerk auf eine handelsübliche mikroporöse Membran aufgebracht, um eine hochgradig flüssigkeitsabweisende Membran mit hierarchischen porösen Strukturen zu schaffen. Die mit Nanofilamenten beschichtete Membran verbessert den Destillationsfluss aufgrund der großen inneren mikroporösen Strukturen, während die äußeren nano-porösen Strukturen die Benetzungsbeständigkeit und somit die Salzabscheidung und Betriebsstabilität erhöhen. In dieser Studie werden die Destillationsleistung und das Benetzungsverhalten der neu entwickelten, mit Nanofilamenten beschichteten Membranen in Gegenwart von Verunreinigungen untersucht, die die Oberflächenspannung herabsetzen, wie z. B. Tenside, die das Risiko der Membranbenetzung erhöhen. Membranverschmutzung durch natürlich vorkommende organische Vebindungen wie z.B. Proteine ist eine der schwerwiegendsten Arten des Membranverschmutzung, da es die Membranleistung durch die Anreicherung unerwünschter Substanzen auf der Membranoberfläche oder in den Poren verringert. Die Resistenz der Membranen gegen Proteinadsorption wird in dieser Studie ebenfalls untersucht. Im Vergleich zu konventionellen hydrophoben Membranen weisen unsere innovativen multiskaligen porösen Membranen eine hohe Verschmutzungs- und Benetzungs-Resistenz auf und erreichen gleichzeitig einen höheren Destillationsfluss. Diese Studie demonstriert somit einen praktikablen Ansatz zur Optimierung von MD-Prozessen für die Abwasser- und Salzwasserbehandlung.

Schlüsselwörter:

Entsalzung, Membrandestillation (MD), superhydrophob, Nanofilamentbeschichtung, Benetzung, Membranverschmutzung.

Abstract

With an ever-growing population, climate change, agricultural, and industrial use, the issue of insufficient clean water is an ongoing one. Seawater desalination has become an important source of clean water in dry locations along the shore. As a result, energy-efficient desalination solutions must be devised to prevent putting undue demand on the limited energy supply. Global desalination capacity has developed in recent decades to assist alleviate water scarcity in locations where supply and demand are out of balance. The existing desalination industry is almost completely built on non-sustainable, industrial-scale procedures that do not address rural water scarcity. One of the most pressing concerns in solving long-term water shortages is the development of small-scale, self-sufficient, and environmentally acceptable desalination technologies.

Membrane distillation (MD) has acquired significant interest as a hybrid thermal/membrane-based desalination technique that may utilize waste or solar heat for small-scale desalination applications as well as for treating high-salinity brines. Recent interest in the technology has been observed due to its unique features such as mild operating temperature, which allows the use of waste or solar heat as a driving force, ultimate rejection for non-volatile components, and low operational pressure, which allows the use of inexpensive, corrosion-free plastic modules. The key obstacles impacting the performance of MD systems are the potential concerns of membrane fouling and wetting. The goal now is to increase the distillation rate while minimizing membrane wetting and fouling.

The first possible issue is membrane fouling, which occurs when the foulants bind to the hydrophobic membrane surface and clog the membrane pores, resulting in drastically decreased water vapor transport. Membrane wetting is the second most common cause of MD operation failure. When a hydrophobic membrane is used in an MD process to desalinate brine water containing amphiphilic molecules such as surfactants and other amphiphilic organics, which attach to the hydrophobic membrane pore surface, exposing the hydrophilic

head and eventually rendering the membrane pores hydrophilic. The result of membrane pore wetting is direct feed water penetration into the distillate stream and a dramatically reduced salt rejection rate.

Super-hydrophobic robust membranes are critical in membrane distillation to create clean water, yet they are susceptible to wetting and fouling. This study provides the challenges involved in membrane fouling in MD and several mitigating approaches. To address this basic obstacle, we coated a fluorine-free nanofilament network over a commercial microporous membrane to create a highly liquid-repellent membrane with hierarchical porous structures. The nanofilament-coated membrane would improve distillation flux with large inner micro-porous structures, and the outside nano-porous structures can boost wetting resistance with high salt rejection and operational stability. In this study, the distillation performance and fouling resistance of fabricated nanofilament-coated membranes are investigated using impurities that reduce surface tension like surfactants, which will increase the risk of membrane wetting. Natural organic fouling is one of the most difficult types of membrane fouling because it reduces membrane performance by accumulating undesired elements on the membrane surface or inside the pores. Protein adsorption resistance to natural organic fouling is also investigated in this study. In comparison to conventional hydrophobic membranes, our innovative multiscale porous membranes exhibit great fouling resistance while attaining higher distillation flux. This study demonstrates a viable method for optimizing MD processes for wastewater and saltwater treatment.

Keywords:

Desalination, membrane distillation (MD), superhydrophobic, nanofilaments coating, wetting, fouling

Acknowledgments

I'd like to thank Prof. Dr. Hans-Jürgen Butt and, in particular, Dr. Michael Kappl for his patience, encouragement, passion, and vast knowledge. Their assistance and advice made my journey much simpler during my study, providing me with the information basis for a great thesis, encouraging me and pointing me in the proper direction, and providing me with the chance to work on this subject.

I'd also like to express my gratitude for receiving financing from the European Union's Horizon 2020 research and innovation program under grant number 801229 (HARMoNIC), as well as funding from project EU SuperClean, to support my work at the completion of my Ph.D.

Furthermore, this journey would have been tough without the assistance of MPIP technicians, as well as the kindness and warmth of all AK Butt members, which is especially crucial for internationals that have far families. Finally, I'd want to thank my family for their unconditional support and the moral beliefs they taught me.

Contents

1. Introduction

The thesis begins with a motivation for the topic, followed by an introduction to the fundamental concepts of Membrane distillation (MD), as well as a literature review on the background of MD, different types of MD configurations, various membranes used in MD, how to characterize the membranes, factors affecting MD process, reasons for scaling and fouling, methods to reduce it, and finally advances in MD technology.

1.1 Motivation

Although water is one of the most plentiful resources on the planet, covering three-quarters of the earth's surface, around 97% of this amount is salty, with only 3% appropriate for people, plants, and animals. Nearly 2.5% of this proportion is trapped in polar ice caps, glaciers, and the atmosphere, leaving just approximately 0.5% available for human use in the form of river water and groundwater. However, due to a variety of factors such as population increase, rising living standards, and climate change, these water supplies are depleting faster than they can be replaced naturally. Most of the world's population still relies on groundwater, which has finite sources, while those living around coastlines rely on seawater as a source of water. Desalination technology is widely used as an alternate approach for harvesting vast amounts of freshwater [1-3].

Desalination is the process of discarding salts, minerals, and other contaminants from seawater. By generating freshwater from salty or brackish natural resources, desalination enables a great usage of existing water resources. In this regard, there are now many more desalination plants scheduled for development or already operational around the world. Over time numerous desalination methods have demonstrated their viability and are being used as acceptable sources. Thermal and membrane desalination are the two basic types of desalination techniques. Thermal-based technologies work by giving thermal energy to salt water to evaporate into water vapor and then condense this vapor to produce drinkable water. Thermal methods are commonly employed in areas with high saline levels and cheap energy prices. Multi-stage flash (MSF), multi-effect distillation (MED), and vapor compression distillation are some of the most often utilized thermal-based technologies [3, 4].

Membrane-based technologies are also gaining popularity because of their lower specific energy consumption, reduced environmental footprint, and more flexible capacity [5]. Microfiltration, ultrafiltration, nanofiltration (NF), and reverse osmosis (RO) are examples of membrane technology. RO is presently the most widely utilized desalination method in the world, accounting for 61% of the global market, followed by MSF (26%), and MED (8%). The majority of these are pressure-driven and rely on pressure difference as a driving factor. Using hydraulic pressure difference as the driving force for mass transfer has its own set of drawbacks. The osmotic-pressure constraint is one of the most significant weaknesses of such pressure-driven membrane processes, particularly in the case of brine desalination and hypersaline wastewaters through RO or NF procedures [4, 6-8].

The existing desalination methods take in massive volumes of high-grade energy, such as electricity, and necessitate big, centralized sites with well-equipped infrastructure. However, for small-scale freshwater production, such as 100 m^3/day RO, MED, and MSF, the energy efficiency and economics are significantly reduced. As a result, traditional desalination procedures are often considered impracticable in sparsely inhabited or underdeveloped locations. Small-scale and cost-effective desalination technologies that need low-grade energy sources, on the other hand, are more acceptable for solving the problem of water scarcity for economically disadvantaged communities [9, 10].

Desalination costs have fallen in recent years because of technological advancements and learning in a world of rising fossil fuel prices. The expense of using renewable energy sources is substantially greater. It has also been shown that the technique of desalination used has a considerable impact on the cost of water desalination [7, 11]. As a result, looking for a new water/wastewater option is appealing.

The "membrane distillation" method is a novel hybrid non-isothermal membrane process that combines distillation with membrane separation. Membrane distillation (MD) is a flexible membrane separation method that is best suited for situations where water is the primary component in the feed to be separated. MD is a term that refers to the diffusive transport of vapor molecules across a microporous hydrophobic membrane. The majority of MD process research has focused on desalination and water/wastewater treatment, among other uses [12].

1.2 Membrane distillation

MD technique was initially patented in 1967 by Findley [13]. Unfortunately, the MD process did not gain popularity until the early 1980s, when better-performing membranes such as Gore-Tex Membrane (expanded polytetrafluoroethylene, PTFE, porous membrane produced by Gore & Associates Co.) and modules were available. Then after several review articles have discussed the growth and advancements in MD [14-18].

MD is a method that combines thermal distillation and the membrane process. MD has several distinguishing characteristics that set it apart from other membrane and thermal technologies. MD differs from hydraulic pressure processes in that the driving force is the difference in vapor pressure of water across the membrane rather than hydraulic pressure. The salt content will only have a little effect on partial water vapor pressure in this sort of operation. As a result, this approach is very beneficial for treating high-saline water [19, 20].

The feed solution can be concentrated in MD to obtain a water recovery rate of 80 to 90% while generating high-grade distillate. In far inland places, this reduces the need for specialized brine management systems. Meanwhile, because the thermal process in MD requires just a moderate working temperature, alternate energy sources like waste heat or solar energy may be used [9]. Furthermore, the MD system may be built as a small-scale and compact unit ideal for small settlements. With these benefits, MD can function as a stand-alone saline water treatment process in distant places where RO and thermal distillation

technology uses are limited [14, 21]. Furthermore, the membrane pore size required for MD is rather larger than those used for RO. Hence, the MD process suffers less from fouling.

Commercial microporous hydrophobic membranes made of polypropylene (PP), polyvinylidene fluoride (PVDF), and polytetrafluoroethylene (PTFE, Teflon), available in capillary or flat-sheet forms, have been used in MD experiments, even though these membranes were originally designed for microfiltration. Because adequate membranes were unavailable in the 1970s, there was only a little development in MD. Later in the 1980s, more appropriate hydrophobic PTFE membranes were introduced, resulting in a rise in academic study and development in MD. In the 1990s, there was a better knowledge of membrane modules and transfer processes, and also alternative designs were tried [22]. In addition, the MD process was coupled with a solar energy source for the first time in a domestic-size desalination machine [23].

1.2.1 Basic Concepts of MD

In MD, the hot salty feed and cold distillate streams are separated by a porous hydrophobic membrane. Because of the temperature difference, water evaporates at the membrane-saline interface and passes through the membrane pores, whereas freshwater condenses on the permeate side. The saline feed water is heated to temperatures (T_f) in the range of 50 to 80 °C, while the permeate side is normally at a temperature (T_c) ranging from 10 to 20 °C Because of the temperature difference across the membrane, water evaporates at the membrane-saline interface and then travels through the membrane pores, freshwater condenses on the permeate side (Figure 1). MD has therefore a strong rejection of any nonvolatile compounds and also a lower operating pressure than RO [9, 16].

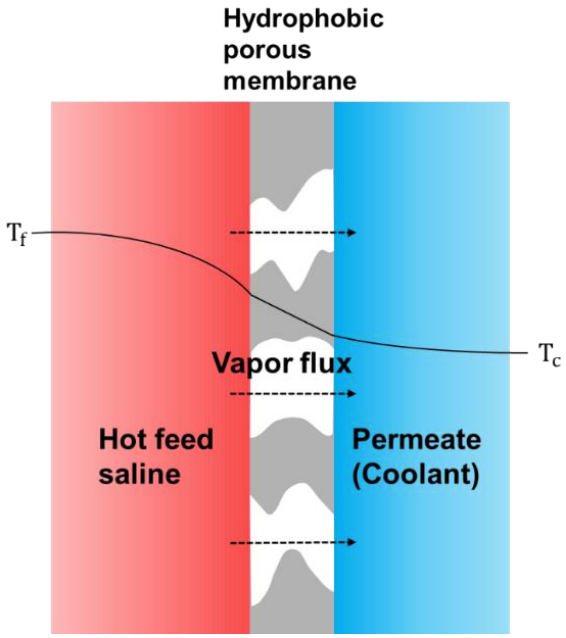

Figure 1: Schematic drawing showing conventional direct contact membrane distillation (DCMD) setup.

During MD, when a vapor pressure gradient is formed across the membrane, the volatile components in the feed solution evaporate, and the vapor molecules are driven through the membrane pores from the feed to the permeate side by the gradient. Depending on the nature of the feed, the permeating vapor may be composed of single or numerous components. The selective property of the MD process is based on the membrane's impermeability to the liquid input, while vapors pass through the porous membrane structure. Therefore, MD membranes should combine several properties: sufficient wetting resistance, to avoid penetration of the liquid into the membrane, high porosity, and large pore size to achieve high vapor flux, and low heat conductivity to minimize thermal loss across the membrane.

1.2.2 MD configurations

Membrane distillation modules are built in various ways depending on how the permeate vapor is collected and condensed. The section below gives an overview of different types of MD module combinations. The hot feed is always maintained in direct contact with one side of the membrane in all types of configurations and with various techniques used on the opposite of the membrane side.

Direct contact membrane distillation

The most prevalent membrane distillation design is direct contact membrane distillation (DCMD). Heat loss via conduction is a key concern in DCMD since the hot feed solution and the cold side come into direct contact with the membrane in this arrangement (Figure 1). As a result, the energy efficiency of this setup is poor. Because this module has the lowest mass transfer resistance, the overall vapor diffusion is faster and so the distillation flux is higher. The diagram displays the membrane's configuration in further detail. The driving force in DCMD is provided by the difference in interfacial temperature across the membrane, and the vapor transport distance is equal to the membrane thickness. The amount of clean water produced instantly adds to the permeate side. The most basic MD configuration is DCMD, which is commonly used in desalination operations and also for aqueous solution concentration in the food sector [19, 24]as well as acid manufacture [25, 26].

Air gap membrane distillation

The second form of MD module design is air gap membrane distillation (AGMD), in which a tiny layer of air is interposed between the membrane and the condensation surface, which is then cooled on the other side (Figure 2). The presence of an air gap and a condensation plate inhibits direct contact between permeating vapor and cooling water, hence slowing heat transfer from the hot feed side to the cooling water. As a result, the AGMD module's internal heat recovery leads to improved energy efficiency than DCMD and reduces heat loss owing to conduction. The presence of an air gap, on the other hand, impedes mass transfer, resulting in decreased distillation flux. AGMD has been studied for various membrane distillation applications, particularly when thermal energy availability is restricted, including ethanol

separation [27], arsenic-contaminated water purification [28], and desalination [29]. When compared to DCMD, the clean water generated by AGMD condenses on the condensing surface near the permeate side and has a separate output.

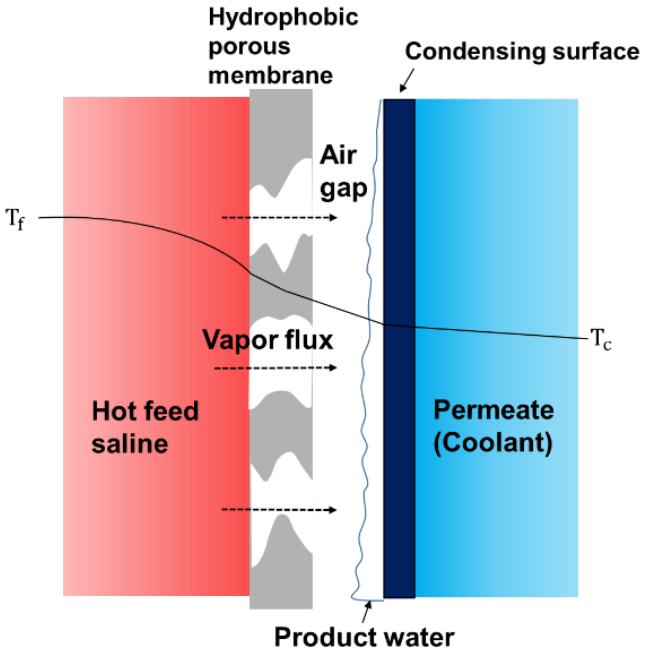

Figure 2: Schematic drawing showing conventional Air gap membrane distillation (AGMD) setup.

Vacuum membrane distillation

The third form of MD module design is vacuum membrane distillation (VMD), in which the permeate side is kept at low pressure, as low as 0.1 kPa [30]. By raising the vapor pressure differential across the membrane, the vacuum produces a driving force for transmembrane flow (Figure 3). Additionally, the approach improves the process by eliminating air from membrane pores and minimizing conductivity losses. VMD can create a greater distillation flux than DCMD and AGMD due to this combination [11]. VMD has several limitations, including an increased danger of membrane wetting (loss of hydrophobicity), the need for membranes with suitable mechanical strength, and an additional energy need for the vacuum pump [21]. VMD is most typically used to extract volatiles from aqueous solutions in applications such as ethanol-water separation [31], removing volatile organic compounds from water [32], desalination [33], and ammonia removal from aqueous solutions [34].

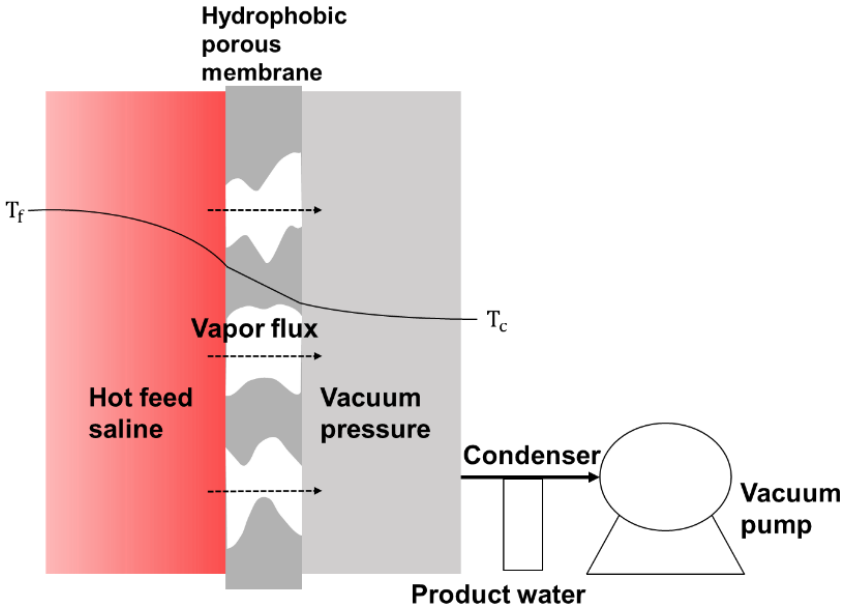

Figure 3: Schematic drawing showing conventional Vacuum membrane distillation (VMD) setup.

Sweeping gas membrane distillation

The next form of MD module design is sweeping gas membrane distillation (SGMD). At the permeate flow side of this membrane distillation arrangement, the permeate is a sweeping gas. The inert gas sweeps vapor from the permeate side of the membrane module and causes it to condense outside of it. The sweeping gas, like the air gap membrane distillation technique, has an air gap, although it is not stationary, which helps boost the mass transfer coefficient. The primary disadvantage of this configuration is that because of the enormous volume of sweeping gas, only a small amount of permeate diffuses, needing a larger condenser in order for the system to work. Figure 4 below depicts the configuration of membrane distillation technology [35, 36].

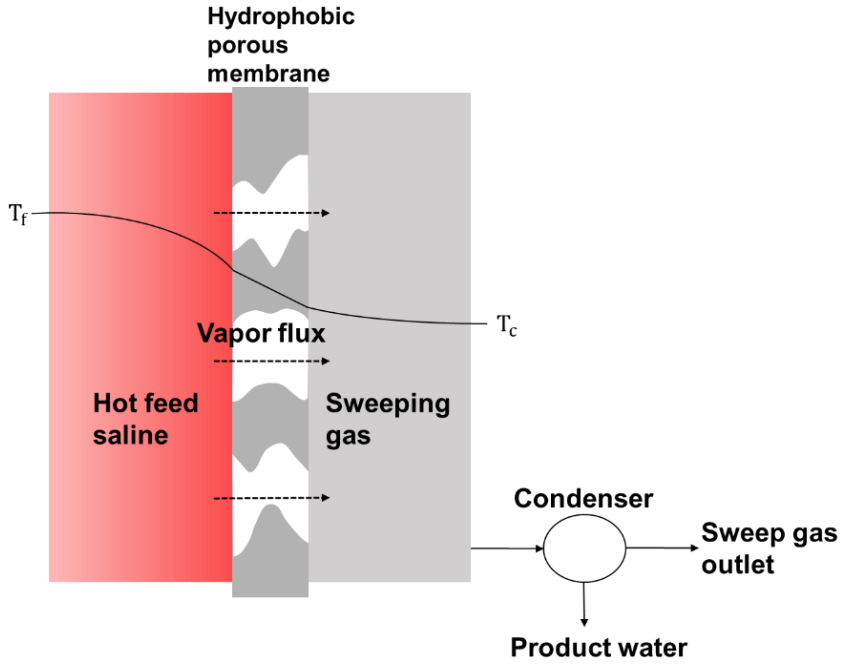

Figure 4: Schematic drawing showing conventional Sweeping gas membrane distillation (SGMD) setup.

A quantitative and direct comparison of distillation flux and energy efficiency under identical conditions is required for the effective selection of the optimal configuration for a certain application. From these four commonly adopted MD configurations, DCMD is the most generally used configuration in laboratory MD research due to its ease of design and assembly, although AGMD has attracted greater attention for commercial applications because of its enhanced energy efficiency and capabilities for latent heat recovery. One of the studies goes into detail on the differences and similarities between DCMD and AGMD to give a better perspective [37]. Eykens et al. also investigated all possible configurations and gave guidance on how to choose an MD setup [38].

1.2.3 Membrane characteristics

The hydrophobic property of the membrane, in general, prevents the solution from accessing the pores, resulting in a vapor-liquid interface at each pore entrance. The MD method employs microfiltration membranes made of hydrophobic polymers such as polypropylene (PP), polytetrafluoroethylene (PTFE), and polyvinylidene fluoride (PVDF) [14, 39, 40]. They exhibit thermal conductivities as low as 0.22- 0.45 W/m.K and high chemical stability at membrane distillation operation temperatures. The majority of the membranes utilized were designed or modified for microfiltration (MF), and few researchers investigated creating or changing these membranes. Membranes with a hydrophobic layer and a hydrophilic layer, or a hydrophobic layer sandwiched between two hydrophilic layers, have also been employed [41-43].

Membrane performance in MD is influenced by a variety of parameters, including membrane hydrophobicity, material chemistry, and morphology-related features such as pore size and

porosity, and pore tortuosity. Being hydrophobic is a basic need for the effective execution of the MD process, which is directly connected to membrane performance stability and is expressed by membrane pore wetting and membrane fouling.

Membrane pore size

If the absolute pressure difference between the liquid and vapor phases is sufficiently minimal, the liquid phase cannot penetrate the membrane pores owing to surface tension, despite the fact that single molecules are much smaller than the membrane pores.

The surface tension cannot maintain the liquid-vapor interface above a specific pressure difference, and the liquid feed enters the membrane pore volume. The liquid entry pressure (LEP) is the name given to this characteristic pressure. It is evident that pressures in MD systems must not surpass the LEP in order for the membrane to retain its separative activity. $\Delta p_{l-g} < LEP$ Eq. 1 Eq. 1 below expresses the key non-wetting condition [44].

$$\Delta p_{l-g} < LEP \qquad Eq.\ 1$$

The Young-Laplace theory outlines the relationship between fluid pressure, surface tension, and surface curvature. The LEP may be readily obtained from the Young-Laplace equation for an ideal cylindrical pore geometry, taking into account the membrane pore diameter d, the surface tension of the liquid phase (γ_l), and the contact angle θ that forms between the fluid and the membrane (Figure 5). Because membrane wetting occurs first at the largest pore, the maximum pore size (r_{max}) of a membrane material is taken into account. Eq. 2 shows that a small values of maximum pore size, a large contact angle, and a high surface tension of the feed solution all contribute to a reliable MD process [45].

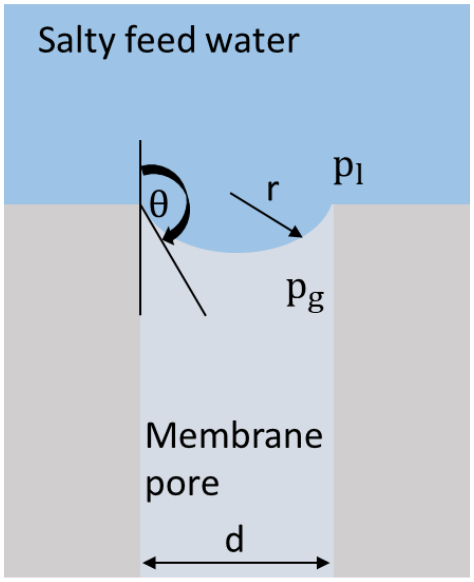

Figure 5: Parameters affecting the LEP values in Young-Laplace equation on a membrane with ideal cylindrical pores.

$$LEP = \frac{-2\gamma_l cos\theta}{r_{max}} \qquad Eq.\ 2$$

From the equations above it is clear that the bigger the pore size, the lower is the liquid entry pressure (LEP). As shown in Figure 6, it is observed how LEP value for PE membranes decrease as pore sizes increases. If the feed pressure is greater than the LEP, the liquid will permeate the pores and the hydrophobicity will be lost, as shown by Eq. 2 . When a low surface tension solution is treated, the influence of pore size becomes obvious. To minimize the wetting of membrane pores, pore size should be kept as small as possible, which contradicts the demand for increased MD permeability. Depending on the kind of feed solution to be treated, an ideal value must be found for each MD treatment.

Pore size distribution is also taken into account in several of the research. Because of the pore size distribution of the membranes, many mechanisms of mass transport can occur at the same time. There are also several theoretical model-based research that investigates the influence of pore size distribution on membrane distillation [46-48].

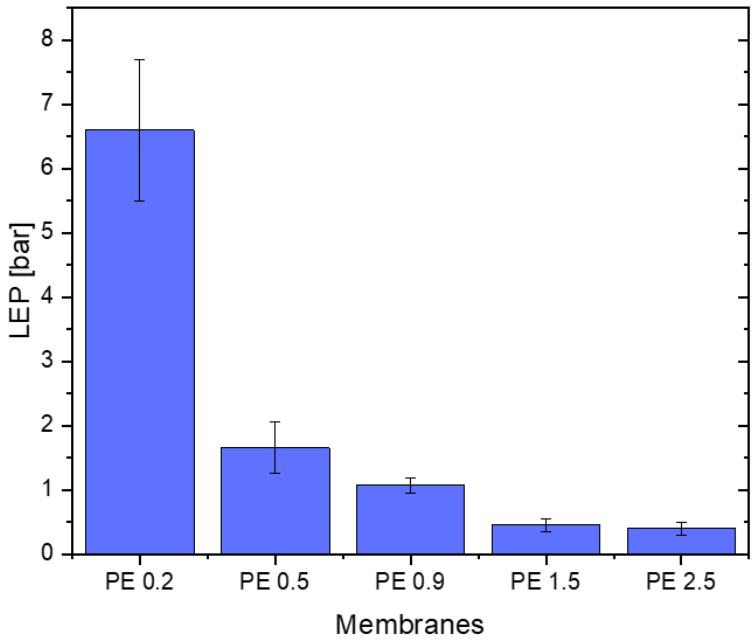

Figure 6: LEP of commercial PE membranes with different pore sizes.

Membrane porosity

High porosity membranes provide higher fluxes independent of MD design because a greater percentage of the surface is accessible for evaporation. In terms of energy efficiency, increased porosities reduce conductive heat transmission through the membrane solid material since the heat transfer coefficient of the air/gas is lower than that of the polymer. In MD setups, typical membrane porosity ranges between 60 and 85% [49].

Membrane tortuosity

Tortuosity is defined as the ratio of the actual length of a particular particle's diffusion way to the thickness of the system under consideration. The greater the tortuosity, the lesser the distillation flux. In MD studies tortuosity is usually considered to be of the order of 2 [50, 51].

Membrane thickness

The thickness of the membrane has a vital impact on the efficiency of heat and mass transport in MD. The membrane should be as thin as feasible to get a high MD permeability thus high distillation flux. Furthermore, thin membranes may minimize the total mechanical resistance of the membranes. The value of optimum thickness is observed to increase with reducing heat transfer coefficients, decreasing feed intake temperature, increasing membrane permeability, and increasing salinity. Also, in order to maximize heat efficiency, the optimum membrane thickness lies in the range of 60 – 150 µm. It should be noted that in the case of AGMD, the impact of membrane thickness is less important than that of the air gap [52, 53].

The kind of polymer utilized also has a significant impact on the membrane's characteristics and manufacturing technique. Gryta et al. investigated the effects of membrane shape and hydrophobicity of membrane materials (water contact angle) on membrane wettability using different types of membranes – PTFE, blending PTFE with PVDF, and PVDF [54]. Here PTFE membranes showed the best hydrophobic properties and so are widely used as a membrane material for MD. The main difference between PTFE and PVDF membranes is that PTFE membranes are more resistant to strong acids and aggressive solutions than PVDF membranes [52, 55]. Only a few writers, on the other hand, have examined the idea of developing novel membranes and membrane module designs explicitly for MD applications [9, 14, 21, 56-58].

1.2.4 Factors affecting Membrane distillation

Feed temperature

The influence of feed temperature on distillation flux has been extensively studied in the various MD setups mentioned. The feed temperature is normally between 60 and 90 ^{o}C, while lower values have been employed. In general, the flux increases exponentially with feed temperature in all MD designs [59]. An increase in the feed temperature raises the vapor pressure in the feed solution channel, which raises the trans-membrane vapor pressure. According to various research, working at high feed temperatures improves evaporation efficiency and overall heat transfer from the feed to the permeate/cooling side, even if the temperature polarization effect rises with feed temperature. Temperature polarization occurs when the temperatures at the membrane surface deviate from the bulk temperatures observed in the feed and distillate. This effect results in a significant loss in driving force for the vapor transport [60]. During the distillation process, when feed concentration rises, we have to add concentration polarization to temperature polarization which also reduces the imposed driving force and so the mass flux.

It should be noted that operating at very high temperatures, such as 90 ^{o}C, may result in a decrease in membrane selectivity and significant scaling issues [61].

Coolant temperature

Because of the exponential increase in vapor pressure with feed temperature, raising the permeate/cooling temperature has less influence than increasing the feed temperature. In AGMD, coolant temperature has no influence on distillation flux because the heat transfer coefficient in the air gap is substantially less than the heat transfer coefficients on the hot and cold sides [62].

Feed concentration

Feed concentration reduces transmembrane flow to some extent in all MD systems. This is due to multiple factors, including reduced vapor pressure owing to salt concentration, a concentration barrier at the membrane surface, and enhanced temperature polarization. However, the effect of increasing feed concentration in several experimental trials ranged from minor to moderate [63, 64].

Feed flow rate

In the MD process under discussion here, we have a salt solution at a high temperature on one side of the membrane and clean water on the other. The difference in temperature and concentration across the membrane causes a vapor pressure differential, resulting in an effective desalination process. According to most research, raising the feed flow rate enhances the distillation flux. This is due to the better mixing of liquid from different zones having different temperatures and concentrations. This leads to more homogeneous temperature and concentration distribution. Also, the temperature at the membrane surface approaches more closely to the input feed temperature due to the turbulence on the feed side [16].

Coolant flow rate

Increased coolant flow velocity promotes heat transfer in the permeate side of the membrane module by lowering the temperature and concentration polarization effects in DCMD, VMD, and SGMD designs. As the temperature difference grows, the distillation flux tends to increase. In the case of an AGMD configuration, where the heat transfer coefficient in the air gap dominates the overall heat transfer coefficient, changes in coolant flow and temperature have negligible influence on the AGMD flux. [16].

Transmembrane temperature difference

The transmembrane vapor pressure, caused by the temperature differential between the feed and permeate/cooling sides of the membrane module, is the driving force in MD. As discussed before the distillation flux grows exponentially with the increase in temperature

difference between the hot and cold sides. As the difference in temperature reduces, the distillation flux also decreases. It should be emphasized that such tendencies are controlled by feed flow rates and are linked to temperature and concentration polarization effects. [16, 60, 65].

1.3 Challenges in Membrane distillation

Minimal MD research has been done at the issues involved in its practical applications. These issues include membrane fouling, wetting, and long-term operational consequences. It is critical to assess membrane fouling development in MD in the context of drinking water supply. Fouling is an issue that affects all membrane functions. Foulants are elements in feed water that are maintained on the membrane surface or in the membrane pores during the fouling phenomena, which are precipitations of organic and inorganic debris or biofilms. Fouling reduces membrane process efficiency, lowers product quality, and eventually reduces membrane life span, incurring additional operational expenses. As a result, more complete knowledge and management of membrane fouling is required [66-69].

In MD, the link between membrane hydrophobicity and fouling development needs to be studied. The hydrodynamic conditions i.e. transmembrane pressure, flowrate and temperature at both sides, etc., as well as the chemical composition of the feed liquid have a significant impact on membrane fouling. Fouling can produce a decrease in distillation flux due to undesired deposits on the membrane surface and pores, as well as partial or total membrane wetting because the deposits lower the hydrophobicity of the membrane via adsorption, resulting in membrane wetting [70-73]. As a result, a membrane's separation qualities may deteriorate, and wetting may develop [74].

Despite the presence of fouling in MD, much MD research lacks in-depth assessments of fouling development [34]. One of the major impediments to commercial MD adoption has been noted as a lack of knowledge of fouling and wetting processes in MD and their related mitigation. As a result, additional research is being conducted on this topic. The number of published MD articles on the issue of membrane fouling has steadily risen over the last two decades, particularly for MD scaling development [75]. The bulk of hydrophobic membranes used for MD includes PTFE or PVDF or in other cases are made via fluorination. Fluorinated organic molecules, on the other hand, are harmful to the environment and are no longer acceptable. PTFE membranes are additionally pricey due to the lengthy manufacturing process and the cost of the material itself [43, 75-78].

However, MD has yet to be commercialized since it requires scientific study, especially in the realms of membrane fouling and membrane pore wetting which reduces membrane permeability and compromises treatment efficiency.

1.3.1 Membrane fouling

The kind of membrane fouling is determined by the source of feed water, foulant properties, and feed water chemistry. Membrane fouling in MD operations can be caused by a number of foulants, including scalants in the form of salts (e.g. $CaSO_4$ and $CaCO_3$) – Inorganic fouling/scaling, then the presence of particulates, colloidal matters – Colloidal fouling, later deposition of natural organic matter (NOM) – Organic fouling and biological species such as bacteria, fungi, and algae that cause biofilm development – Biofouling [66, 67, 69].

The MD membrane is the most important component of an MD system. Hydrophobic membranes characterize conventional MD membranes. To avoid direct liquid absorption via the micropores, hydrophobicity is essential. However, when hydrophobic membranes are utilized in MD to treat wastewater, two major issues may arise, resulting in MD operation failures [73]. The first issue that may occur is membrane fouling, and the second is membrane wetting.

Membrane fouling is a common issue in all membrane processes. It refers to the buildup of undesired elements on the membrane surface or within the membrane pores, which affects mass transfer across the membrane and causes a decrease in distillation flux and in some cases also reduces salt rejection. When a fouling layer forms on the membrane's surface, it adds hydraulic and thermal resistance to the mass transfer coefficient. The degree of resistance is estimated using the fouling film's properties, such as the thickness and porosity of the deposited layer. In the case of the non-porous fouling layer, it leads to both thermal and hydraulic resistance. Whereas when the fouling layer is porous, it will depend on its porosity as a comparison to the membrane’s porosity and also thickness to determine the effect of thermal resistance [66].

According to the literature, membrane fouling is more severe in the pressure-driven membrane process than in the MD method. However, fouling in MD is recognized as one of the major challenges impeding the long-term adoption of MD technology. When comparing fouling in the MD process to fouling in the pressure-driven membrane process, it is discovered that fouling in the MD process is still understudied and poorly understood. However, all identified types of fouling that occur in any membrane-based process are also present in the MD process [79, 80].

Membrane fouling is a complex phenomenon. It is difficult to explain the mechanism of fouling occurring since it is influenced by several parameters that are all interconnected. To ensure a thorough knowledge of the fouling mechanism, a detailed approach to prevent fouling development should be adopted. Because an acceptable mitigation strategy differs depending on the kind of fouling, it is more feasible to study each form of membrane fouling separately. Fouling is a complicated phenomenon that is impacted by several parameters. Tijing et al. (2015) classified the parameters that might influence fouling development into

three categories: operating conditions, feed water and foulant characteristics, and membrane characteristics [69, 73].

Gryta's (2000) work was one of the first MD drinking water application studies to highlight the occurrence of membrane fouling [81]. After that Karakulski and Gryta (2005), for example, detected $CaCO_3$ precipitation on the MD membrane surface using concentrated tap water [82]. Gryta et al. (2008) also studied the formation of fouling layers in various feed solutions such as protein effluent, brine, bilge water, and demineralized water [68].

Surface roughness is one of the membrane features that have a significant impact on membrane fouling by modulating the membrane's hydrophobicity. More air can be trapped in micro- and nano-sized membrane surface pores with higher surface roughness [83]. As a result of the increased fraction of the solid-gas interface in the overall combination of solid-liquid and solid-gas interfaces on the membrane surface, the membrane surface becomes more hydrophobic. According to Zhao et al. (2015), increasing membrane roughness diminishes the contact strength between the foulant particle and the membrane surface. As a result, foulants stick to and detach from the membrane surface with ease [69, 84].

It is known that the most difficult sort of fouling comes from feed solutions containing hydrophobic pollutants such as oil and hydrophobic organics. These pollutants form a nonporous layer of fouling that is difficult to remove due to strong hydrophobic-hydrophobic interactions formed between the contaminants and the membrane surface [68].

The following section describes the different types of fouling encountered in the MD process in detail, their origins, and the effects on the membrane surface, characteristics, and MD performance.

1.3.1.1 Inorganic/scaling

The subject of inorganic fouling in MD has gotten a lot of attention in the literature [67]. Inorganic fouling or scaling is the deposition of solid inorganic compounds such as calcium carbonate, calcium sulfate, silicate, sodium chloride, aluminum oxide, iron oxide, calcium phosphate, $MgCl_2$, $MgSO_4$, ferric oxide, $SrSO_4$, and $BaSO_4$ on the membrane surface or inside the pores [69, 85, 86]. The inorganic components present in the feed solution goes through series of steps leading to crystallization.

The most common scale forms are caused by the presence of sparingly soluble salts in the feed solution, such as $CaSO_4$, $CaCO_3$, and CaC_2O_4. These salts have limited water solubility yet are not entirely insoluble. Temperature changes, solvent evaporation, and concentration polarization all increase the concentration of dissolved salts in the feed solution. Furthermore, Membrane scaling during MD is mostly caused by the direct precipitation of sparingly soluble salts such as $CaSO_4$, $CaCO_3$, and silicate on the membrane surface [87]. Most salt solubility rises with temperature, and these salts do not crystallize on heat transfer surfaces unless their concentrations are quite high. Scale deposits are created by salts whose

solubility is normally restricted and decreases with increasing temperature in the majority of situations [88]. Hsu et al. (2002) showed a decrease in distillation flux with saltwater, relating high temperature application to membrane fouling in MD [19]. Supersaturation on the feed side occurs when the concentration exceeds the equilibrium solubility product, resulting in the nucleation process. Nucleation is the process by which a limited number of ions, atoms, or molecules form the typical pattern of a crystalline solid [87, 88].

Several factors can influence how quickly the scaling occurs, including supersaturation, temperature, water composition, flow parameters, substrate material, and the presence of any nucleation sites. During supersaturation, various ions begin to attract one other, resulting in the formation of crystals in the bulk solution or on the membrane surface. During the MD experiments, when, the small crystals of Ca salts or others depending on the feed solution prepared could potentially act as nucleation sites for the crystallization of further larger crystals. Crystallization occurring in bulk solution is termed as homogeneous nucleation, and crystal nucleation on the membrane surface is referred to as heterogeneous nucleation. Typically heterogeneous nucleation is more likely than homogeneous nucleation. When water vapor diffuses through the membrane, the rejected salt collects in the boundary layer near the membrane at higher concentrations than in the bulk which can lead to heterogeneous nucleation and result in the formation of crystals (Figure 7).

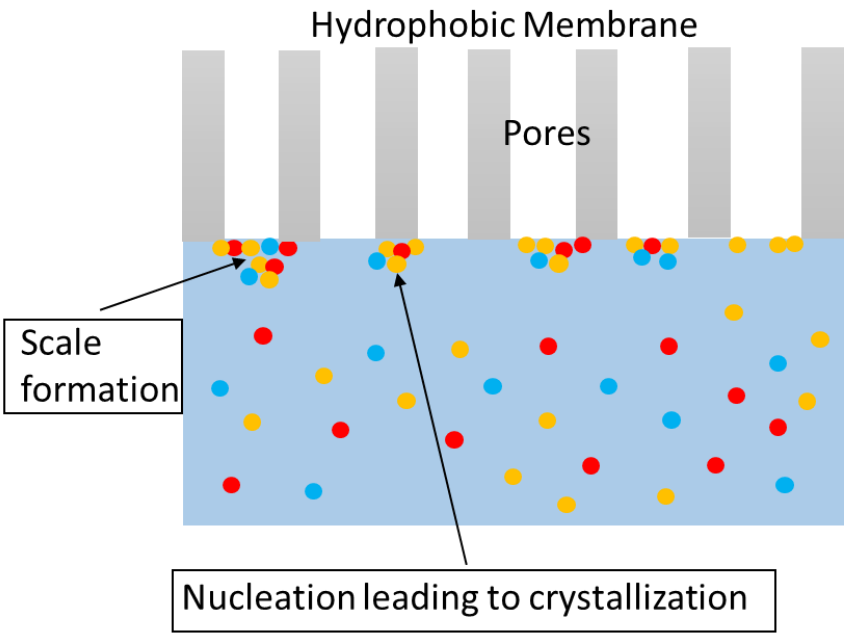

Figure 7: General steps for inorganic fouling/scaling during the MD process

Despite the fact that the membrane distillation process operates at low pressure, both crystallization processes can occur in MD. In the MD system, both crystallization processes coexist, making inorganic fouling a complicated process. According to one study, heterogeneous crystallization is more dominant in unstirred batch systems, but scaling occurs in both homogeneous and heterogeneous crystallization processes in continuous flow

systems [89]. Concentration polarization is recognized to be the principal cause of increasing concentration of the feed solution, resulting in the development of crystallization processes.

During the crystallization process, many layers of deposits form on the membrane's surface. The deposition layer has higher temperature polarization and thermal durability, which minimizes driving force across the membrane (Figure 8). Distillation flux will be lowered as a result [56, 87, 90, 91]. Gryta investigated various scaling effects on PP membranes and discovered a dramatic decrease in distillation flux owing to the deposition of considerable amounts of scalants on the membrane surface [88, 92]. Crystals generated on the membrane surface may potentially penetrate into the interior of the pores, causing harm to the MD module. As a result, the concentration of salt solutions contaminated with scarcely soluble chemicals in the MD process necessitates their continual removal from the feed, for example, by crystallization.

To avoid scaling development on the membrane surface, it is critical to understand the mechanism of inorganic fouling crystallization. Because inorganic scalants are difficult to remove from the membrane surface and pores, preventing fouling development serves as a fouling mitigation approach for inorganic fouling. As a result, inorganic fouling is regarded as one of the primary obstacles preventing the MD process from being used in large-scale desalination applications. Inorganic fouling is caused by a variety of reasons, including membrane shape, feed solution type, and operating conditions.

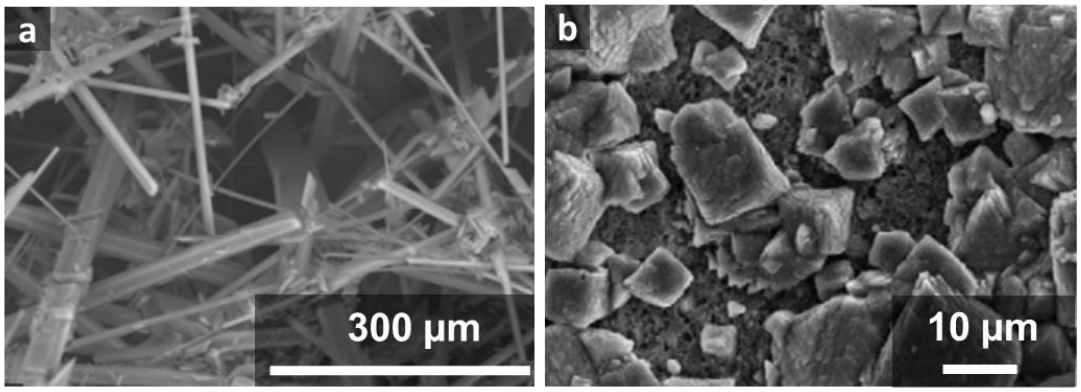

Figure 8: SEM image of (a) $CaSO_4$ deposits precipitated on PTFE membrane [87] (b) $CaCO_3$ layer on PP coated fluoro-silane [49]

Temperature is one of the most important elements in the scaling and fouling of MD membranes. Salt solubility and crystal formation, in particular, vary greatly over the temperature range important to MD systems. Importantly, the solubility of specific salts can be associated with temperature either favorably or negatively. The solubility of sodium chloride, for example, rises with temperature, but that of calcium carbonate, magnesium hydroxide, and calcium phosphate decreases. This negative connection of solubility with temperature is common for alkaline salts, which rely on the dissociation of water into hydrogen and hydroxide to produce scale; at higher temperatures, such dissociation increases [80]. Salts with inverse solubilities, such as calcium sulfate and calcium carbonate, are frequently the most saturated in desalination feed solutions (calcium sulfate concentration is

higher in the case of seawater as a feed while calcium carbonate concentration is higher in groundwater sources). In general, greater temperature increases the likelihood of scaling in common feed solutions [90, 93].

1.3.1.2 Colloidal fouling

Colloids are tiny particles floating in water that cause fouling in many feed water solutions. Colloids can range in size from a few nanometers to a few micrometers. Although different membrane technologies may remove bigger particles, small particles can cause major fouling concerns. Colloidal fouling is sometimes classified as both inorganic and organic fouling in the literature. As a result, colloidal particles can be classified as inorganic foulants or organic macromolecules. The primary inorganic sector of colloidal foulants found in natural water sources includes silica, aluminum silicate minerals, clay, silt, iron oxides/hydroxides, and debris [67, 94, 95].

Silica is significant because its tiny size makes it difficult to remove using pretreatment procedures such as microfiltration. Silica appears in water in three forms: colloidal silica, particle silica, and dissolved silica (or mono silicic acid). When supersaturation occurs and silica begins to polymerize on the membranes, the latter can cause significant fouling in MD systems. In one study, colloidal silica is used in combination with Ca salts and one observed strong fouling for DCMD process [95]. In another study silica scaling caused greater DCMD flux decline than gypsum and calcium carbonate scaling [96]. Similar fouling effects were also observed in another study [97].

The removal of the foulant by acid and drying of the membranes only temporarily restored the initial distillation flux [93, 96]. This occurred despite the feed being nano-filtered upstream of the MD membranes. SEM-EDS investigation revealed that the deposit was mostly silicon, with traces of iron, calcium, and zinc. SEM examination also showed that the flux decrease was caused by clogged membrane capillaries rather than a deposited layer of foulants. Because of the blockage, the feed flow rate was lowered, which increased temperature and concentration polarization, lowering the module flux. While silica fouling does not produce as rapid a flux drop as calcium carbonate, it remains a worry since it is difficult to clean. Acids that are usually employed to dissolve the crystalline scale are ineffective on uncharged silica. When there is a high concentration of silica in the feed, the authors recommend avoiding hollow fiber membranes with feed flow inside the capillaries [82, 97].

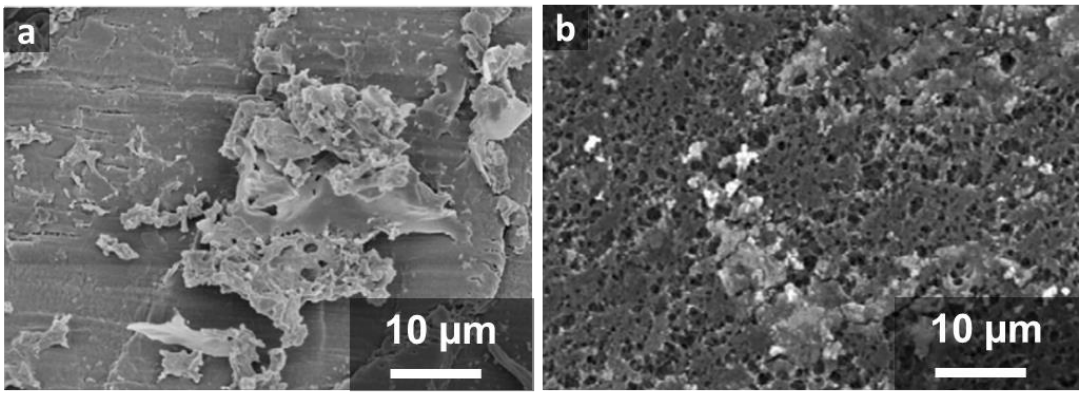

Figure 9: SEM image of (a) Silica deposits precipitated on PTFE membrane [97] (b) Iron oxide fouling on PP membrane [85]

Other foulant is iron oxide which is also a common and major particle foulant studied in MD. Iron oxide fouling can be made up of a range of compounds, such as iron oxides, iron hydroxides, and iron oxide-hydroxides. These compounds are normally crystalline, although they can also exist in hydrated forms. Iron oxide scale is not expected to be present in ordinary feed waters, but it is a scaling danger owing to the rusting of steel and even stainless steel components in distillation systems. Corrosion fouling not only causes clogging issues, but it may also cause membrane degradation due to surface erosion (mechanical damage by corroded flakes and chunks in motion through the narrow flow passages) [85].

Additional iron oxide fouling occurred in Gryta's research as a result of acid cleaning (HCl) of the feed side. The volatile acid was able to pass through the membrane as gaseous HCl to a limited extent, acidifying the permeate and inducing oxidation of the stainless steel components on the permeate side of the system. Even at concentrations of less than 50 g/L HCl, substantial reactions with the stainless steel components can occur. As a result, Gryta suggests utilizing acid-resistant high-grade steel or plastic for MD systems [85].

In comparison to other scale forms in MD, iron oxide is unlikely to arise with adequate system design. It is less detrimental to distillation flux, but it is still a major source of wettability and is extremely difficult to eliminate. Because of the reduced working pressure characteristic of the MD process, plastic components may be used, potentially eliminating most iron from the system [93, 98].

1.3.1.3 Natural organic fouling

Natural organic matter (NOM) components that provide a risk for MD are common in wastewater as well as some lake and ocean water samples. NOM is comprised of proteins, amino sugars, polysaccharides, and humic compounds. The fouling generated by NOM can influence the membrane's permeability as well as its rejection of dissolved materials. Ionic strength, pH, ions present, membrane surface structure and chemistry, molecular weight, polarity, distillation flux, and hydrodynamic and operational parameters all influence membrane fouling in the presence of organic molecules [72, 99, 100].

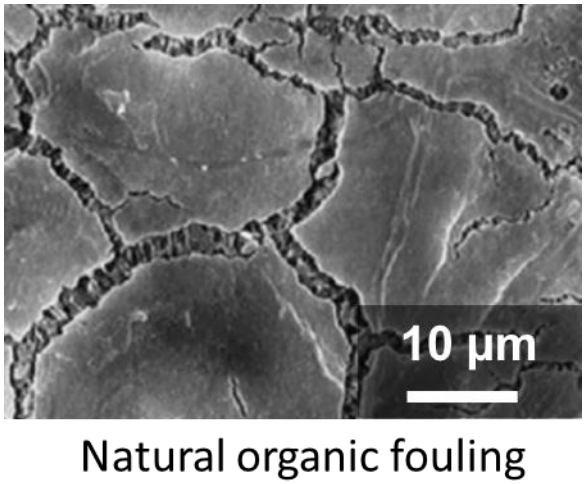

Figure 10: SEM image of protein deposits on PP hollow fiber membrane [68]

NOM may adsorb on the membrane's surface via a variety of processes, including particular chemical affinity, electrostatic and hydrophobic interactions. NOM deposition can: (a) adsorb or deposit inside the membrane's pores, either partially or completely blocking water passageways; (b) form a separate gel-like layer on the membrane's surface, thus blocking the pores; and (c) bind particles and NOM together, forming a low permeability particle/NOM layer on the membrane's surface [68].

In one of the studies, humic acid (HA) was employed. It was observed that HA was first deposited inside the membrane's pores, and then it was deposited on the blocked region. The fouling behavior of HA is influenced by the solution's pH and ionic strength, the concentration of monovalent and divalent ions, the surface characteristics and structure of the membrane, and the working circumstances. The pH of a solution has a large impact on HA fouling [101].

Khayet et al. (2004) investigated how HA solution treatment can minimize fouling in MD. MD was used to treat HA solutions containing NaCl and $CaCl_2$ at concentrations comparable to those found in natural waters. Microporous PTFE and PVDF membranes were used in the tests. When humic acid-containing salts were investigated, larger salt rejection factors with extremely low distillation flux decline were reported in DCMD application when compared to pressure-driven membrane separation procedures. These findings show that MD is an appealing technique for treating HA solutions [70].

Organic fouling that causes wetting has not been well studied. Previous research has discovered structural and surface charge changes in protein organics as temperature rises. Bovine serum albumin (BSA) is a protein with a molecular weight of approximately 66,000 Da. One of the primary causes of protein fouling in MD is high operating feed temperature. According to Tijing et al., BSA fouling in the MD process is insignificant when the BSA feed content and feed temperature (i.e., 20-38 °C) are low [73]. Gayathri Naidu et al. (2014) used synthetic model solutions of HA, alginate acid (AA), and BSA to evaluate fouling development in the DCMD system at feed temperatures of 50 ^{o}C and 70 ^{o}C. A 40-50% distillation flux reduction was found at higher temperature, with BSA and HA displaying major fouling tendencies and AA showing minor fouling due to its hydrophilic nature. The study of the

fouled membrane revealed that the BSA feed solution had more substantial deposits on the membrane surface (35.2% more carbon mass than the HA foulant) but less significant pore penetration [71]. Wenli Quin et al. (2017) demonstrated the combination effects of AA, BSA, and HA in the presence of colloidal silica particles in another investigation. Combination of BSA protein with colloidal silica in the feed solution enhanced the rate of fouling forming larger aggregates which resulted in a significant decrease in distillation flux as well as partial pore wetting [94].

Researchers have explored several ways to manage fouling phenomena, such as considering feed pretreatment(s), increasing feed flow rate causing turbulent flow regime, applying periodic hydraulic and/or chemical cleanings, increasing membrane surface roughness and/or changing its surface charge [102]. Some investigations have shown that organic fouling in DCMD is irreversible [70, 103]. Other studies, however, claimed the reversibility/cleaning of organic fouling, such as the complexes formed by calcium ion (Ca^{2+}) and organic matter that precipitates only on the membrane surface, forming a thin deposit layer that is completely eliminated by a simple cleaning with water and 0.1 M sodium hydroxide solution. It was observed that just washing the membrane with deionized water via the feed channel at a flow velocity of roughly 1 m/s allowed for the recovery of up to 98% of the distillation flux [71].

According to one study, MD is a viable approach for recovering ammonia from animal feces. It was discovered that pretreatment with microfiltration was adequate to lower the danger of organic fouling and boost ammonia mass transfer. It was also discovered that washing with NaOH/citric acid was adequate to restore the ammonia flow regardless of manure preparation [104].

Temperature increase causes humic acid and other organic compounds especially proteins to decompose. In fact, the temperature rise may be employed as an effective humic acid cleaning approach in reverse osmosis membrane systems. However, distillation flux rises at higher temperatures for MD, which may result in a larger concentration of organic molecules at the membrane interface due to the concentration polarization effect.

1.3.1.4 Bio-fouling

Biofouling is defined as the deposition and accumulation of microorganisms on the surface of the membrane and within its pores, which finally results in the creation of a biofilm. The biofilm is made up of microbial cells and extracellular polymeric substances (EPS) that covers the membrane's surface. Biofouling has been a major issue for reverse osmosis membranes; it is also anticipated to be an issue with practical MD systems. However, the operating parameters of the MD process, particularly high temperatures and salinity, can severely limit microbial development in MD installations. Temperature may have a substantial impact on biofouling due to microbe’s inability to tolerate high temperatures and thermal impacts on organic compounds. Most environmental organisms will not survive and so will not develop on MD membranes at temperatures over 60 °C, according to M. Krivorot et al research's using hollow fiber membranes [105]. As a result, the difficulties caused by biofouling in membrane processes such as nanofiltration, ultrafiltration, or reverse osmosis should not be as prevalent in MD systems. Organic fouling, on the other hand, may be more relevant in MD [105].

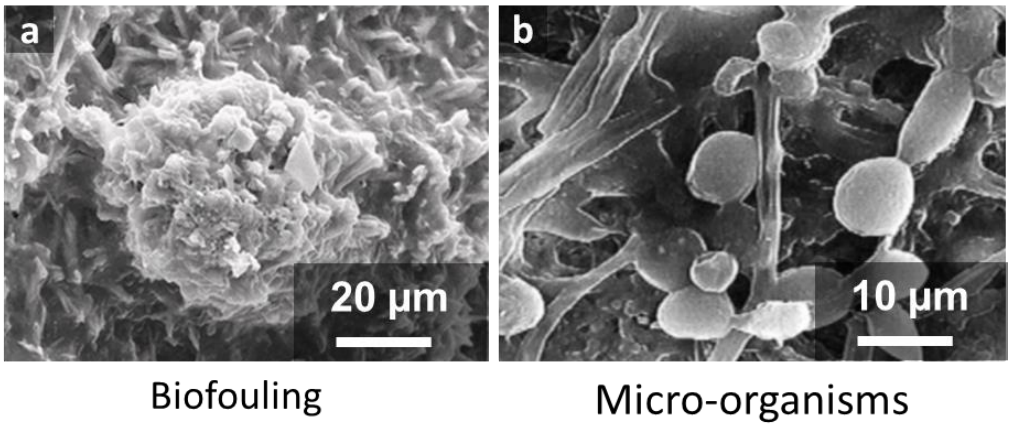

Figure 11: SEM image of heavily bio-fouled membrane with (a) extracellular polymeric substances [105] (b) micro-organisms [102]

Bacteria and microorganisms abound in water systems. While chlorination kills germs, it can be harmful to several popular MD membrane materials. Bacteria invade and excrete EPS in normal biofilm development and this EPS can be difficult to remove from membranes as they attach to the surface. When compared to inorganic scaling and fouling, these biofilms are generally 75-95% water and rather permeable [106, 107].

Gryta (2002), MD conducted a study on a bioreactor using saline wastewater containing yeast, Pseudomonas and Streptococcus faecalis bacteria, and the fungus Penicillium and Aspergillus [108]. The DCMD hollow fiber PP membranes (pore size: 0.22 µm) were unable to keep Streptococcus bacteria out of the distillate. No bacteria were identified at the membrane surface at 90 °C and salt concentrations of up to 300,000 ppm, showing that these circumstances inhibited bacterial development. Bacteria and fungus were discovered at the membrane when the temperature was reduced to 80 °C [108].

Biofilms, particularly in seawater, frequently contain microorganisms in addition to bacteria. Although there are no direct MD studies with marine microorganisms in the literature. Very few relevant superhydrophobic materials similar to MD membrane materials have been studied with seawater. Zhang's study evaluated seawater fouling in submerged hydrophobic and superhydrophobic surfaces during a 6-month period. Surfaces made of polysiloxane and PTFE were investigated. The hydrophobic surface fouled within a day, whereas the superhydrophobic surface (contact angle 169°) withstood fouling for around three weeks. After two months, however, both surfaces were significantly contaminated. The loss of biofouling resistance was mostly attributable to the loss of air bubbles across the membrane when the air dissolves into the surrounding water [109].

In summary the literature does not yet provide specific parameters for preventing biofouling since biofouling is affected by several elements such as salt concentration, feed composition, residence period, pre-treatment, microorganism presence, operational temperatures, membrane type, and cleaning frequency [110-112].

1.3.2 Membrane wetting

Membrane pore wetting can occur due to the loss of membrane hydrophobicity for the feeds containing wetting compounds (e.g., oils, surfactants). The metrics used to measure the membrane's wetting resistance are the liquid entry pressure (LEP), as stated above in section 1.2.3, and the membrane's surface wettability, as measured by the water contact angle (WCA). The surface wettability is greatly reliant on the surface's free energy and contact angle. Young's equation (Eq. 3) is widely used to determine the wettability of a liquid droplet on a flat, smooth surface [113]. In the equation, γ_{sv}, γ_{sl}, γ_{lv} represents surface tension between solid and vapor phase, solid and liquid phase, liquid and vapor phase, and θ is the contact angle between liquid and membrane.

$$cos\,\theta = \frac{\gamma_{sv}-\gamma_{sl}}{\gamma_{lv}} \qquad Eq.\ 3$$

Wetting is classified into four kinds in general: non-wetted, surface-wetted, partially wetted, and completely wetted. Surface wetting causes the liquid/vapor interface to move partially inward of the membrane cross section. Distillation flux may then progressively decrease as temperature polarization increases, lowering the temperature of the evaporating surface inside the pore. In the case of surface wetting, the membrane still provides a liquid/vapor interface for separation, whereas in the case of partial wetting, scaling due to feed evaporation can occur inside the pores along the meniscus [114, 115]. Furthermore, crystal development within the pores enhances the pace of scale formation by preventing the diffusive transit of solutes and solvents between wetted pores and the feed bulk, hence increasing solute concentrations locally. Under some situations, however, the liquid incursion into the pore has been seen to generate a brief flux increase due to the shorter vapor diffusion route through the dry section of the pore.

Partial wetting might occur as the feed liquid penetrates further into the membrane pores. If the majority of pores are still dry, the MD procedure can still work. However, partial wetting where the pores are blocked by organic or/and inorganic compounds can reduce distillation flux due to a reduction in the active surface area for mass transport associated with partial wetting or it can cause an increase in distillation flux, and decrease in salt rejection due to wetting of some pores (i.e. vapor transport is overtaken by liquid transport) followed by a rapid decrease due to steady blockage of pores by foulants depending on the experimental conditions [82, 116]. Partial wetting also causes distillate water quality to deteriorate. Surprisingly, all of the hydrophobic membranes employed in MD, such as PP, PTFE, and PVDF, have demonstrated partial wettability over time [117].

In the case of full wetting, the MD membrane ceases to function as a barrier, the feed liquid completely floods the membrane, resulting in a viscous flow of liquid water through membrane pores, rendering the MD process inoperable [86, 115].

The pore-wetting issue is always connected with hydrophobic MD membranes. Wetting limits MD for various applications, including desalination, the removal of trace volatile organic

compounds from wastewater, and the concentration of ionic, colloidal, or other non-volatile aqueous solutions, as well as other solutions with a high fouling tendency. Significant partial wetting into the membrane, similar to employing thinner membranes, may increase its effective thermal conductivity and hence reduce the MD thermal efficiency, resulting in a drop in distillation flux. Yet, when complete pore wetting occurs as a result of water bridging, the membrane's water flow increases over time as salty water also penetrates the membrane pores, resulting in a decrease in salt rejection. [86, 118, 119].

LEP reduces when organic substances or surfactants are present in the feed solution, and the membrane pores may get wetted. As discussed before LEP is affected by pore diameter, pore geometric structure, and also the surface tension of the feed solution, and the contact angle between the membrane surface, and liquid. However, LEP cannot adequately explain the process of membrane wetting [120].

Although avoiding wetting in MD is the most important process requirement, it has not been well explored, and only a few studies have attempted to overcome wetting difficulties in MD membranes. Some writers have researched how to increase the hydrophobic characteristics of membranes by using innovative materials or by changing surface chemistry and surface geometry using nanoparticle coating and surface fluorination. However, when addressing feed solutions containing large concentrations of surface-active species, these membranes are still sensitive to pore wetting [121].

So far, no membrane has been developed that can withstand both wetting and fouling. An omniphobic membrane that has been demonstrated to resist surfactant wetting is actually oleophilic underwater. Oil droplets in the feed easily fouled an omniphobic membrane, reducing distillation flux by obstructing the membrane pores. A composite membrane with an in-air hydrophilic surface that is fouling resistant, on the other hand, failed to reduce surfactant wetting of the membrane [69, 115, 122, 123]. Small amphiphilic chemicals can easily penetrate the membrane surface and damage the hydrophobic substrate. MD may become broadly useful in desalinating hypersaline wastewater with complicated compositions if a new membrane that is both wetting and fouling-resistant can be developed.

An omniphobic membrane, which can resist wetting to both water and low surface tension liquids, has recently been proposed as an MD membrane. M. Elimelech and Tung created omniphobic membranes for MD with hierarchical re-entrant topologies using fluorinated nanoparticle deposition on microporous nanofiber substrates [124, 125]. Despite the fact that the modified membranes were omniphobic, the production processes were difficult and required many modification steps.

The olive oil manufacturing process generates a substantial amount of watery waste, which is referred to as 'olive mill wastewaters' (OMW). OMW discharge in water reservoirs (groundwater, surface waters, seashores, and sea) without pre-treatment causes serious difficulties for the entire ecosystem since OMW effluents have low pH and biodegradability, as well as exceptionally high solids and organic component concentrations. One of the research looks at the use of MD to treat waste water with OMW. El-Abbassi et al. focused on pre-treatment options before to MD and discovered that microfiltration outperformed

coagulation/flocculation [111]. Gryta and Karakulski evaluated the effect of crude oil concentration and discovered that greater oil concentrations resulted in membrane wetting and hence lower permeate quality [82]. Membrane fouling due to the affinity between the hydrophobic oil and the hydrophobic membrane, and the organic compounds sufficiently lowering the liquid surface tension to wet the membrane. Furthermore, surfactants, amphiphilic molecules that stabilize oil emulsions, can reduce surface tension and enhance the likelihood of membrane wetting.

Membrane wetting is a well-known problem in MD processes, and the research discussed above has thrown some insight into how to improve MD for handling oily feeds. However, there is a knowledge gap on which of the three essential ingredients in real oily wastewater streams (oil, surfactant, and salt) has the most critical influence on MD performance, which inhibits the use of MD for such purposes.

1.4 Outline of thesis

After the literature study we discuss the experimental part where we report on reliable fabrication technology to create a new class of non-fluorinated superhydrophobic membranes, using silicone nanofilaments (NFs) coating of commercial microporous membranes. At the start of this research, the NF coatings were tested on several hydrophilic membranes such as polyethersulfone (PES), cellulose acetate (CA), and hydrophobic membrane polyvinylidene fluoride (PVDF), polytetrafluoroethylene (PTFE) with varying pore sizes. Even without surface fluorination, the nanofilament-coated membranes exhibit exceptional superhydrophobicity when compared to commercial membranes. The wetting properties of the fabricated NF-coated membranes were evaluated by determining the liquid entry pressure (LEP), water contact angle, water sliding angle, and gas permeability to carefully consider mass transfer resistance, and distillation flux to assess MD performance. The minimum pressure required by the liquid to enter the membrane pores is denoted by LEP, and the LEP value should be as high as feasible to avoid membrane wetting. According to the testing results, the fluorine-free nanofilament coating might very well greatly raise the LEP of coated membranes, avoiding wetting of membranes with large pore diameters. More crucially, because the coating thickness can be adjusted within micrometers, the nanofilament-coated membranes can retain excellent vapor diffusion over large pores. We show experimentally that the maximum LEP of NF-coated membranes can surpass 11.5 bar, more than double the value of commercial membranes with 0.2 µm pore size. Considering all substrates, nanofilament coating on PES membranes exhibits excellent results with a 45 to 60% increase in distillation flux compared to commercial polytetrafluoroethylene (PTFE) and polyethylene (PE) membranes in normal desalination where the feed water consists of pure salt water.

Membrane fouling and wetting are the major challenges for the long-term MD process. After achieving successful results with standard desalination, NF-coated PES membranes were selected to study the anti-fouling and anti-wetting performance. One of the principal membrane foulants in wastewater treatment has been identified as protein-like molecules. Because of the significant foulant-membrane affinity, the hydrophobic membrane surfaces

exhibit an exceptionally high potential to become fouled by proteins during the MD process. To examine anti-fouling effectiveness, bovine serum albumin (BSA) is used as a model organic foulant protein. The surface morphology of membranes exposed to BSA was studied using a scanning electron microscope, and the amount of BSA adsorbed on the membrane surface was measured in real-time using confocal microscopy. We also studied the BSA fouling in MD by comparing the distillation flux and salt rejection for hydrophobic PTFE membranes, and superhydrophobic NF-coated membranes. The presence of low surface tension impurities in the feed solution, such as surfactants, causes membrane wetting during MD fouling. Sodium dodecyl sulfate (SDS) is employed as a model contaminant for low surface tension foulant in this investigation. To evaluate SDS fouling, the presence of SDS on the membrane surface was investigated using Fourier transform infrared spectroscopy (FTIR). The manufactured composite NF-coated PES membranes have a superhydrophobic surface with strong anti-fouling and anti-wetting properties, indicating a viable application for MD. In comparison to standard PE and PTFE membranes, we found that NF-coated PES membranes had little or no adsorption of BSA protein. In the case of surfactants, we investigated the wetting qualities of membranes in the presence of SDS, and NF-coated PES membranes outperform conventional PE and PTFE membranes in terms of liquid repellency.

2. Fabrication of superhydrophobic porous membrane

This chapter describes a reliable fabrication technology to create a new class of non-fluorinated superhydrophobic robust membranes for distillation. Using this technique, silicone nanofilaments are coated on commercial polyethersulfone (PES), cellulose acetate (CA), polyvinylidene fluoride (PVDF), and polytetrafluoroethylene (PTFE) membranes with various pore sizes.

Major issues in MD involve low permeate flux, membrane pore wetting, long-term stability, and membrane fouling. To enhance the MD efficiency, an ideal membrane should maximize the membrane pore size and porosity, leading to high distillation flux and requiring fewer materials for manufacturing. However, in conventional membranes, increasing pore size is limited (to typically ≤ 0.2 µm) to maintain the required high liquid entry pressure (LEP) to prevent membrane wetting. Here, LEP is the minimum pressure required by the liquid for entering the membrane pores and the LEP value should be as high as possible to prevent membrane wetting. As these two points contradict each other, our approach is to use commercial core membranes with larger pore sizes and then add a much thinner superhydrophobic layer of silicone nanofilaments (NFs) on both sides as shown in Figure 12 to form the multiscale porous membrane [126-128]. Hence the microporous inner layer gives higher flux and the nanoporous outer layer improves the wetting resistance.

In the emerging field of membrane distillation, PTFE and PE membranes are commonly used due to their stable hydrophobic surface chemistry. We have therefore chosen such membranes as reference standards. This study uses DCMD and AGMD configurations to compare the novel NF-coated membranes with commercial PTFE and PE membranes.

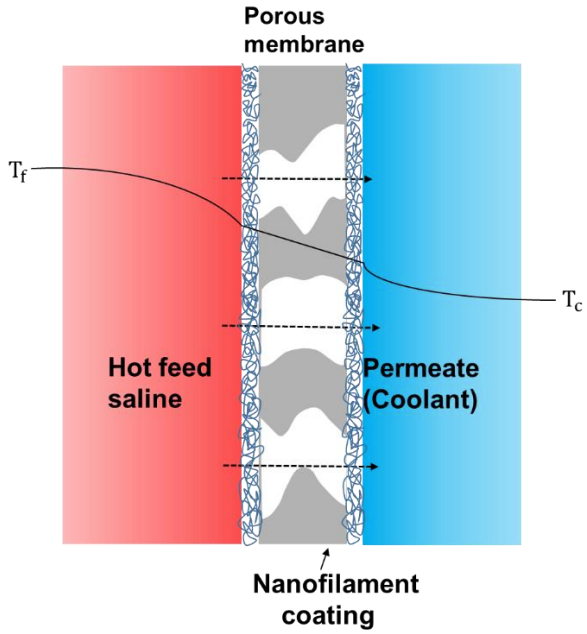

Figure 12: Design of multi-scale porous membrane with nanofilament coating

For creating the superhydrophobic coating on commercial membranes, polysiloxane NFs were grown on the surface via the hydrolysis of trichloromethyl silane (TCMS). To fabricate a homogeneous water-repellent layer of nanofilaments, the membrane surface needs to be hydrophilic. The presence of polar functional groups and hydroxyl groups on the surface is required.

For fabrication, the commercial membranes are first activated via oxygen plasma (Diener electronic GmbH & Co KG - Plasma-Surface-Technology, Germany) with the following parameters, 90 W for 2 min at a flow rate of 6 cm^3/min to create hydroxyl groups on the surface. After plasma activation, the hydrophilic membranes are immersed in an organic solvent containing TCMS and trace amounts of water. By judiciously adjusting the water content in the solvent to 180 ppm, TCMS can hydrolyze in a proper manner. These hydrolyzed silane molecules then react with the hydroxyl groups on the membrane surface and induce a surface polymerization of polysiloxanes, forming silicone NFs (Figure 13). The methyl groups on the NF surface make them a low surface energy material. Furthermore, the coiled and interwoven structure of nanofilaments leads to an overhanging morphology with inward curvature. This combination of low surface energy and surface topography renders the NF-coating superhydrophobic and can stabilize an air cushion below the liquid-solid interface and maintain the so-called Cassie–Baxter wetting state.

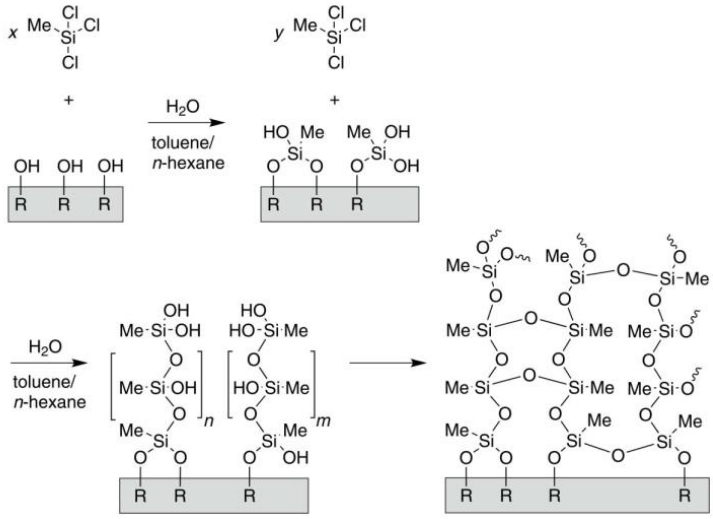

Figure 13: Reaction mechanism for nanofilaments formation on the surface

In the initial part of the study, we successfully coat the nanofilaments on commercial hydrophilic membrane PES. The nominal pore diameter (average pore diameter according to manufacturer specifications) of the PES membranes ranges from 0.1 µm to 8 µm, which is suitable for developing multilayer membranes with hierarchical pore sizes. For convenience, the notation “Membrane material - Nominal pore diameter”, e.g. PES-8 for PES membranes with 8µm pore size will be used throughout this thesis. After achieving successful results on hydrophilic PES membranes, we implemented similar coatings on hydrophilic CA, hydrophobic PVDF, and PTFE membranes.

The porous hydrophilic membranes used in this study were PES membranes which were provided by Sterlitech corporation with a nominal thickness of 110-150 µm and hydrophilic CA membranes were supplied by Dorsan filtration and labsolute. Also, hydrophobic PVDF membranes were supplied by Dorsan filtration and hydrophobic PE membranes were supplied by Solupor membrane (Lydall performance materials). PTFE membranes were supplied by Donaldson filtration solutions. The average thickness of the PE membrane is 110 µm and the mean pore size is 0.2 µm. The PTFE membranes have polypropylene (PP) as a substrate, the total average thickness is of 150 µm and the mean pore size is of 0.2 µm.

2.1 NF coating on PES membrane

As shown in Figure 14, the NF on PES membranes forms a network structure covering the top surface of the membrane completely including the large pores. Even for a PES-8 membrane with a nominal pore diameter of 8 µm, the NFs still can cover the majority of the openings on the top surface.

Figure 15 shows the cross section image of NF-coating on the PES-8 membrane. We can clearly observe a layer of NFs created on top of the membrane. Growth of NFs within the inner porous structure does occur as well, but the formed inner coating is sufficiently thin to avoid a significant change in membrane porosity and pore size. This low coating coverage inside the membrane may originate from a lower efficiency of plasma treatment within the membrane and a lower growth rate due to the longer diffusion distances for hydrolyzed silane. As the maximum thickness of the NF layer is ~500 nm, we can expect that the inner coating will not strongly hinder the vapor diffusion inside the membranes.

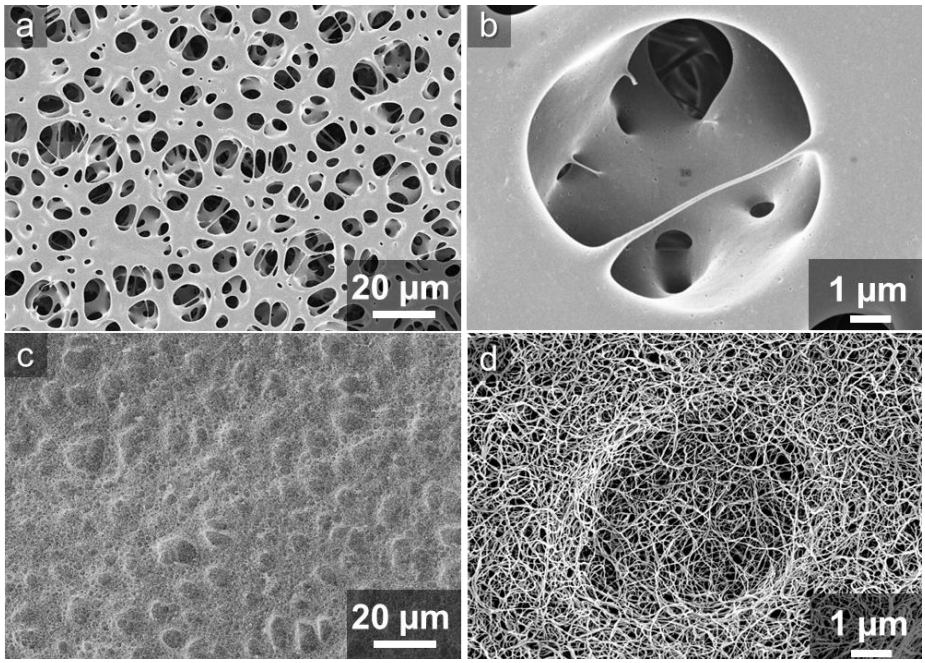

Figure 14: SEM images of (a, b) original PES-8 membranes with pore size of 8 µm and (c, d) nanofilament coated PES-8 membrane. Images b and d are magnified versions of a, and c respectively.

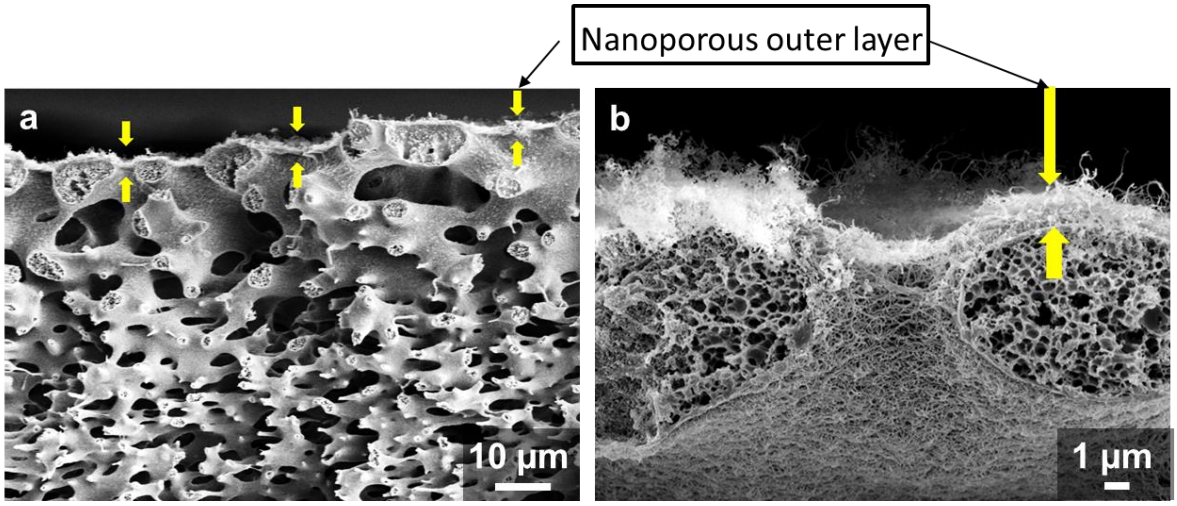

Figure 15: SEM images showing the (a, b) cross section of nanofilament coated PES-8 membrane. Images b is magnified view of a.

2.2 NF coating on CA membrane

After having successful coated nanofilaments onto PES membranes, our next target was to try coatings on other hydrophilic membranes to prove the universality of our approach. Cellulose acetate (CA) membranes with different pore sizes ranging from 0.22 µm to 5 µm were used. Even in case of CA membranes, they demonstrate the similar results of NF-coating morphology compared with the PES membranes (Figure 16). However, we note that some surface openings cannot be perfectly covered by the network of nanofilaments, probably owing to the different original surface topography of CA membranes.

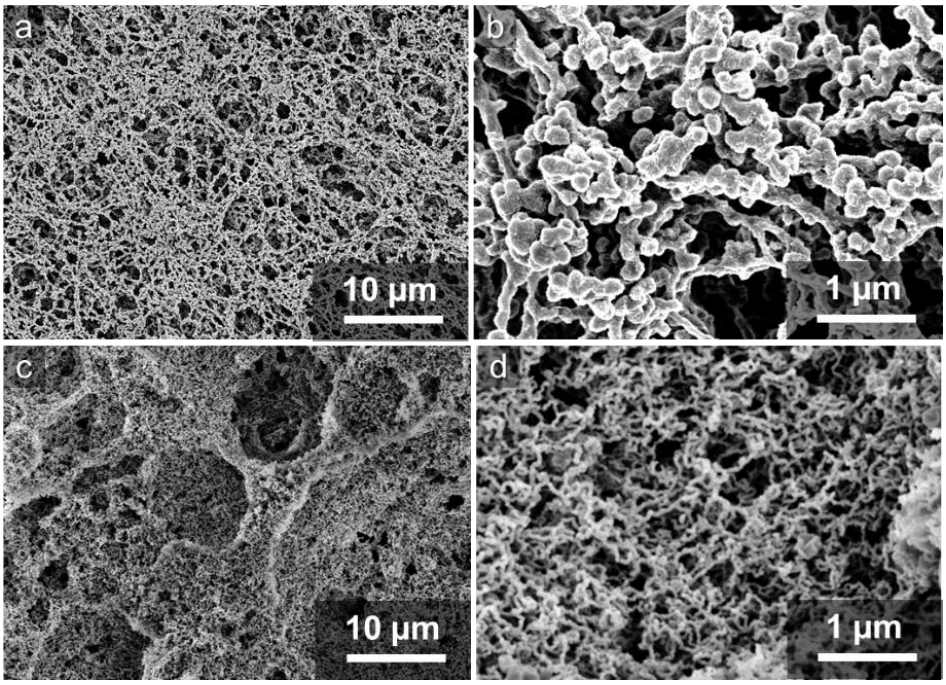

Figure 16: SEM images of (a, b) original CA-5 membranes with pore size of 5 µm and (c, d) nanofilament coated CA-5 membrane. Images b and d are magnified versions of a, and c respectively.

2.3 NF coating on hydrophobic membranes

Similar coatings were then studied on hydrophobic membranes such as PVDF (Figure 17) and PTFE (Figure 18). SEM images show a morphology identical to hydrophilic membranes PES and CA covering majority of the pores. As a result, it is obvious that these coatings are fairly general and easy to apply to diverse materials.

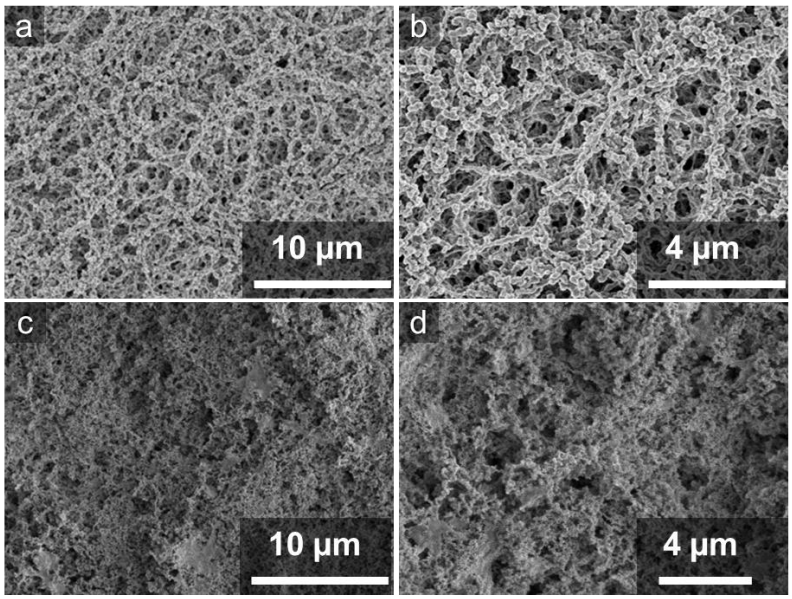

Figure 17: SEM images of (a, b) original PVDF-0.45 membranes with pore size of 0.45 µm and (c, d) nanofilament coated PVDF-0.45 membrane. Images b and d are magnified versions of a, and c respectively.

PTFE membranes are chemically stable and inert in general, making them acceptable for use with harsh organic solvents, strong acids, and alkalis. As a result, we sought to see if the PTFE membrane substrate promotes NF development following treatment with oxygen plasma. Surprisingly, the morphology of NFs covering the membrane surface was comparable also in case of PTFE membranes (Figure 18).

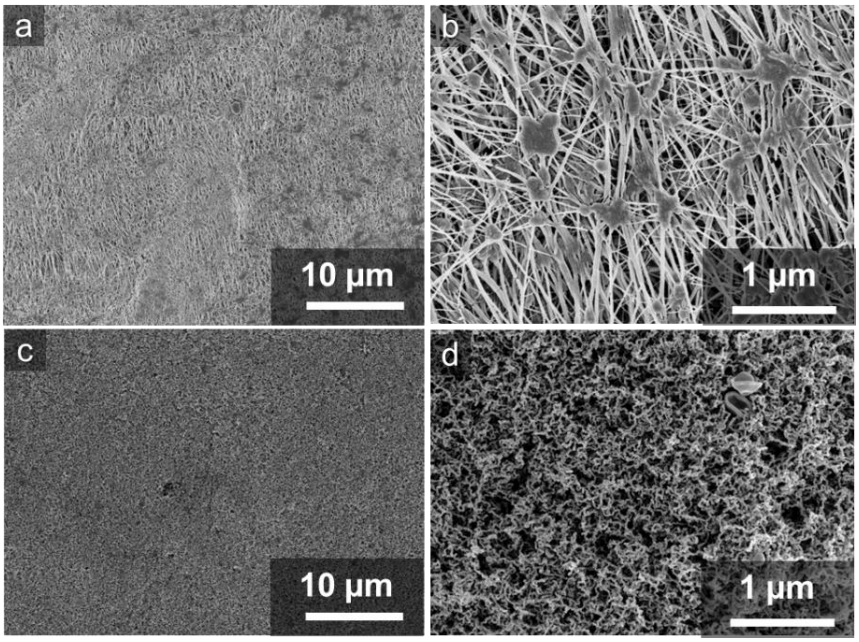

Figure 18: SEM images of (a, b) original PTFE-1 membranes with pore size of 1 µm and (c, d) nanofilament-coated PTFE-1 membrane. Images b and d are magnified versions of a, and c respectively.

The optimized manufacturing conditions for various core membranes is identified after repeated testing and modification, as shown in Table 1.

Table 1: Fabrication protocol for all membranes

Membrane material	Pre-treatment	Solvent	Concentration of TCMS	Reaction time
PES	O_2 plasma, 90W for 2 min, 7 sccm oxygen flow rate	1:1 mixture of saturated heptane (water content: 90 ppm) and toluene (water content: 270 – 275 ppm)	0.2 ml TCMS per 100 ml solvent	16 hours
PVDF		Toluene (water content: 165 – 170 ppm)	0.1 ml TCMS per 100 ml solvent	
PTFE				
CA	Hexane rinse for 2min			

3. Membrane characterization

3.1 Characterization methods

3.1.1 SEM

Membranes to be tested were imaged by scanning electron microscope (SEM) Zeiss LEO 1530 Gemini SEM and to improve conductivity samples were coated with a 7 nm platinum layer using CCU-010 compact coating unit.

3.1.2 Gas permeability test

Gas permeability test is employed to analyze the mass transfer resistance of NF-coated membranes [129]. The experimental apparatus used for the measurements is shown in Figure 19 b. The membrane to be tested is mounted on the membrane holder (Figure 19 a) which was connected to the nitrogen source. When nitrogen flows through the tested membrane, the transmembrane pressure was measured by manometer and permeation flux was obtained by precise flow sensors (SMC Deutschland GmbH, PFMV505-1 and PFMV530-1). In this study, we characterized the gas permeability of tested membranes with effective area of 63 mm^2 under transmembrane pressures from 0 to 70 mbar.

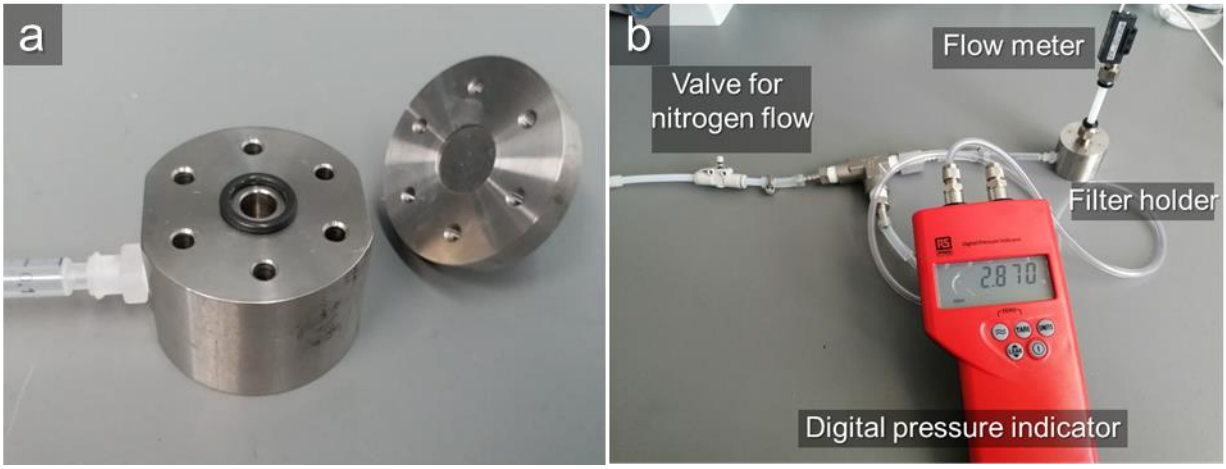

Figure 19*:* (a) Filter holder (b) Image of gas permeability testing setup.

3.1.3 Liquid entry pressure (LEP) test

The liquid entry pressure (LEP) is defined as the minimum transmembrane pressure that is required for the feed solution to penetrate the membrane pores. Therefore, the hydrostatic pressure during operation should be lower than LEP to avoid membrane wetting [130]. LEP is a significant characteristic of MD membranes and should be as high as possible. The pressure depends on the pore size, the hydrophobicity, and the surface morphology of the membrane.

In this work, LEP of tested membranes was measured by using a custom designed apparatus (Figure 20 a). The membrane is mounted inside a filter holder, which connects to a syringe pump. By pumping the salty water into the holder with a very low and constant flow rate (1

mL/min), the hydrostatic pressure applied on the tested membrane gradually increases. The pressure was monitored using a pressure sensor and the data was recorded using a data acquisition system (Figure 20 b). Once the applied pressure exceeds the capillary pressure of the membrane pores, liquid penetrates the membranes, leading to a pressure drop. The obtained peak in the pressure vs. time plot value gives the LEP of tested membrane.

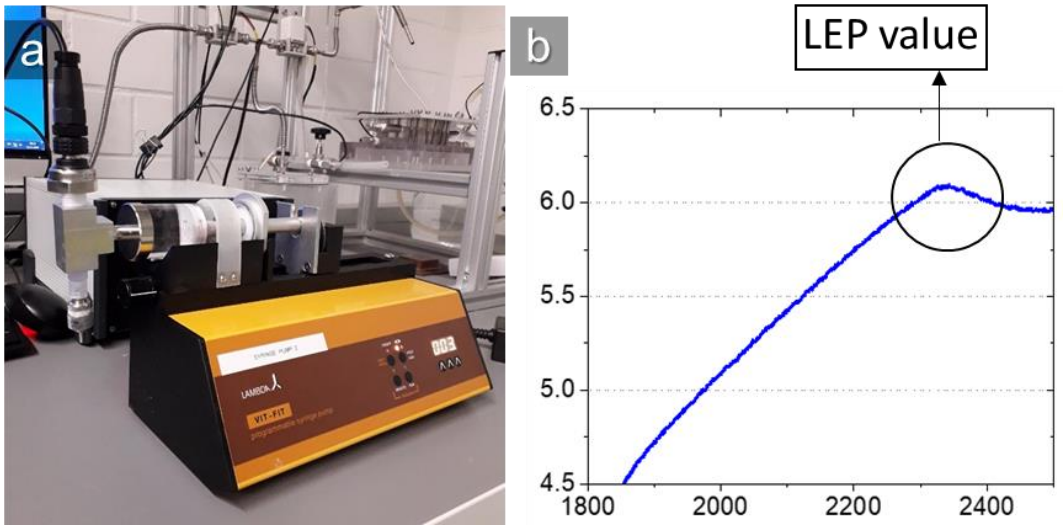

Figure 20*:* (a) Schematic of LEP testing setup (b) Image of LEP testing setup. (c) Pressure in membrane holder as a function of time during a typical liquid infusing process.

3.1.4 Contact angle

The water contact angle on tested membranes (PE, PTFE, fluorinated, and NF-coated hydrophilic membranes) is measured to characterize the surface wettability. The static contact angle and droplet sliding angle of a water droplet with a volume of 5 µl were measured using the DataPhysics OCA35 goniometer. The static contact angle and sliding angle were determined by 3 – 5 individual measurements at different positions of each samples.

3.1.5 AGMD setup

For testing the performance of our membranes, our Air Gap Membrane Distillation (AGMD) setup was used. The operating parameters of all AGMD tests are listed in Table 2. The temperatures and flow rates of feed and cooling water are chosen based on the recommendation values in a pilot AGMD system and literature studies. All the MD experiments were carried out over 48 hours to test the membrane durability for long-term operation.

Table 2*:* Operating parameters for AGMD tests

Variables	Value	Units
Feed temperature, T_f	75-80	°C
Feed flow rate, $\dot{V}_f$	1	L/min
Coolant temperature, T_c	15-20	°C
Coolant flow rate, $\dot{V}_c$	2.0	L/min
Air gap width, δ_g	3.5	mm
Effective membrane area, *A*	19.22	cm^2
Concentration of NaCl	3.5	wt%
Feed conductivity @ 22 °C, σ_f	54	mS/cm
Test duration, *t*	48	h

AGMD tests were carried out with the use of a custom-built AGMD setup that included an AGMD module, feed water and coolant circulating loops, a digital balance, a conductivity meter, and a data collecting system (Figure 21). The membrane under test was installed in the AGMD module between a feed flow channel and a condensing surface. A 0.5 mm thick support mesh was utilized to keep the membrane in a planar shape and decrease membrane deformation caused by the pressure differencel between the feed flow and the air gap. To establish the requisite air gap in the MD module, an acrylic spacer was employed. The overall width of the air gap between the membrane and the condensing surface was 3.5 mm.

Using a magnetic coupling water pump, feed saline water was heated to the required temperature and fed to the AGMD module. The coolant flow loop used a chilled water bath circulator to manage the condensing surface temperature (F25-HE, Julabo). Distilled water was collected in a glass flask as it slid down the condensing surface by gravity. For calculating the distillation flow of tested membranes, a digital balance (SPX 2202, Ohaus) continually recorded the weight of collected distilled water. The conductivity meter was used to measure the conductivities of feed and distilled water in order to calculate salt rejection during membrane distillation.

To monitor the liquid temperature at the inlet and exit of the feed flow channel and coolant flow channel, four Pt100 temperature probes (PM-1/10-1/8-6-0-P-3, Omega) were used. To continually monitor the flow rate and pressure in the feed and coolant loops, two flow meters (FT110, Gems) and two pressure transducers (IPSLU-M12, RS-Pro) were put in the pipelines. The AGMD testing setup's sensors were all electrically coupled to a data collecting system comprised of two National Instruments (NI) analog input modules (PCI 6251 and NI-9216). During the MD tests, the measured data was sent to the computer, which could be watched in real-time and saved using self-written LabView programs.

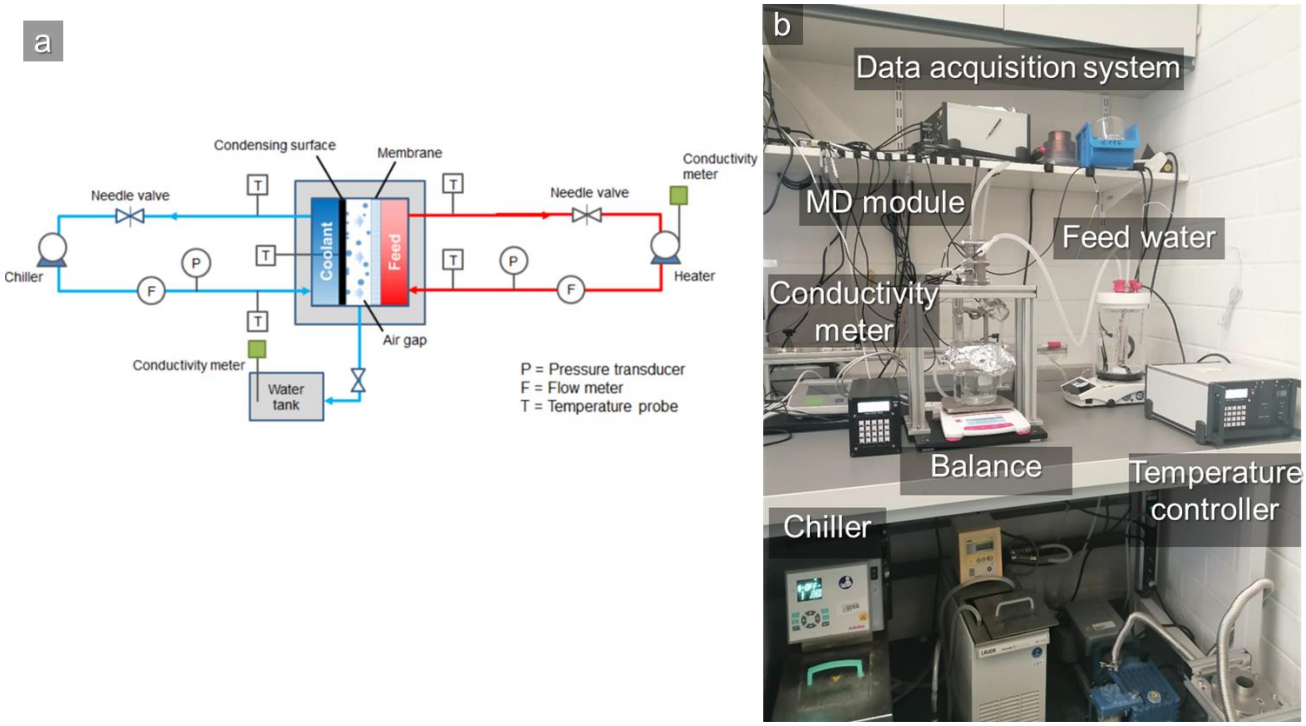

Figure 21*:* (a) Schematic of the air gap membrane distillation (AGMD) testing system.(b) Air gap membrane distillation testing setup

3.1.6 DCMD setup

The acrylic gap spacer and condensing surface from the MD module were removed and replaced by a silicone rubber gasket on both sides of the membrane to prepare the DCMD configuration. This puts the membrane under test in direct contact with the salty feed water on one side and the cooling water on the other side. In the case of DCMD, the distilled water produced goes directly into cooling water tank. As a result, the distillation flux is calculated from the increase of the water level in the cooling water tank during the experiment. All of the other sensors were identical to the ones used in the AGMD configuration.

It should be emphasized that all of these characterization configurations were developed by postdoctoral researcher Dr. Youmin Hou during his stay at MPIP.

3.2 Results and discussion

3.2.1 Gas permeability data

The additional layer of NFs on the membrane surface could create significant mass transfer barrier for vapor diffusion in NF-coated membranes. So it is not a priori clear, if the comination of NF layers with large pore size core membranes can give higher overall flux compared to standard commercial MD membranes Therefore, to get a first impression of the possible mass transfer for the different membranes, we measured the gas permeability of bigger pore size NF-coated membranes, commercial PE-0.2, and PTFE-0.2 membranes before carrying out the more complex and time-consuming MD distillation experiments.

PES membrane

Figure 22 depicts the observed gas permeation flow vs transmembrane pressure for commercial PE-0.2 and PES-3 membranes before and after nanofilament coating. The permeation flux of nanofilament coated PES-3 membranes is 60% lower than that of virgin PES-3 membranes. Because of the large pore size of the inner part, NF-coated PES-3 membranes displayed ten times higher nitrogen flow than the ordinary PE-0.2 membrane. When paired with high pore size core membranes, the improved gas permeability of NF-coated PES membranes demonstrates that the nanofilament coating not only improves the non-wetting quality of the membrane surface but also ensures a sufficiently low mass transfer resistance for effective vapor transport.

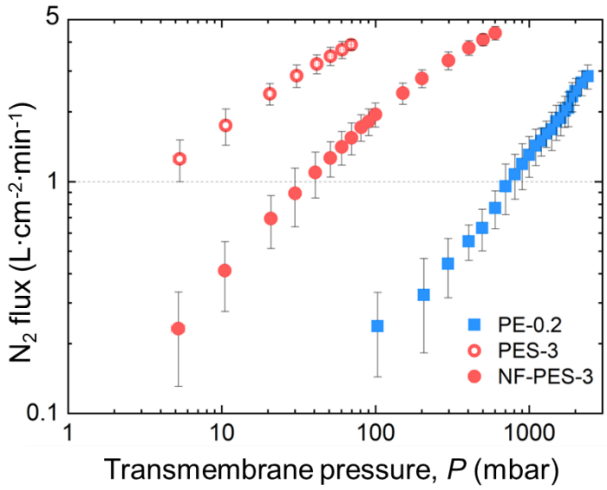

Figure 22: Gas permeation flux as a function of flow pressure for PE-0.2 and NF-coated PES membranes.

CA membrane

Using the same setup shown in Figure 19, gas permeability data for CA membranes were obtained. Figure 23a shows the measured gas permeation flux as a function of the transmembrane pressure for CA membranes before and after nanofilament coating. For CA-5 membranes, the permeation flux is reduced by 30% due to nanofilament coating. Still because of larger pore size of inner section, NF-coated CA-5 membranes show approximately 8 times more nitrogen flow compared to the commercial PE-0.2 membrane (Figure 23 b). The enhanced gas permeability of NF-coated CA membranes indicates that the composite membrane with nanofilament coating and CA core membrane can ensure a low mass transfer resistance for efficient vapor transport.

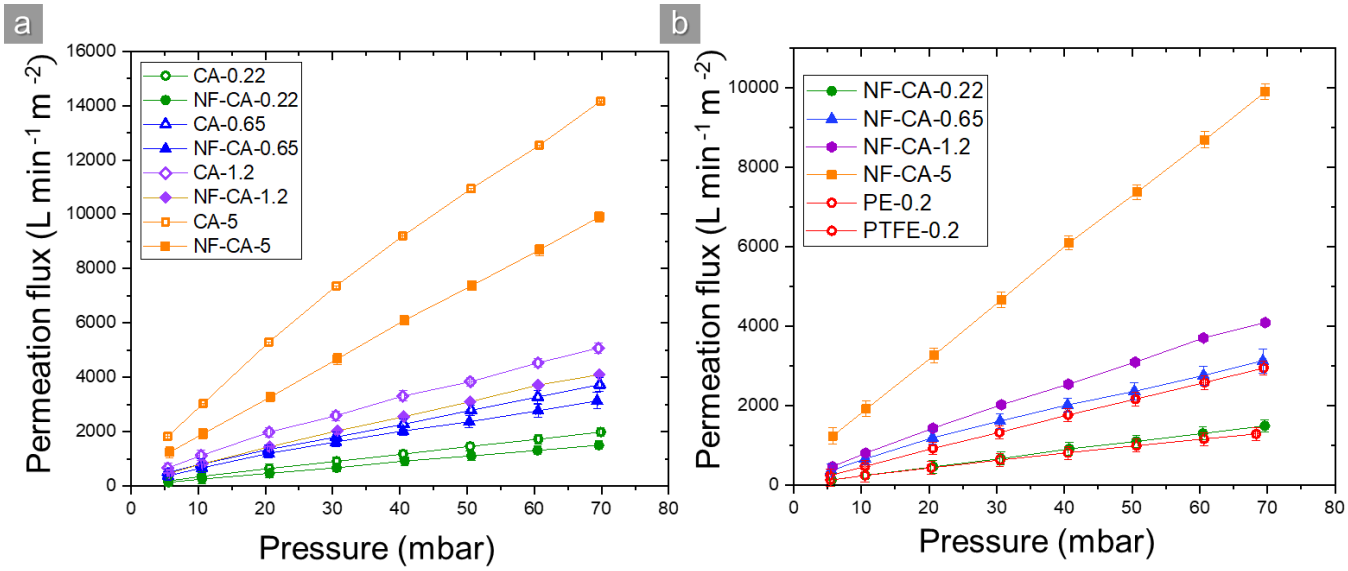

Figure 23: Gas permeation flux as a function of flow pressure for (a) CA membranes before and after NF coating (b) for NF-coated CA membranes in comparsion to commercial PE-0.2 , PTFE-0.2 membranes.

PTFE membrane

Later also NF coated PTFE membranes were evaluated for gas permeability and compared with original ones. The permeation flux of NF-PTFE-1 is nearly double that of PTFE-0.2 (Figure 24).

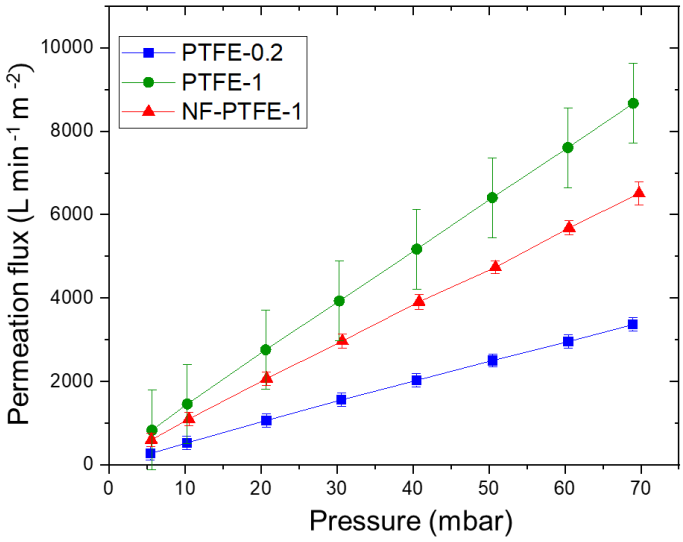

Figure 24: Gas permeation flux as a function of flow pressure for PE-0.2 and NF-coated PES membranes.

The increased gas permeability of all NF-coated membranes with different substrates indicates that the nanofilament coating not only improves the membrane surface's nonwetting feature but also ensures a sufficiently low mass transfer barrier for effective vapor diffusion.

3.2.2 LEP data

LEP is the key parameter in membrane distillation to determine how wettable a membrane is to different liquid solutions. After verifying that NF-coated membranes have greater gas permeation flux than commercial hydrophobic membranes, the wetting resistance of these membranes is tested. As with hydrophilic membranes, they would get wet rapidly as water is absorbed by the membrane. Therefore, the hydrophilic membranes are first fluorinated and then compared to NF-coated and commercial membranes.

PES membrane

NF-coated PES-0.1 and PES-1.2 membranes exhibited extremely high LEP which exceeded the limit of our testing setup (11.5 bar). As the pore size of NF-PES membranes increases to 3 µm, the LEP of NF-coated membrane gradually goes down but stays above 4 bar for all cases. The reason for a decrease in LEP value can be due to the imperfect growth of nanofilaments with larger pore sizes. Also, the effective pore diameter of the NF-PES-3, NF-PES-5, and NF-PES-8 membranes was still smaller than 0.3 µm according to the theoretical estimation of the Young-Laplace model. LEP values of all NF-coated PES membranes are well above the safety threshold values which is 2 bar (below threshold values the membranes will be more susceptible to wetting) hence they can easily be used for MD (Figure 25).

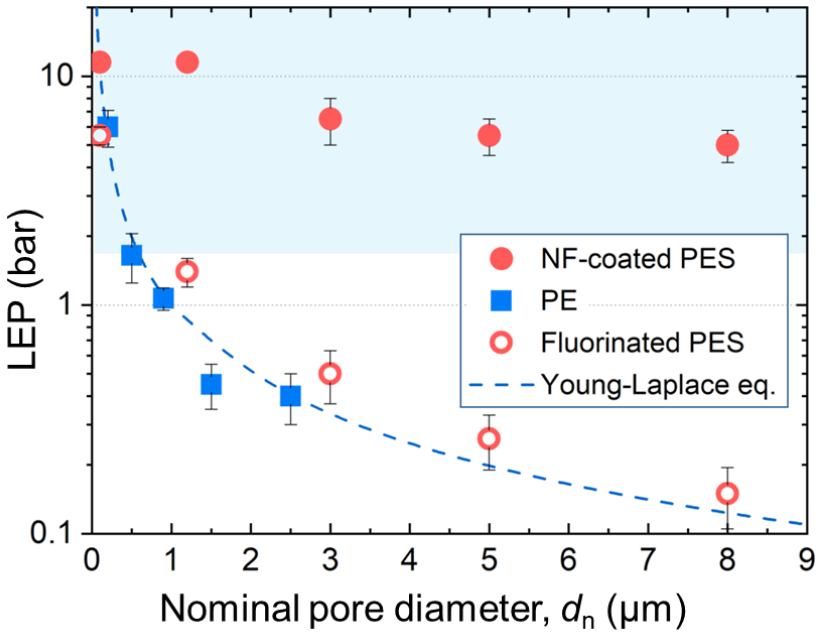

Figure 25: Liquid entry pressure as a function of nominal pore diameter for the nanofilament-coated PES, PE, and fluorinated PES membranes. The dashed line denotes the theoretical prediction of LEP for single-scale porous membranes from the Young-Laplace equation.

CA membrane

Nanofilament coated CA membranes exhibited LEP values well above the safety threshold value of 2 bar except for CA-5 with the largest pore size. For LEP values of less than 2 bars, there is some risk of membrane wetting during the distillation operation.

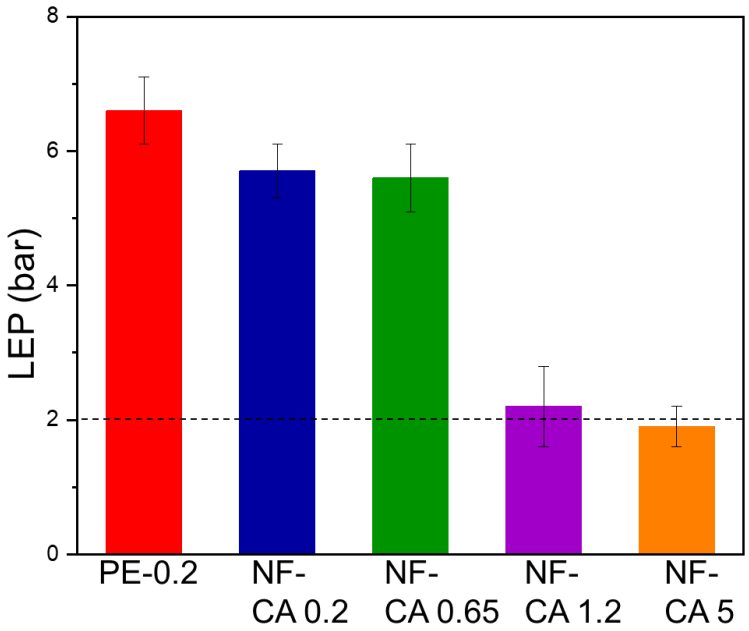

Figure 26: LEP values for commercial PE-0.2 and nanofilament coated CA membranes with different pore sizes

PVDF & PTFE membranes

The LEP values show that NF-coating significantly enhances the wetting resistance of hydrophobic membranes (Figure 27). In this respect, hydrophobic membranes with larger pore sizes may be used in MD to produce higher distillation flux. As PVDF membranes were hydrophilic in nature when supplied by the supplier, they were fluorinated and then used for LEP testing.

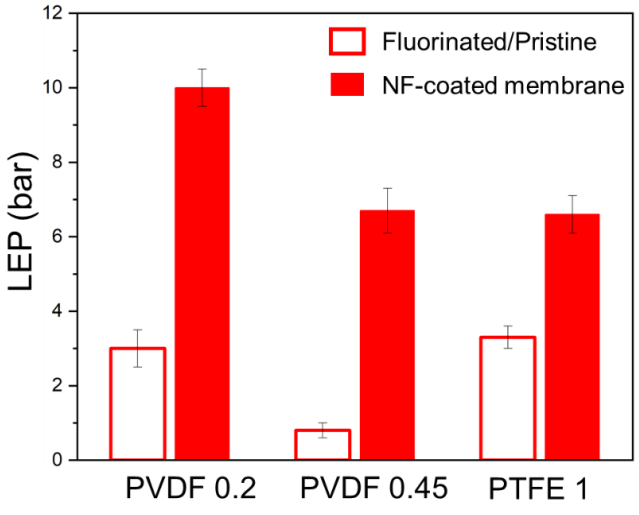

Figure 27: LEP values for original and NF-coated hydrophobic PVDF and PTFE membranes

3.2.3 Contact angle data

Water contact angle and sliding angle were measured on all the membranes. However, in the case of a hydrophilic membranes, they were fluorinated before the measurement. Fluorination and NF-coating have been shown to efficiently lower the surface energy of hydrophilic membranes. All the NF-coated PES, PVDF, and CA membranes exhibit the same super-water repellency after being coated with nanofilaments (Table 3). When compared to fluorinated membranes, the NF-coated membranes exhibit exceptionally low sliding angles indicating that NF coating can not only have a smaller structure but also a lower surface energy. However the fluorinated membranes are not superhydrophobic because the surface energy is not low enough.

Table 3: Contact angle measurement of tested membranes

Sample		**Contact angle / °**	**Sliding angle / °**
PE-0.2		129 ± 3	42 ± 5
PTFE-0.2		140 ± 2	25 ± 6
Fluorinated	PES-1.2	136 ± 3	sticking / no sliding
	PVDF-0.2	148 ± 2	55 ± 1
	CA-0.2	139 ± 2	60 ± 1
NF-coated	PES-1.2	155 ± 2	< 1
	PVDF-0.2	156 ± 2	< 1
	CA-0.2	155 ± 2	< 1

3.2.4 Durability of membranes

Immersion in Milli-Q @ RT

To verify the long-term stability of PE, PTFE and NF-coated membranes, they were immersed in Milli-Q water at room temperature for as long as 30 days. Hydrophobic PE and PTFE membranes were used as a comparison with NF-coated membranes by evaluating the degradation in their wetting properties after 7 days and 30 days. The membranes to be tested were dried under nitrogen stream and used for measuring water apparent receding contact angle θ_r^{app} and contact angle hysteresis θ_{CAH}. After 7 days of immersion, the commercial PE and PTFE membranes exhibit clear degradation in their wetting properties. For hydrophobic PE membranes the θ_r^{app} deteriorates from ~98° to ~40° (Figure 28 d), indicating the considerable loss of liquid repellency. Likewise, the rising of θ_{CAH} on PE membranes also reflects the increasing hydrophilicity on surface. For hydrophobic PTFE membranes, θ_r^{app} also deteriorates from ~116° to ~64° along with increasing θ_{CAH} to ~75°. However the nanofilament coated membranes maintained their super liquid-repellency with θ_r^{app} > 150° and θ_{CAH} less than 10° (Figure 28 e).

Subsequently after 30 days of immersion test, the commercial PE and PTFE membranes degrade further with θ_r^{app} of ~12° and ~45° and θ_{CAH} of ~84° and ~75°, respectively, indicating complete loss of surface hydrophobicity. Nanofilament coated membranes show loss of superhydrophobicity with θ_r^{app} of ~121° and θ_{CAH} of ~35° (Figure 28 g,h,i), but are still very hydrophobic.

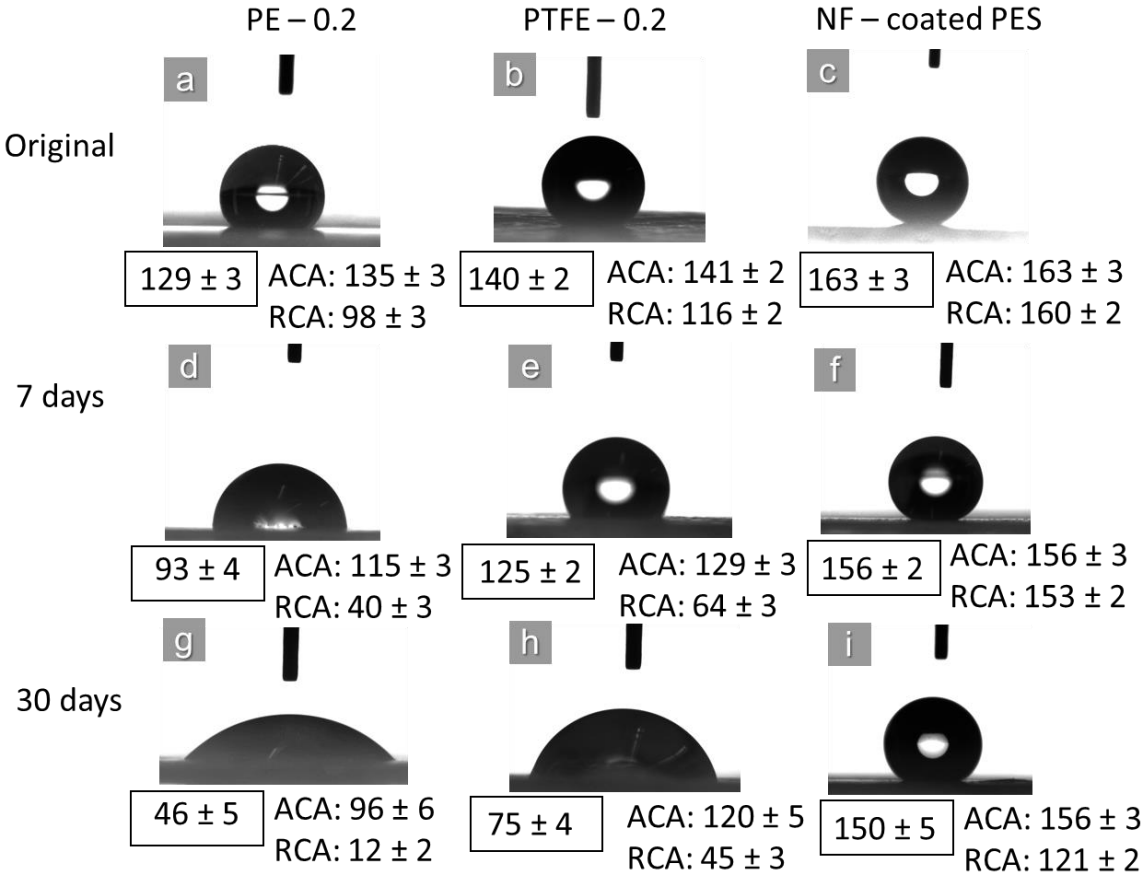

Figure 28: Membrane surface before (a,b,c) and after 7 days (d,e,f) , 30 days (g,h,i) immersion in Milli-Q water at room temperature

Immersion in distilled water at 80 ^{0}C

Membranes must be in contact with hot water for hours or days during MD desalination, which might change their physical characteristics and surface chemistry [131, 132]. PE, PTFE, and NF-coated PES membranes were submerged in Milli-Q water at 80 °C for up to 1 month to assess the potential deterioration of membrane surfaces. After immersing membranes for 7 days, 15 days, and 30 days and drying the membrane surfaces under a nitrogen stream, we evaluated the apparent receding contact angle θ_r^{app} for water and the contact angle hysteresis θ_{CAH}.

It was obvious that the hydrophobic PE membrane loses its hydrophobicity when immersed in Milli-Q water at room temperature; however, it was surprising to see that after 7 days of immersion at high temperatures, even the hydrophobic PTFE membrane begins to degrade and loses its hydrophobicity with a θ_r^{app} of 42 °, which decreases to 25 ° after 1 month, with θ_{CAH} of ~ 90 ° only after 7 days of immersion. NF-coated membranes, on the other hand,

are still hydrophobic with θ_r^{app} of 138 ° and θ_{CAH} of ~ 12 ° after 30 days of immersion (Figure 29).

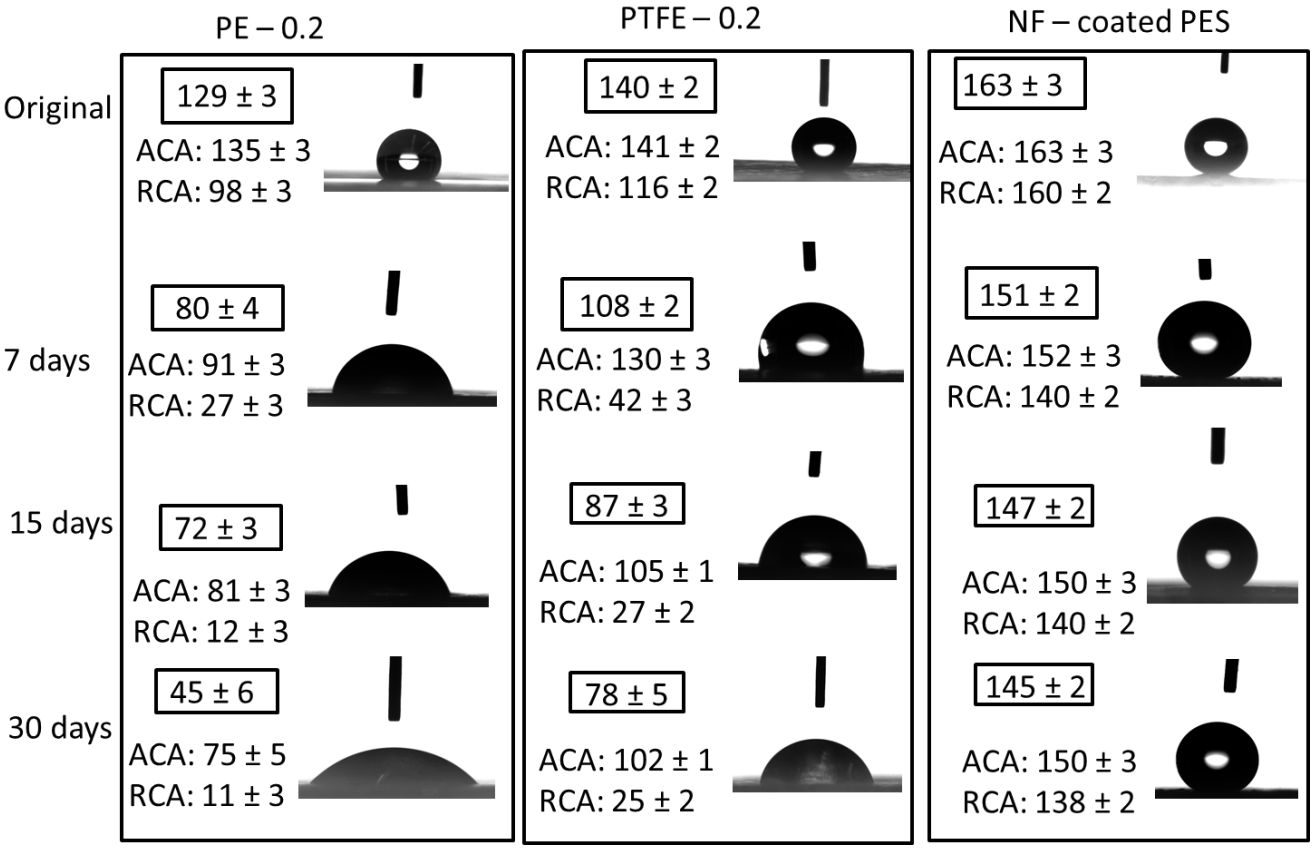

Figure 29: Membrane surface before and after 7 days, 15 days, and 30 days immersion in Milli-Q water at 80 °C.

Immersion in salt water @ 80 ^{0}C

Following the investigation of the impact of immersion in Milli-Q water at high temperatures, the membranes were submerged in NaCl water at the same concentration as seawater (35 g/l). In this circumstance, the hydrophobicity of all membranes degrades considerably quicker.

Unexpectedly, the θ_r^{app} of PTFE membranes reduces to ~ 33 ° in 7 days which falls even more to ~ 19 ° in 1 month. In this case, even NF-coated membranes show degradation with θ_{CAH} of > 85 °. It seems that the salt ions present in water increases the process of hydrophobicity loss, and quicker deterioration of the membranes (Figure 30).

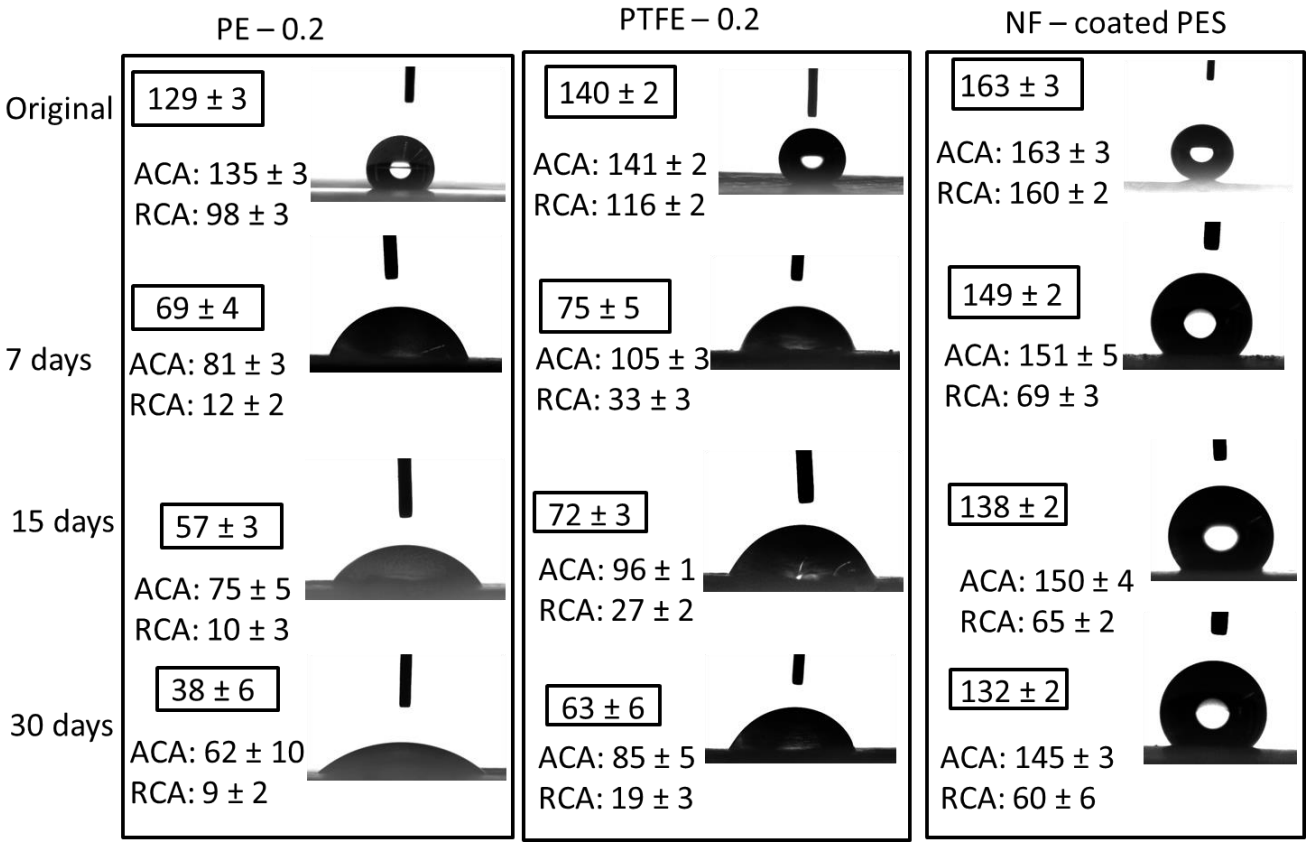

Figure 30: Membrane surface before and after 7 days, 15 days, and 30 days immersion in salt water at 80 ^{o}C.

Exposure to acid conditions (18% HCl)

MD is one of the potential membrane processes that is still being researched [25, 101]. In order to check the chemical stability of NF-coated membranes in harsh conditions like acids, we examined the deterioration of wetting characteristics of NF-coated PES, NF-PVDF, and NF-PTFE membranes after 3 hours immersion in 18% HCl solution. The NF-PTFE and NF-PVDF membrane exhibits no pinning of a water droplet even under extreme circumstances (Figure 31 b, c). However, NF-PES membrane shows unambiguous pinning of a droplet to the membrane surface (Figure 31 a). This leads to the conclusion that the surface chemistry of nanofilament coated hydrophilic substrate PES appears to be more influenced than PVDF and PTFE. To investigate further, other tests such as SEM/EDX and FTIR must be performed.

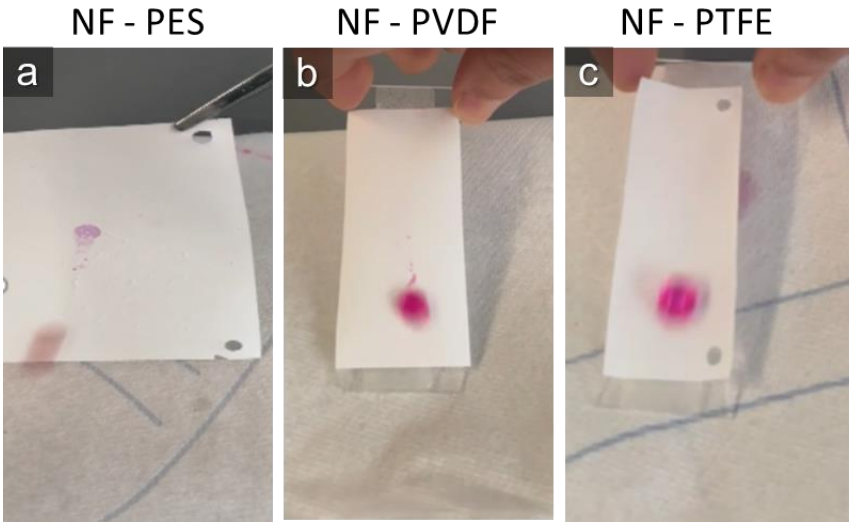

Figure 31: Membrane surface before and after 7 days, 15 days, and 30 days immersion in salt water at 80 ^{o}C.

3.2.5 AGMD performance

3.2.5.1 PES membrane

To compare the distillation performance for different membranes, we plot the correlation between the distillation flux and water conductivity (Figure 32 a). It is vital to monitor the conductivity of the water produced on a regular basis, since an increase in conductivity indicates a salt leak into the permeate side. Depending on the amount of leak, the distillation flux may rise. All the NF-coated PES membranes show a high salt rejection during 48 hours MD test with a feed temperature of 80 ^{o}C and coolant temperature of 20 ^{o}C . The conductivity of collected water fully meets the criteria of distilled water (0.5 to 3 µS/cm). The MD fluxes of NF-coated PES membranes rise obviously with an increasing nominal pore size of the original membranes. When the nominal pore diameter of the NF-coated PES membrane increases to 5 µm, we observe a significant increase in distillation flux, which is more than 80% higher than the NF-coated PES-0.1 membrane. Compared with the MD flux of commercial PTFE-0.2 membrane (11.0 L m^{-2} h^{-1}), the NF-coated PES-5 membrane also shows 40% enhancement of distillation rate (15.6 L m^{-2} h^{-1}). The NF-coated PES-8 membrane also demonstrates a durable desalination performance (permeate conductivity = 1.36 µS/cm), as the LEP (5 bar) is well above the threshold value (1.5 bar). Owing to the large porous paths inside the membrane, the NF-coated PES-8 membrane achieves 60% higher MD flux than the commercial PE-0.2 reference membrane. On the contrary, all the fluorinated PES membranes show leaking issues with salty feed water penetrating during distillation process. Although the LEP values of the fluorinated membranes are higher than the hydrostatic pressure of feed flow, the conductivity of permeate water with values ranging from 400 µS/cm to 13500 µS/cm clearly indicates salt penetration. The experimental results shown in Figure 32 a clearly demonstrate that our nanofilament coating is capable of converting the hydrophilic polymeric membranes into superhydrophobic membranes with excellent membrane distillation performance.

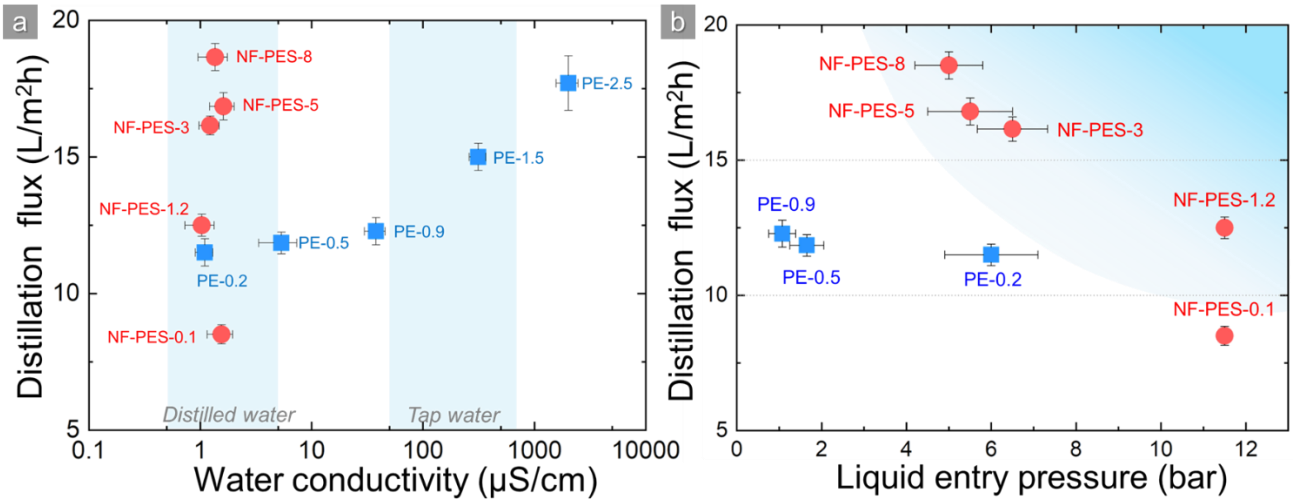

Figure 32: (a) Experimental distillation flux as a function of conductivity of produced water for 48-hour MD test. (b) Distillation flux as a function of liquid entry pressure for the commercial PE benchmark membranes

The ideal membrane for distillation should combine high LEP value and distillation flux. Optimization of both aspects simultaneously in a single layer membrane by adjusting pore size cannot work, as high LEPs demands small pore diameters, whereas distillation flux will profit from large pores and high porosity. Figure 32 b shows the correlation between the distillation flux and liquid entry pressure for our NF-coated membranes in comparison to the commercial PE membranes. The blue shaded area in Figure 32 b highlights the target area for membranes to achieve best distillation performance. Clearly, NF-coated PES membranes offer a significant improvement as compared to the commercial PE membranes. The NF-coated PES-1.2, NF-coated PES-5 and NF-coated PES-8 membranes all offer higher distillation flux, reaching an up to 60% improvement over the existing state of the art commercial membranes. The membranes with highest flux (NF-PES-5 and NF-PES-8) do compromise on a lower LEP compared to the PE membranes, but still exhibit sufficiently high LEP values for stable operation with excellent salt rejection. The NF-PES-1.2 has both higher distillation flux and LEP compared to the commercial reference. While the NF-PES-0.1 has lower flux than the PE-0.2 membrane it would allow operation at much higher pressure gradients (that could be used to improve flux) or operation with low surface tension liquids for applications other than desalination.

Commercial PTFE and NF-coated membranes were evaluated for 1-week AGMD investigations after achieving steady MD flux for 48 hours. In the instance of AGMD, NF-PES-8 demonstrated 33% higher distillation flux than PTFE-0.2, with salt rejection greater than 99.9%. For a continuous 170-hour experiment, the NF-coated membrane exhibits a stable flow of 5.6 L/m^{2}h, whereas the flux of PTFE-0.2 decreases slightly with time from 4.3 L/m^{2}h to 4 L/m^{2}h (Figure 33). It should be noted that the distillation flux for NF-PES membranes is lower during the one-week experiment for two reasons. One evident difference is that the feed temperature is lower, and the PES membrane is coated with a thick coating of NFs to make it more resistant. The flow reduces with increasing thickness from the previous experiment but remains larger than the PTFE membrane.

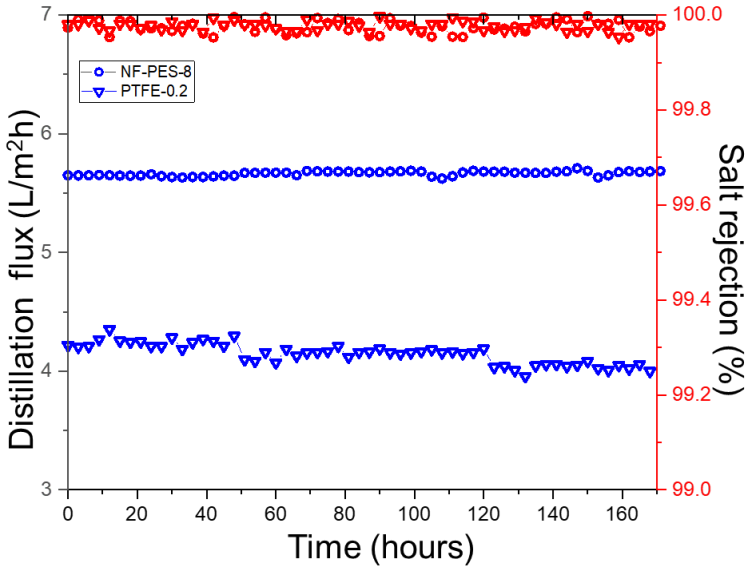

Figure 33: AGMD water flux and salt rejection as a function of time for PTFE-0.2 and NF-PES-8 at feed temperature of 60 °C and cooling water temperature of 20 °C.

3.2.5.2 CA membrane

Following the success of NF-coated PES membranes in AGMD, NF-coated CA membranes were investigated. Figure 34 shows AGMD data for nanofilament coated CA membranes for smallest pore size 0.22 µm and largest pore size 5 µm. Although the LEP value for this membrane was at the border range where one expects stable wetting resistance, the NF-coated CA-5 membrane showed stable operation during 48hrs AGMD experiments. The conductivity of the distillate did increase slightly during the first 24 hours, but stabilized afterwards and water quality remained in the distilled water quality range for the whole 48 hour test. However, the increase in permeate flux for the CA-5 membrane compared to CA-0.22 was much lower than expected from gas permeability test results. Increase in water flux is only 13% with increase in pore size of the core membrane from 0.22 µm to 5 µm.

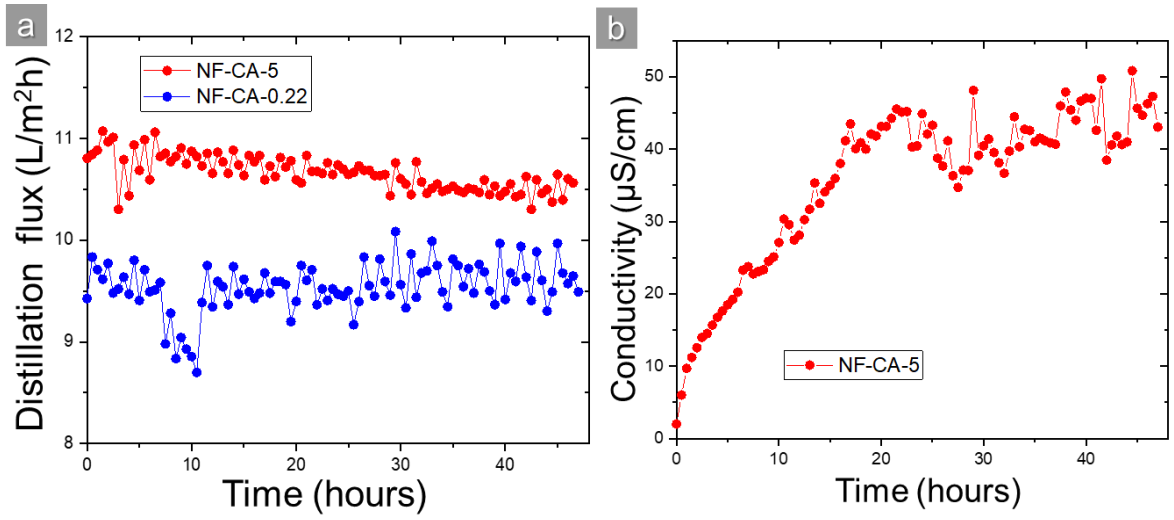

Figure 34: AGMD data for NF-coated CA-0.22 and CA-5 (a) Distillation flux as a function of time (b) Conductivity of water produced as function of time.

Comparison of CA membranes from different suppliers

We studied several CA membranes from different manufacturers to understand the reason for reduced distillation flux for NF-CA-5 membranes. Figure 35 shows CA-0.22 membranes from two different suppliers – Labsolute & Dorsan. The surface morphology of the CA membranes are very different from both suppliers. Also the top and bottom images from Dorsan show different morphologies where bottom side of the CA membrane exhibit more flat surface. However, the SEM image from Figure 35 d and Figure 36 a, they both look very similar. It means that the bottom part of CA-0.22 from Dorsan shows similar morphology to PES-0.1 membrane which gave successful NF coatings with high wetting resistance properties. Figure 37 shows the SEM images for cross section of CA-0.22 membranes from both the suppliers. It is observed that CA-0.22 from Labsolute has an additional polyester web inside the CA membrane to improve its mechanical properties. Such an additional support structure is absent in case of CA-0.22 from Dorsan.

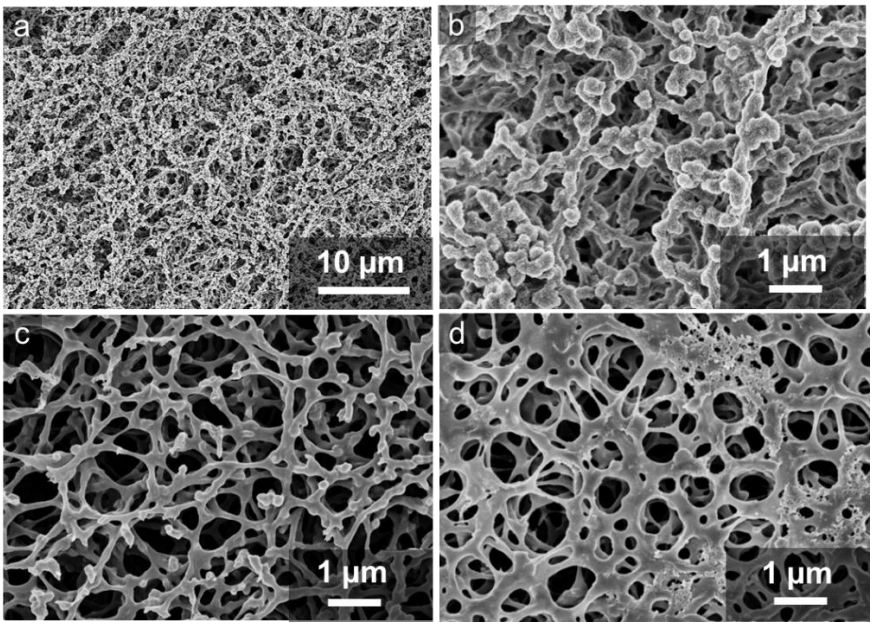

Figure 35: SEM images original CA-0.22 from (a,b) Labsolute with image b magnified version of image a (c,d) Top and bottom of CA-0.22 membrane from Dorsan

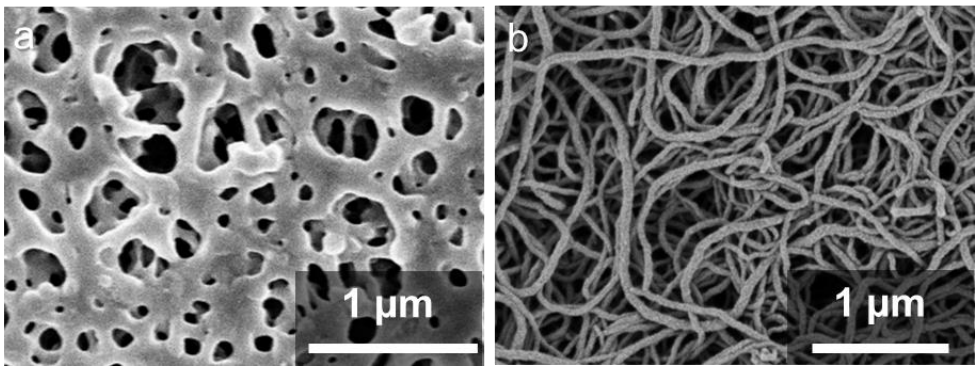

Figure 36*:* SEM images nanofilament coated PES-0.1 membrane. Image b is magnified version of a respectively.

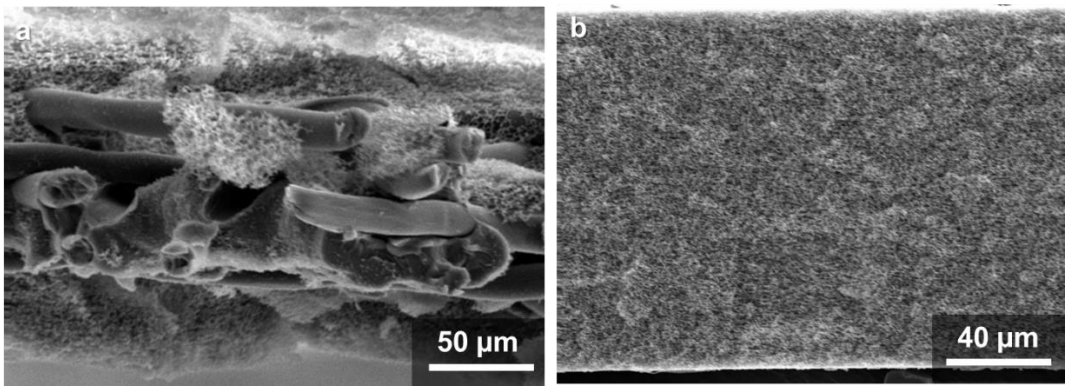

Figure 37: SEM images showing the cross section of original CA-0.22 membrane (a) with polyester web from supplier Labsolute (b) without polyester web from supplier Dorsan.

Later, gas permeability is tested using the setup described in section 3.1.2 to examine the influence of the polyester web on the permeability of CA membranes from both providers. Figure 38 gives gas permeability for both CA-0.22 membranes with and without polyester web. It is observed that without a polyester web, the nitrogen gas flow increases by 24% even for the same nominal pore size.

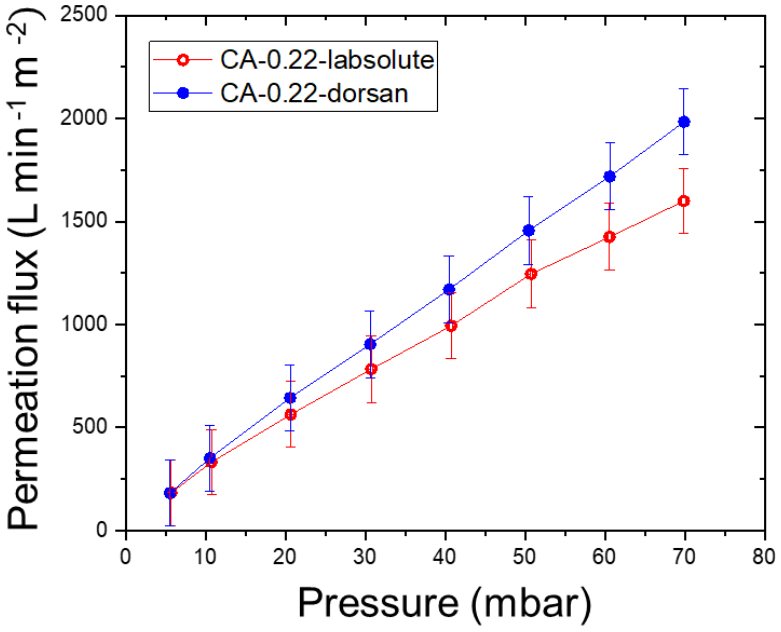

Figure 38: Gas permeation flux as a function of flow pressure for CA-0.22 membranes from suppliers Labsolute and Dorsan.

All NF-coated CA membranes with different pores sizes were compared with NF-coated PES membranes to compare the effect of polyester web in gas permeability data (Figure 39). It was observed that presence of polyester web for large pore size for CA-5 decreases gas permeability by 58% when compared to NF-coated PES-5. However when we compare NF-coated CA-1.2 without polyester web, gas permeability is 35% higher than NF-coated PES-1.2. This can be one reason for lower permeate flux during AGMD in Figure 34.

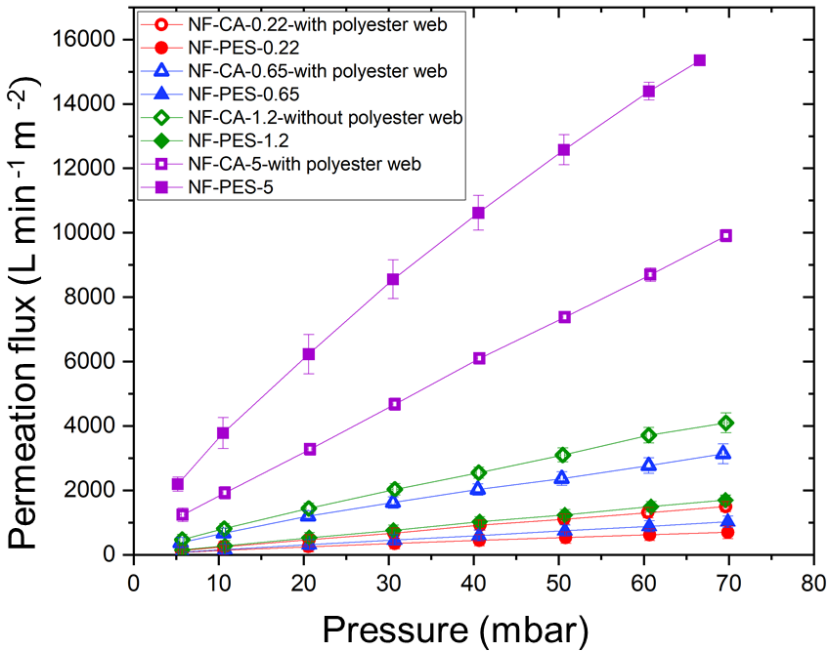

Figure 39: Gas permeation flux as a function of flow pressure for nanofilament coated CA & PES membranes with different pore sizes.

3.2.6 DCMD performance

3.2.6.1 PES membrane

For direct contact membrane distillation (DCMD), commercial PTFE and NF-coated membranes were tested. To prepare the DCMD setup for AGMD, the gap spacer and condensing surface on the condensate side were removed (For details see section 3.1.6). DCMD studies were carried out at feed temperatures (T_f) of 60°C and 80°C, as well as condensate side temperatures (T_C) of 20°C.

When compared to hydrophobic PTFE-0.2, NF-coated PES membrane with a pore size of 8 µm delivers 50% greater distillation flux at a lower T_f of 60°C. Even at greater T_f, the distillation flux of NF-coated PES membrane is 27% higher than that of PTFE membrane. DCMD studies were conducted for 12 hours and revealed steady flow in both PTFE and NF-coated membranes with salt rejection greater than 99.9% (Figure 40).

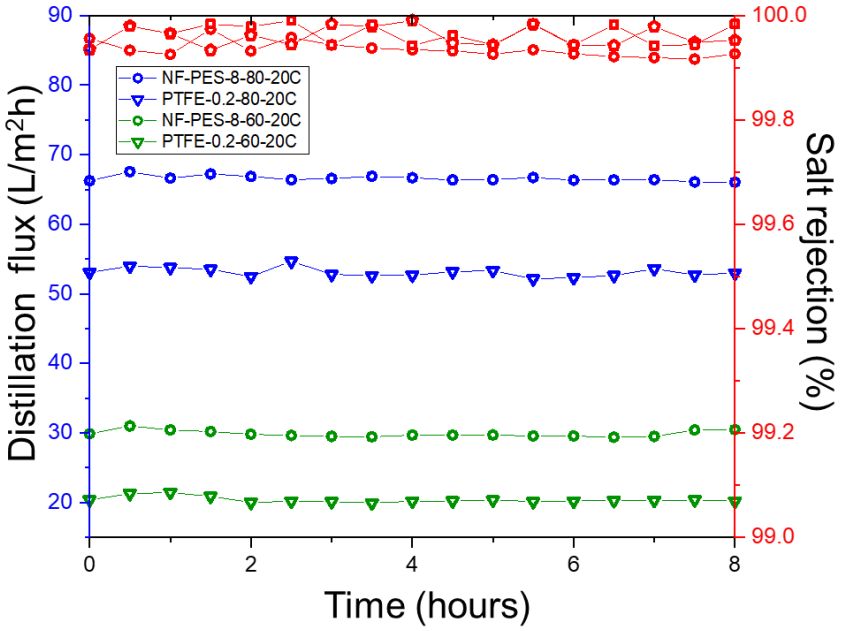

Figure 40: DCMD flux and salt rejection as a function of time for NF-PES-8 and PTFE-0.2 at feed temperature of 60 °C and 80 °C, with cooling temperature of 20 °C

DCMD studies were also carried out continuously for 7 days. Even after 7 days of continuous DCMD operation at 60°C T_f , NF-coated membranes have a 24% greater distillation flow than PTFE membranes. For continuous long-term experiments, NF-coated membranes exhibit steady flux of 24.8 L/m^{2}h, but PTFE membrane flux declines with time from 20.2 L/m2h to 19.2 L/m^{2}h with salt rejection of more than 99.9% in all cases (Figure 41). It should be emphasized that for the one-week experiment, the PES membrane is covered with a thick layer of nanofilament to make it more robust. With increasing thickness, the flow decreases from the prior experiment but remains greater than the PTFE membrane.

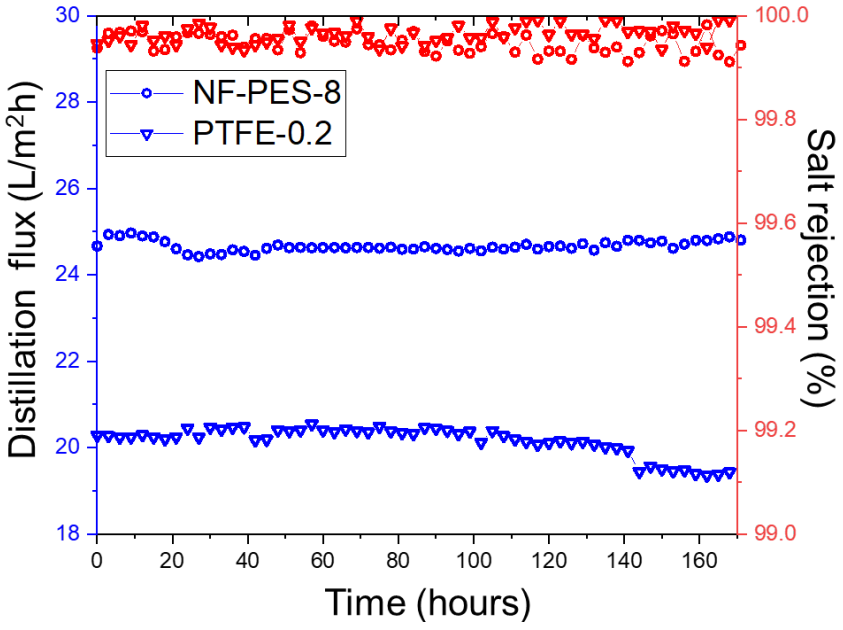

Figure 41: DCMD water flux and salt rejection as a function of time for PTFE-0.2 and NF-PES-8 at feed temperature of 60 °C and cooling water temperature of 20 °C.

4. Anti-fouling & Anti-wetting tests

4.1 Materials

Bovine serum albumin (BSA) was purchased from Sigma-Aldrich. Sodium dodecyl sulfonate (SDS) was purchased from MP Biomedicals Germany GmbH.

4.2 Methods

4.2.1 Confocal laser scanning microscope (CLSM)

CLSM was applied to examine BSA protein adsortion on the membranes. The fluorescent dye Nile Red was used to label the BSA protein. Confocal microscopy was performed using Leica TCS SP8 (Leica Microsystems GmbH, Germany) with 20 x numerical aperture objective. Nile Red was excited with 458 nm argon laser. Membranes to be tested were glued to a glass slide and clamped onto open flow channels so that the membranes closed the channel, forming its top. The in- and outlets of the flow channel were connected to a peristaltic pump. This pump was used to control the continuous flow of BSA / Nile Red solution through the channel. Membrane surfaces facing the flow channel were observed with the confocal microscope while BSA solution continuously flowing along them. Fluorescence of Nile Red was detected by two separate channels in the red (488nm) and green (561 nm) spectral range. Nile red emits in red when being in a hydrophilic environment like water whereas it emits in green when being in a hydrophobic environment like the membrane surfaces used for MD.

4.2.2 Surface tension of SDS and salt mixture

The surface tension of SDS and salt combination was tested because the values in the literature usually referred to simply SDS or surfactant mixtures at different temperatures. [133, 134]. When salt is added to the SDS solution, there is a drastic drop in the surface tension of the solution (Table 4). For characterizing the wetting properties, we used 0.2 mM of SDS with 0.59 M NaCl which has a surface tension of ~35 mN/m.

Table 4: Measured surface tension values for SDS and NaCl solution

SDS (mM)	NaCl (M)	Temperature (^{o}C)	Surface tension (mN/m)
0.1	0	25	69 ± 2
	0.59	25	41 ± 1
	0.59	75	38 ± 1
0.2	0	25	55 ± 2
	0.59	25	36 ± 1
	0.59	75	35 ± 1

4.2.3 Contact angle in presence of surfactant

For investigating the wetting properties of the membranes in presence of SDS, we prepared a mixture of 0.2mM SDS and 0.59 M NaCl. The water contact angles and contact angles with the SDS + NaCl mixture were measured on the membranes (PE, PTFE, NF-coated PES membranes). The static contact angle and contact angle hysteresis of a water droplet were measured using a DataPhysics OCA35 goniometer. For the measurement, a 5 µl droplet was deposited on the membrane surface, and later 20 µl of SDS + water droplet was added and then removed from the droplet. The measurement was consequently repeated at three different positions per substrate. The error of the advancing and receding contact angle measurements is ± 2 ^{o}.

4.2.4 Fourier Transform Infrared Spectroscopy (FTIR)

The absorption spectrum of distinct molecular groups is analyzed in FTIR to reflect the presence of chemical components by wavelength and intensity. PE, PTFE, and NF-coated PES membranes were immersed in SDS solutions with a concentration of 10 mM (surface tension: 33 mN/m) and a mixture of SDS-0.2 mM + NaCl-0.59 M (surface tension: 35 mN/m) for 1 hour and 1 week. Later to detect the presence of SDS on the membranes, attenuated total reflectance Fourier Transform Infrared (FTIR) spectroscopy (Bruker Tensor II with Platinum ATR-unit, Germany) was used. For each spectrum, 32 scans were recorded with a resolution of 4 cm $^{-1}$ at room temperature. The obtained spectra were baseline corrected and then deconvoluted over the region 4000 – 500 cm $^{-1}$ depending on the sample.

4.3 Results & Discussion

4.3.1 BSA fouling

4.3.1.1 SEM-data

For the first try, all the membranes were immersed in 500 mg/l BSA solution for 24 hours. The membranes to be analyzed were then rinsed with distilled water and dried under nitrogen before being imaged using SEM. For NF-coated PES membranes, we could not identify any adsorbed proteins by SEM. Thus, NF-coated PES membranes are expected to be less prone to fouling by proteins than commercial hydrophobic membranes. In contrast, layers of adsorbed BSA cover PE and PTFE membrane surfaces (Figure 42). Such results have also been reported by other studies [71, 135, 136].

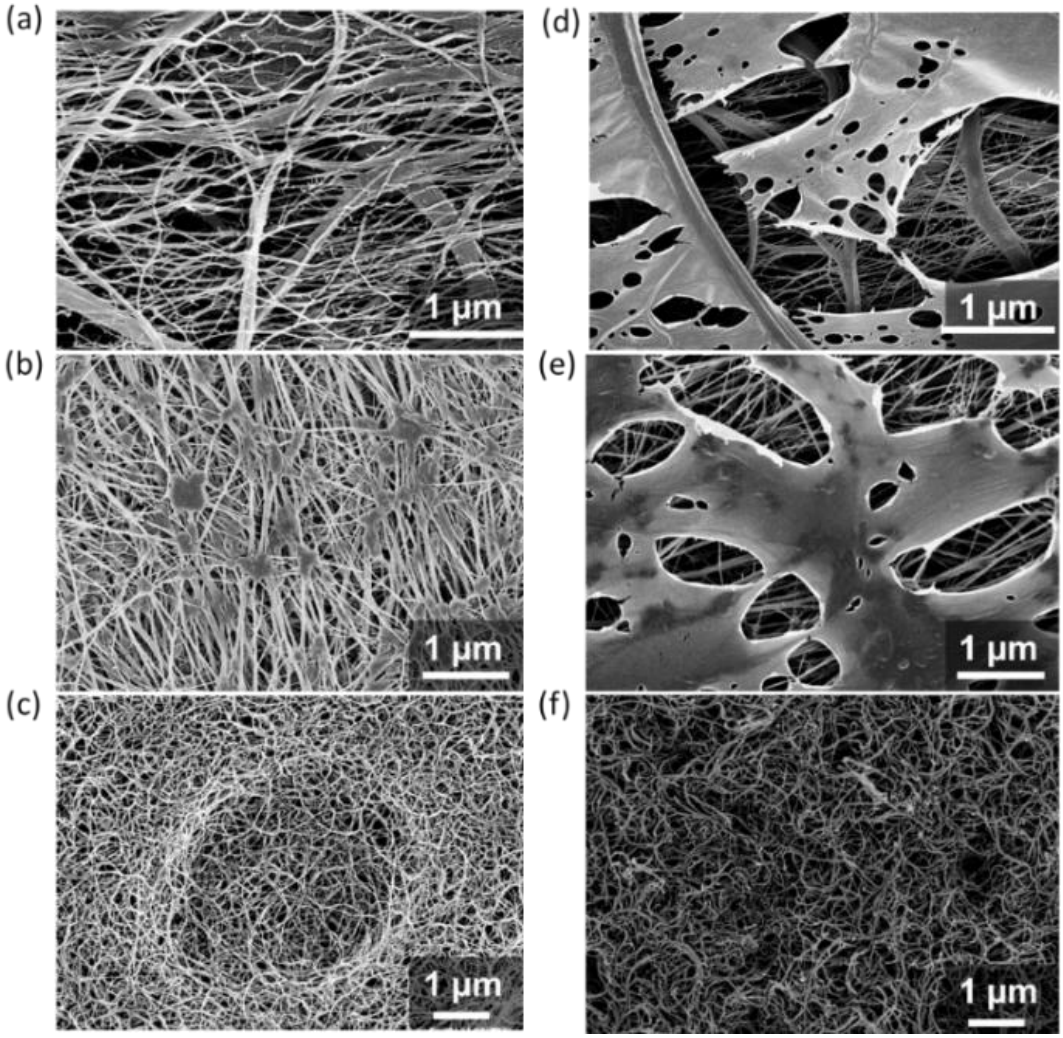

Figure 42: SEM images of (a, b, c) virgin PE, PTFE, and NF-coated PES membranes (d, e, f) PE, PTFE, and NF-coated PES membranes after 24 hours immersion in 500 mg/l BSA solution.

4.3.1.2 Confocal detection of BSA adsorption

To monitor BSA adsorption in real-time, we exposed membranes to a flow of dyed BSA solution for 1 hour while imaging the membrane surface by confocal microscopy. The dye was excited with a 458 nm argon laser. The objective was focused near the membrane interface. Then dyed BSA was allowed to flow along the membrane surface. The measurements were performed within a central 1024 x 256-pixel frame. Total fluorescence intensity was measured for 1 hour (3600 secs) with an interval of 0.357 frames/sec. The result was saved as a video data file and then analyzed using Fiji software giving the plot of the fluorescent intensity over time for the respective membranes.

Figure 43 a gives the increase in the intensity of fluorescence in the hydrophilic medium (Red fluorescence) over time for PE, PTFE, and NF-coated membranes. Considering the red fluorescent intensity equivalent to BSA adsorption in the water close to the membrane interface, it is observed that PE membranes show about 3 times more BSA adsorption than NF-coated membranes. However, PTFE and NF-coated membranes fall in the same range.

Figure 43 b gives the increase in the intensity of fluorescence in the hydrophobic medium (Green fluorescence) over time for PE, PTFE, and NF-coated membranes. In this case, considering the emitted green fluorescent intensity equivalent to BSA adsorption on the membrane surface, it can be concluded that PE does show approximately 3 times more BSA adsorption than nanofilament-coated PES membranes. Also, over time PTFE membranes show roughly 2 times more BSA adsorption than NF-coated PES membranes with an increasing trend. Although in the case of NF-coated PES, membranes exhibit very stable adsorption for 1-hour BSA flow.

Finally from the confocal images in Figure 43 c, it is observed that PE membranes show complete coverage with a green signal confirming protein BSA is adsorbed on the membrane surface. PTFE membranes show BSA adsorbed on some parts of the membrane but not completely covered (Figure 43 d). However, NF-coated PES membranes show very less intensity for the green signal compared to the red signal confirming very low adsorption of BSA on the membrane surface (Figure 43 e). In addition, as compared to PE and PTFE membranes, the strength of the green signal on NF-coated membranes is quite low.

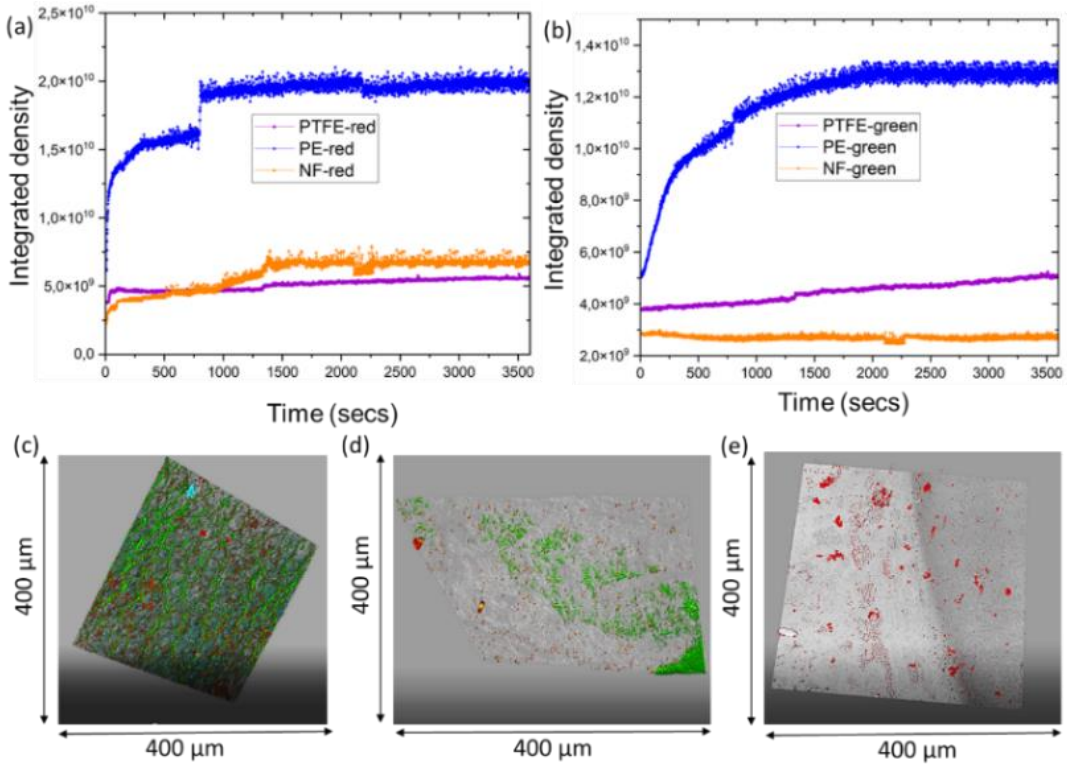

Figure 43: Confocal microscopy data (a) Fluorescence intensity as a function of time for red spectral range, indicative of BSA adsorbed in a hydrophilic environment. (b) Fluorescence intensity as a function of time for green spectral range, indicative of BSA adsorption in a hydrophobic environment. Confocal images for (c) PE (d) PTFE (e) NF-PES membranes (overlay of both green and red spectral ranges).

4.3.1.3 AGMD in the presence of BSA

To check for possible membrane fouling during membrane distillation, the AGMD setup described in section 3.1.5 was used to conduct membrane distillation experiments in the

presence of BSA. AGMD fouling experiments were conducted using 1000 mg/l BSA in 0.59 M NaCl feed. The temperature of the inlet feed solution containing salt and BSA (T_f) was kept at 53 °C. This relatively low value of T_f was chosen based on the fact that above 53 °C, BSA starts to coagulate. This coagulation leads to the formation of large aggregates that adsorb to the pipes of the distillation setup and cause complete clogging of the whole system. The temperature of the distillate inlet stream (T_c) was kept at 15 °C for all experiments. The feed and distillate volume flows were 1 L/min and 2 L/min respectively. All the AGMD experiments were carried out over at least 48 hours. For all membranes, an initial MD run with salt water without BSA was carried out for one hour, before switching to BSA containing salt water.

Figure 44 b shows BSA fouling results for our NF-coated PES-8 membranes compared to commercial PTFE-0.2 membranes. In the case of the pure salt water feed solution, NF-coated PES-8 membranes showed a ~25% higher distillation flux than PTFE-0.2 (Figure 44 a).the In presence of BSA, the PTFE-0.2 membrane showed a ~23% decline in flux directly after restarting the distillation experiment with the new feed solution. The NF-coated PES-8 membrane shows an almost completely unaffected flux with only a ~2% decline over 48 hours of AGMD experiments.

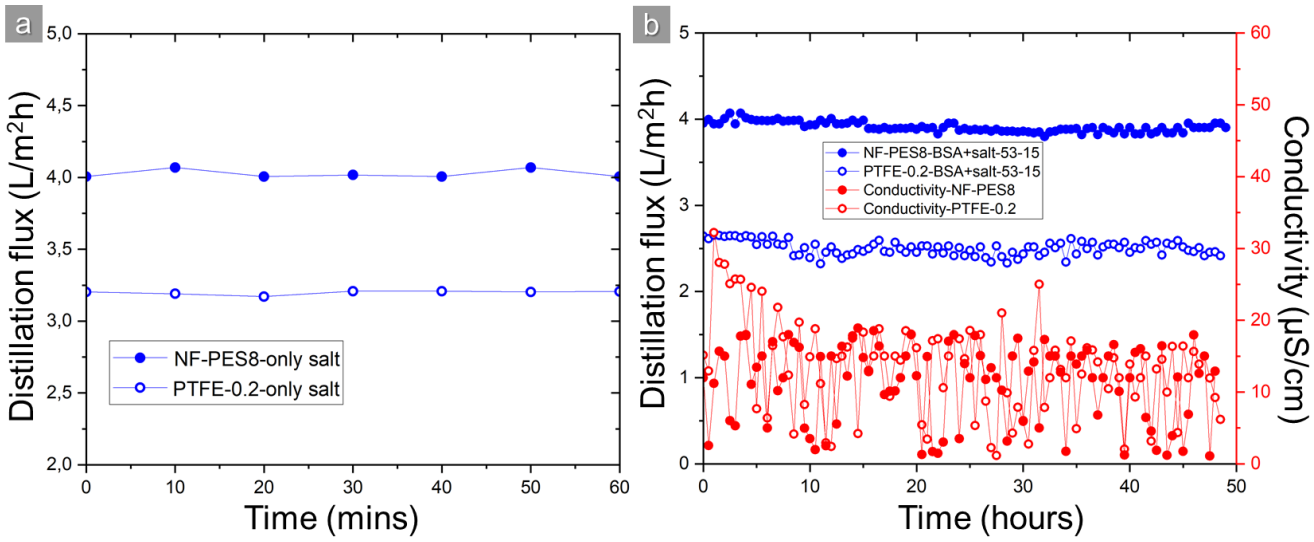

Figure 44: AGMD distillation flux as a function of time for original PTFE 0.2 and NF-coated NF-PES-8 membranes (feed temperature T_f of 53 °C, distillate temperature T_c of 15 °C) (a) initial run for 1h using only salt in the feed solution (b) with 1000 mg/L BSA and salt in the feed solution.

To check the adsorption of BSA to the membranes during membrane distillation, we did SEM imaging for the samples after the AGMD operation. Membranes were taken out of the distillation setup, shortly rinsed with distilled water, and then dried in the air before transferring them to the SEM. It was observed that for PTFE-0.2, a layer of BSA forms on the membrane surface covering some areas completely and having cracks in some areas that expose the bare membrane structure (Figure 45 b).

For the NF-coated PES membranes, we observe only very weak coverage by BSA on most of the membrane area and no crack formation (Figure 45 d). However, more BSA seemed to

adsorb in areas where the NF layer covers the large PES pores. In addition, shrinkage of this adsorbed layer during drying seems to have damaged the NF coating along the pore edges, possibly due to stress concentration at the edges during the drying process (Figure 45 d). This should not be a problem during continuous operation of the membrane but needs to be considered for the case of intermittent operation with complete drying in between process cycles.

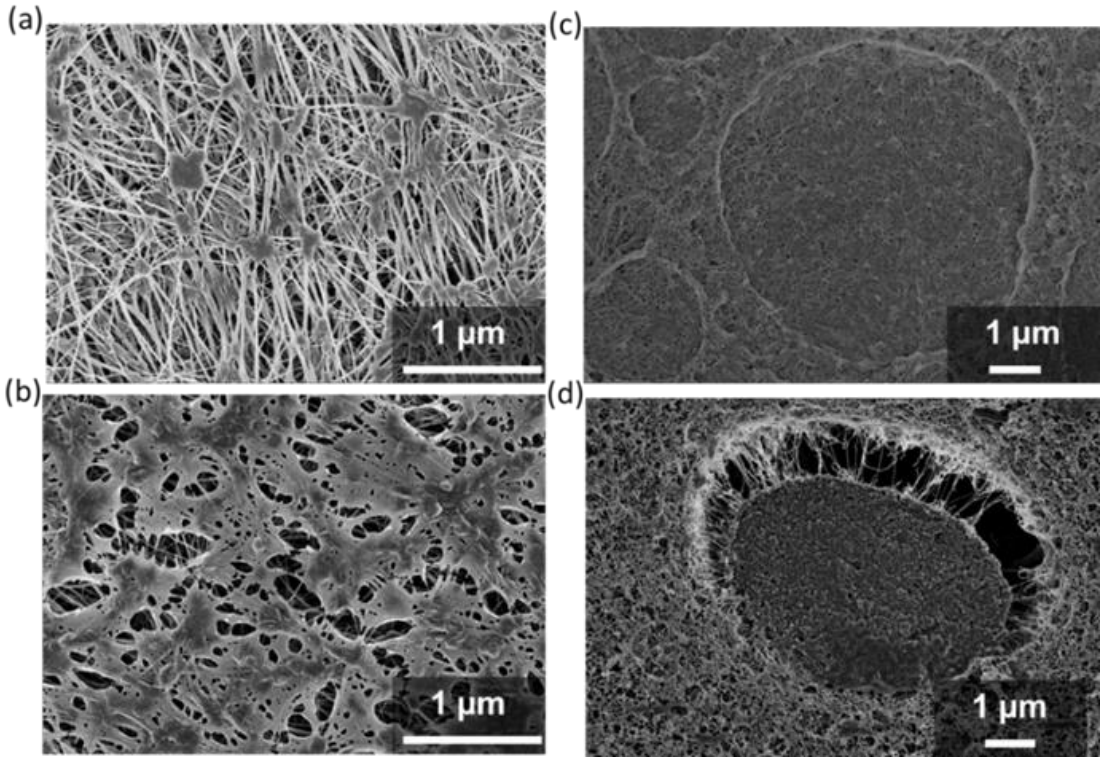

Figure 45: SEM images of (a, b) PTFE-0.2 membranes before and after AGMD operation and (c,d) NF-PES-8 membranes before and after AGMD operation in presence of salt and BSA for 48 hours.

4.3.1.4 DCMD in presence of BSA

BSA fouling is investigated in the DCMD setup (described in section 3.1.6) for NF-PES-8 and PTFE-0.2 membranes in the presence of BSA. DCMD studies were done for 1 hour solely in the presence of salt. In this situation, NF-PES-8 membranes had a ~ 30% greater distillation flow than PTFE-0.2 membranes (Figure 46 a). When 1 g of BSA is injected after 1 hour, PTFE-0.2 membranes have an approximately 8% drop in flux in a 9 hours of DCMD experiments with partial wetting because the conductivity is always in the range of 60 - 120 uS/cm. NF-PES-8 membranes, on the other hand, exhibit essentially consistent flux with just a 2% reduction in flux and salt rejection that is always greater than 99.9% (Figure 46 b).

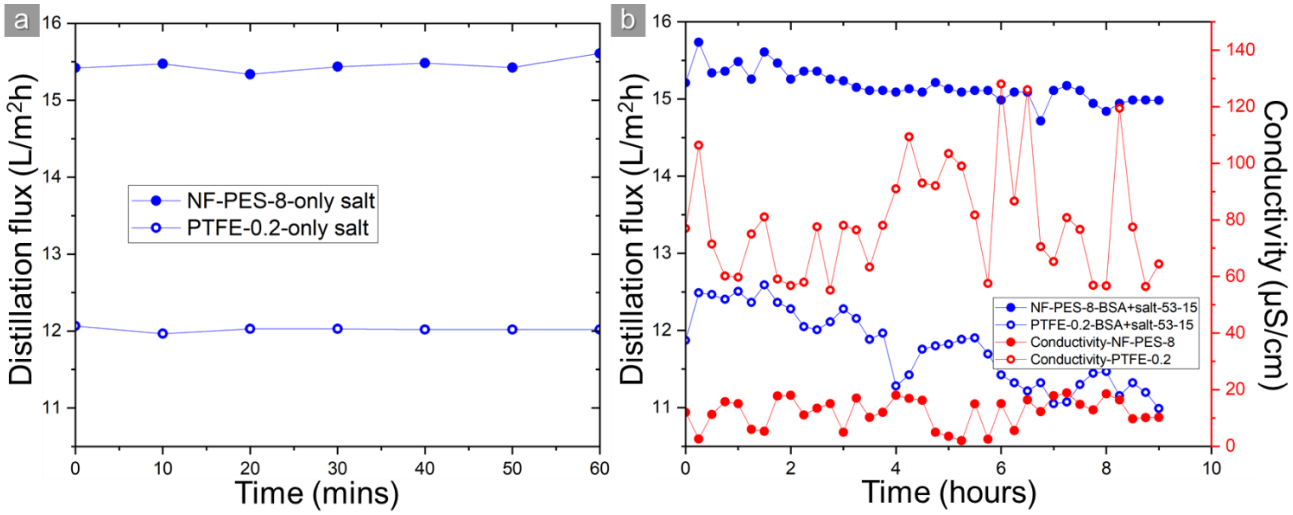

Figure 46: DCMD distillation flux as a function of time for original PTFE 0.2 and NF-coated NF-PES-8 membranes (feed temperature T_f of 53 °C, distillate temperature T_c of 15 °C) (a) initial run for 1h using only salt in the feed solution. (b) with 1000 mg/L BSA and salt in the feed solution.

4.3.2 SDS fouling

4.3.2.1 Wetting properties – SDS

In the case of PE membrane, the mixture of SDS + salt wets the membrane as the static contact angle (SCA) decreases from ~129° to ~84°, whereas contact angle hysteresis (CAH) increases from ~37° to ~77° indicating considerable loss of liquid repellency (Figure 47 a, d). The hydrophobicity also decreased on commercial PTFE membranes, as SCA decreases from ~140° to ~114 ° and CAH increased from ~25° to ~67 ° (Figure 47 b, e). However, NF-coated PES membranes are still superhydrophobic with SCA of ~147° and CAH of ~31°. Hence NF-coated PES membranes show better repellency even with SDS + salt mixture having surface tension as low as ~35 mN/m (Figure 47 c, f).

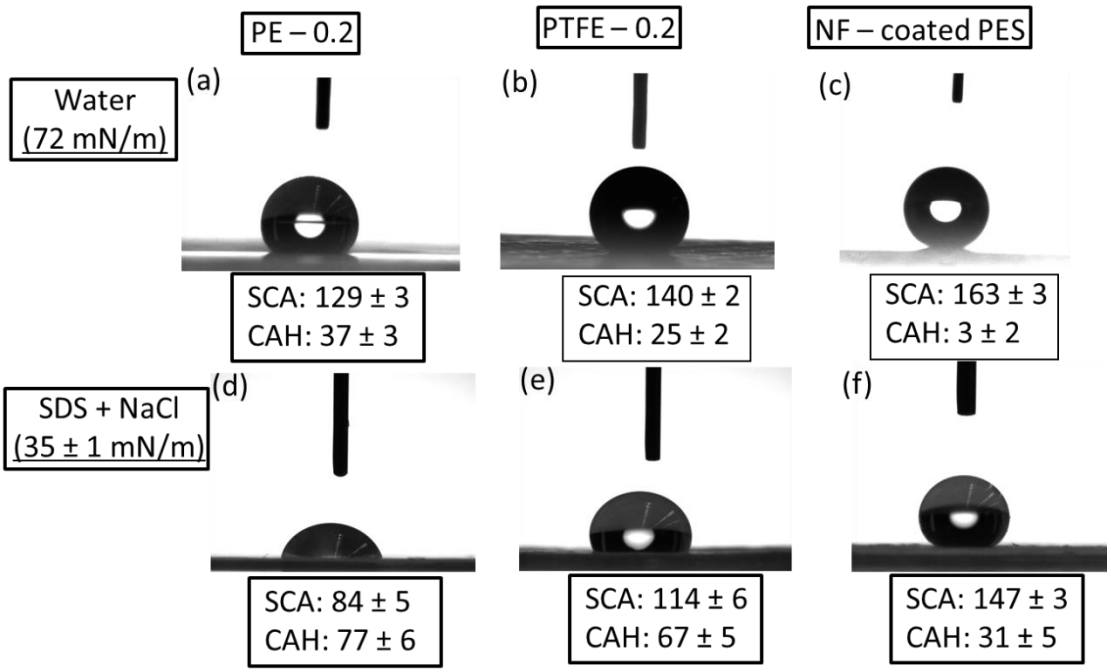

Figure 47: Static contact angle (SCA) and contact angle hysteresis (CAH) for pure water (surface tension of 72 mN/m) for (a) PE (b) PTFE (c) NF-PES membranes. SCA and CAH for 0.2 mM SDS + 0.59 M NaCl (surface tension of 35 mN/m) as liquid on (d) PE (e) PTFE (f) NF-PES membranes.

4.3.2.2 FTIR – SDS

PE, PTFE, and NF-coated PES membranes were immersed in SDS solutions with a concentration of 10 mM (surface tension: 33 mN/m) and a mixture of SDS – 0.2 mM + NaCl-0.59 M (surface tension: 35 mN/m) for 1 hour and 1 week. Later to detect the presence of SDS on the membranes, Fourier Transform Infrared Spectrometer (FTIR) was used. SDS has a distinctive peak at 1080 cm-1 and 1216 cm-1 for S=O and S–O bonds, respectively. Also for CH_2 symmetric and asymmetric stretching at 2851 cm-1 and 2926 cm^{-1} [83, 118]. Because it was unable to distinguish the difference in peaks from membrane or SDS in PE membranes, the presence of SDS was detected by S–O and S=O bonds. Figure 48 (a, b, d) shows the immediate adsorption of SDS on PE and PTFE membranes. On the contrary, NF-coated PES membranes did not show any distinct peaks except after 1-week immersion in the mixture of salt and SDS, where the peak for CH_2 symmetric stretching with higher intensity was observed (Figure 48 e, f).

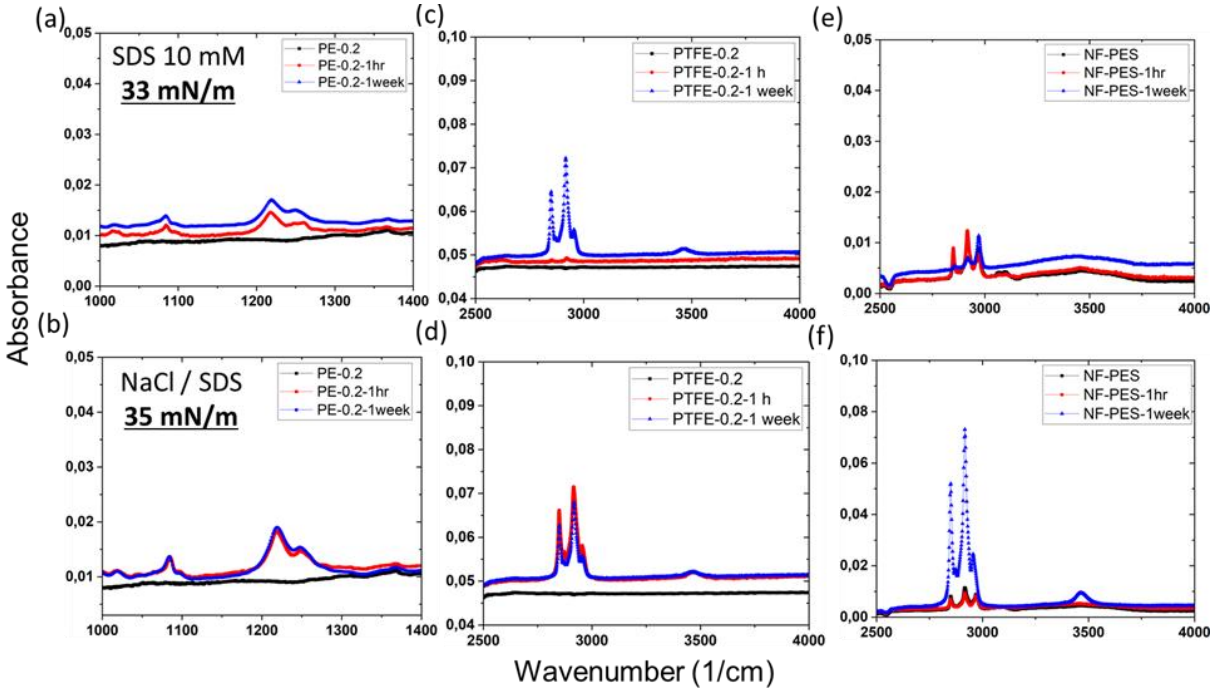

Figure 48: FTIR spectra for PE, PTFE, NF-coated PES membranes for original and after SDS immersion in (a, c, e) 10 mM SDS (b, d, f) 0.2 mM SDS + 0.59 M NaCl for 1 hour and 1-week immersion.

4.3.2.3 AGMD – SDS

For investigating the anti-wetting properties of the NF-coated membranes during AGMD in presence of surfactants we used 0.01 mM of SDS with 0.59 M NaCl in the feed solution (surface tension: 55 mN/m). The temperatures used were T_f: 65°C and T_c: 15°C. The feed and distillate volume flows were 1 L/min and 2 L/min respectively. All the AGMD experiments were carried out over 48 hours. NF-PES-8 membranes exhibited ~ 7 % higher distillation flux than PTFE-0.2 with stable water flux for 48 hours and no increase in water conductivity (

Figure **49**).

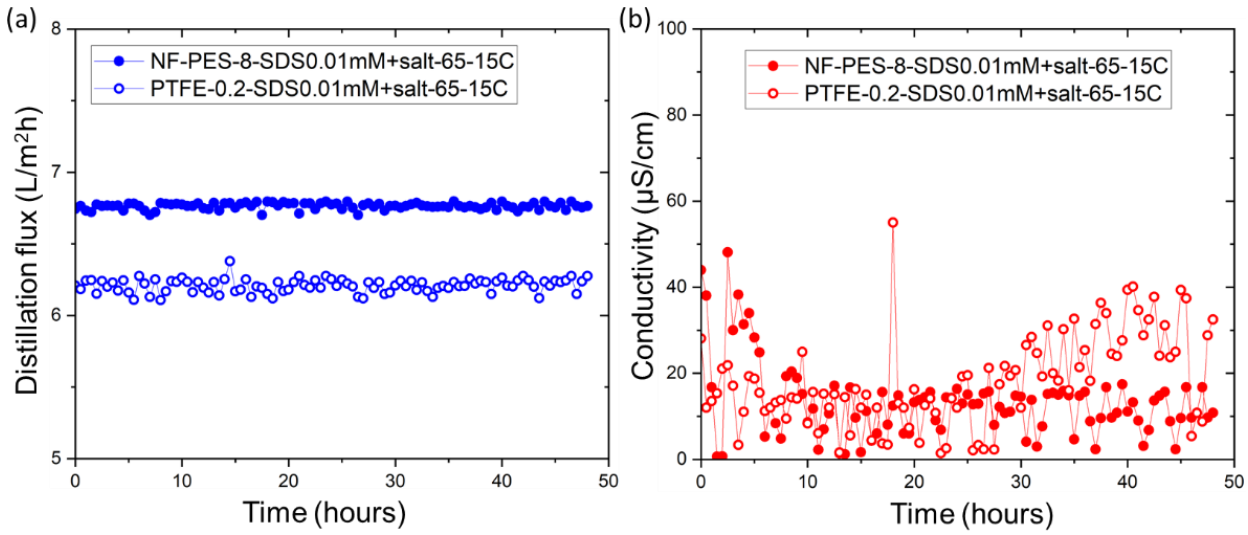

Figure 49: (a) AGMD distillation flux as a function of time and (b) water conductivity over time for original PTFE 0.2 and NF-coated NF-PES-8 membranes with 0.01 mM of SDS + 0.59 M salt at T_f of 65 °C and T_c of 15 °C

AGMD experiments were also conducted with a much higher concentration of 0.2 mM of SDS with 0.59 M NaCl (surface tension: ~ 35 mN/m). Figure 50 a represents AGMD data only in presence of salt at feed temperature of T_f = 80 °C and a distillate temperature of T_c = 20 °C with no increase in conductivity for 48 hours long experiment. Presence of SDS in the feed solution had no significant influence on the distillation flux (Figure 50 b). However, in the presence of SDS the PTFE-0.2 membrane shows partial wetting as conductivity of the permeate increases to ~ 150 µS/cm in the beginning of the experiment and gradually increases to ~ 500 µS/cm in 48 hours using a feed temperature of T_f = 80°C and a distillate temperature of T_c = 20°C. The NF-coated PES-1.2 membrane was also tested at same temperatures, where we observed 17% increase in distillation flux compared to PTFE-0.2. Under these harsher conditions, the NF-PES-1.2 membrane also exhibited a slight decrease in wetting resistance, as the conductivity of the distillate increased to 200 µS/cm within 48 hours which exceeds the range of distilled water quality, but is still in the range of drinking water (< 500 µS/cm).

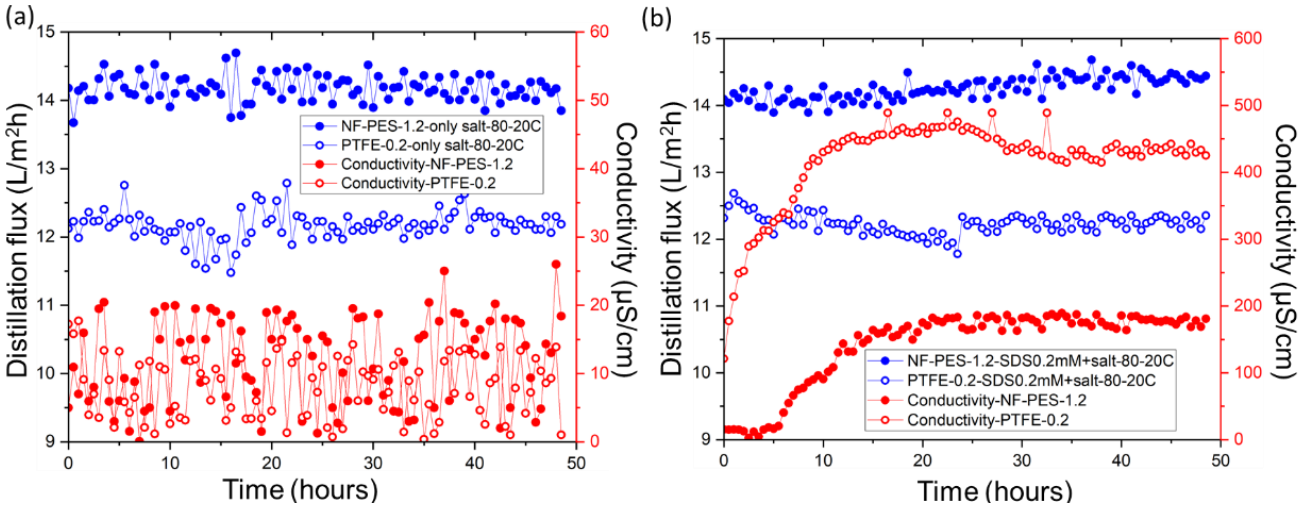

Figure 50: (a) AGMD distillation flux as a function of time and (b) water conductivity over time for original PTFE 0.2 and NF-coated NF-PES-1.2 membranes with 0.2 mM of SDS + 0.59 M salt at T_f of 80 °C and T_c of 20 °C

4.3.2.4 DCMD – SDS

DCMD tests using SDS 0.1 mM and 0.59 M salt (surface tension: 41 mN/m) were conducted with PTFE-0.2 and NF coated PES-8 membranes. As shown in Figure 51, the PTFE membrane shows minor wetting with conductivity being increased to ~100 µS/cm in 9 hours. Nevertheless, NF coated PES membranes show ~ 6 % higher distillation flux than PTFE-0.2 but were unsuccessfull and started to show gradual wetting after 2 hours of testing and after 9 hours the conductivity of water produced increases to ~500 µS/cm and shows increasing trend.

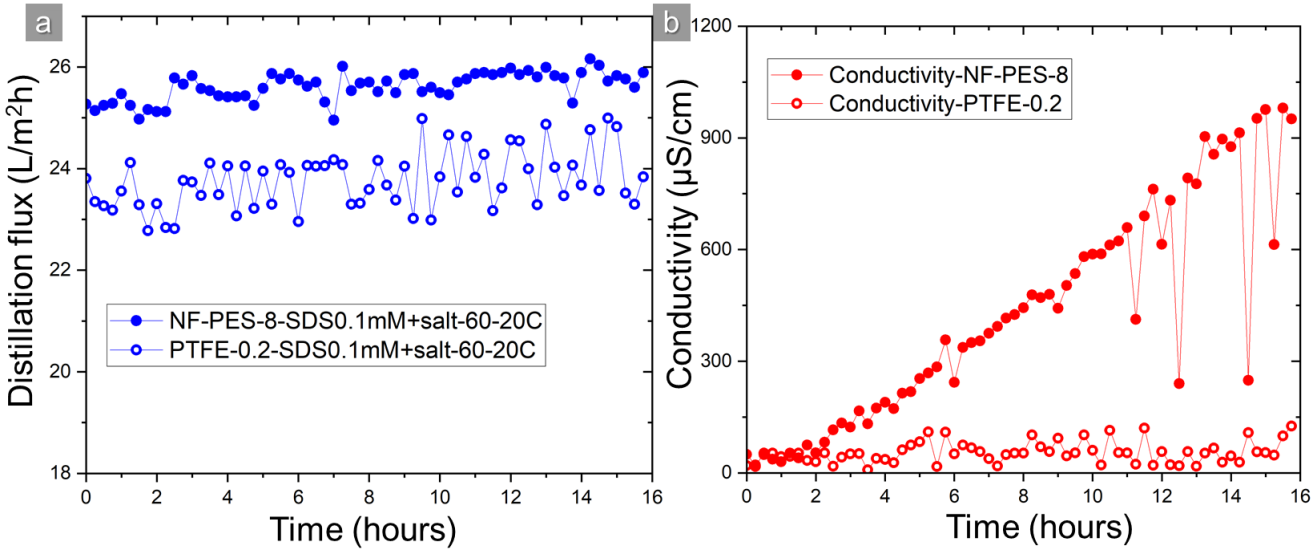

Figure 51: (a) DCMD distillation flux as a function of time and (b) water conductivity over time for original PTFE 0.2 and NF-coated NF-PES-8 membranes with 0.1 mM of SDS + 0.59 M salt at T_f of 60 °C and T_c of 20 °C

Hence it can be concluded that NF coated PES membranes demonstrate better performance in AGMD than in DCMD, this can be because in case of DCMD, membrane is in direct contact with the feed side and permeate side. Thin NF coating is not stable enough for long term contact with low surface tension liquids.

5. Experiment with various superhydrophobic membranes

5.1 Plasma-treated membranes

Plasma-treated PTFE membranes with pore sizes of 0.1, 0.2, and 1 μm, and also hydrophilic cellulose acetate (CA) membrane after plasma treatment with a pore size of 0.2 μm were provided by NCSR-Demokritos.

Initially, these membranes were textured inside an Alcatel Reactive Ion Etcher (RIE) to induce directional (anisotropic) etching and result in roughness creation perpendicular to the surface of the membranes. To further explain the roughness mechanism we mention that small amounts of etching inhibitors sputtered from the quartz plate (covering the electrode) deposit on the surface of the polymer during O_2 plasma etching (the surface concentration in inhibitors is less than 4%). They act as local micromasks during anisotropic polymer etching and result in nanograss formation, which grows versus time in nanofilaments, and eventually bundled nanofilaments. The same process has been used for roughness creation in various polymeric materials in other plasma reactors, and it is extremely reproducible. The plasma etching inherently widens the pores thereby increasing the vapor transfer diffusion. After the O_2 plasma texturing, membranes were transferred inside a high-density Inductively Coupled Plasma (ICP) reactor equipped with a helicon source (at 13.56 MHz), the MET system of Adixen for the deposition process. This step incorporates Octafluorocyclobutane (C_4F_8) plasma to deposit a thin hydrophobic film of 30nm (as measured on flat Silicon wafer), reduce the surface energy, and render the surface of the membranes superhydrophobic. From now on, we will refer to the textured and hydrophobized membranes as plasma-treated membranes. It should be stressed here that other less fluorinated or non-fluorinated gases may be used for membrane hydrophobization, such as CHF_3, or hydrocarbons. However, C_4F_8 plasma deposited films have lower surface energy. The plasma-treated PTFE and CA membranes were first evaluated for standard desalination in an AGMD setup (section 3.1.5), and then for fouling with BSA and SDS in AGMD tests.

5.1.1 Gas permeability – Plasma treated membranes

Figure 52 depicts the flow of gas permeation vs transmembrane pressure for all PTFE membranes (plasma treated and untreated) and CA 0.22 untreated. This test evaluates the mass transfer resistance to ensure that vapor transport through the membrane pores is adequate when utilized in desalination. The gas permeability of PTFE 1 is, as predicted, the greatest due to the large pore size, and at 50 mbar, the plasma treated one has a 30% greater flux than the pristine. At the same pressure, the difference between the two PTFE 0.2 membranes is smaller, but the fluxes are almost identical in the case of PTFE 0.1. This implies that the pore widening impact of plasma treatment is considerably more visible when the original pores are big, and/or plasma deposition closes the hole and recovers the widening

caused by plasma etching. Because of the distinct morphology on the surface, the pristine CA 0.22 membrane has the lowest flux, which corresponds to the highest mass transfer resistance of all membranes.

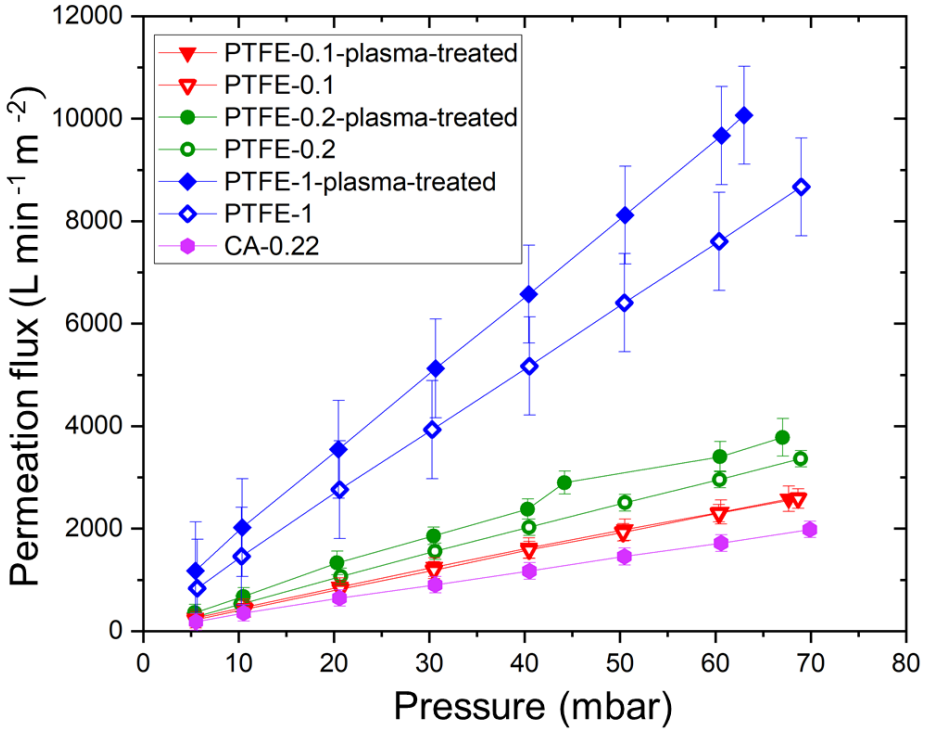

Figure 52: Gas permeation flux as a function of flow pressure for PTFE-0.1, 0.2 and 1 µm pore size (plasma treated and untreated) and CA-0.22 untreated.

5.1.2 Standard desalination – Plasma treated membranes

The long-term operation distillation flux as a function of time is shown in Figure 53 for all membranes applied. The graphs with solid symbols depicting plasma-treated membranes indicate that their performance stays steady throughout the course of the studies. On the contrary, all untreated PTFE membranes had a lower distillation flux, and the fluxes of PTFE 1 and PTFE 0.2 dropped with time, revealing their scaling susceptibility. Untreated PTFE 1 membrane performance consistently decreases from 10.7 to 9.9 L/m2h, but plasma treated membrane performance remains constant at 10.9 - 11 L/m^{2}h. Similarly, untreated PTFE 0.2 flux decreases from 10.3 to 9.7 L/m^{2}h, but plasma treated PTFE 0.2 flux remains constant at 10.8 - 10.9 L/m^{2}h. This demonstrates that plasma treatment-induced superhydrophobicity not only enhances flow by enlarging pores, but also generates robust and resilient structures that can withstand wetting in long-term operations.

Furthermore, even when mass transfer resistance is essentially the same, as in the case of treated and untreated PTFE 0.1 membranes that displayed the same flow in the gas permeability test (Figure 52), the transformation to superhydrophobic can increase performance. This long-term experiment further shows that the suggested method is not only a surface functionalization technique, but has been successfully implemented in the inner

regions of the pores, with no capillary condensation or membrane wetting detected during MD. On the contrary plasma treated CA-0.22 membranes showed lower flux with salt rejection rate of 99.23 % while pristine and plasma treated PTFE membranes exhibited excellent distillation rate and salt rejection higher than 99.9 % always.

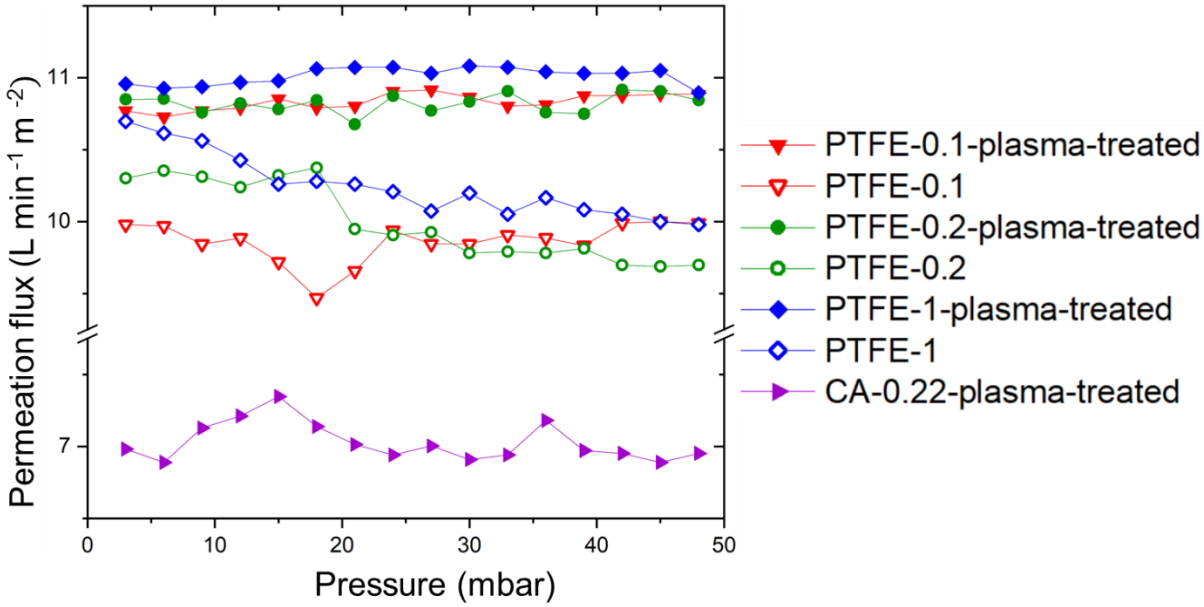

Figure 53: AGMD performance in terms of distillation flux versus time of PTFE 0.1, PTFE 0.2 and PTFE 1 plasma treated and untreated (T_f - 75 ^oC, T_c – 15 ^oC) and plasma treated CA 0.22 (T_f - 65 ^oC, T_c – 10 ^oC)

5.1.3 BSA fouling – Plasma treated membranes

In the case of plasma-treated PTFE membranes, all 3 membranes showed stable flux for 48 hours of experiments with no decline in water flux. Also for smaller pore sizes PTFE 0.1 & PTFE 0.2, there is no decline in distillation flux with BSA when compared with results with only salt in the feed solution and also untreated PTFE membranes from the results above (Figure 54). Plasma-treated CA membranes were also tested and shows ~23% increase in flux with only salt in the feed solution when compared to PTFE-0.2. However, when BSA is added, flux stays stable for initial 5 hours and later gradually decreases over time which after 48 hours is around 6% lower than at beginning of the experiment (Figure 54). Salt rejection in all cases is always > 99.9%.

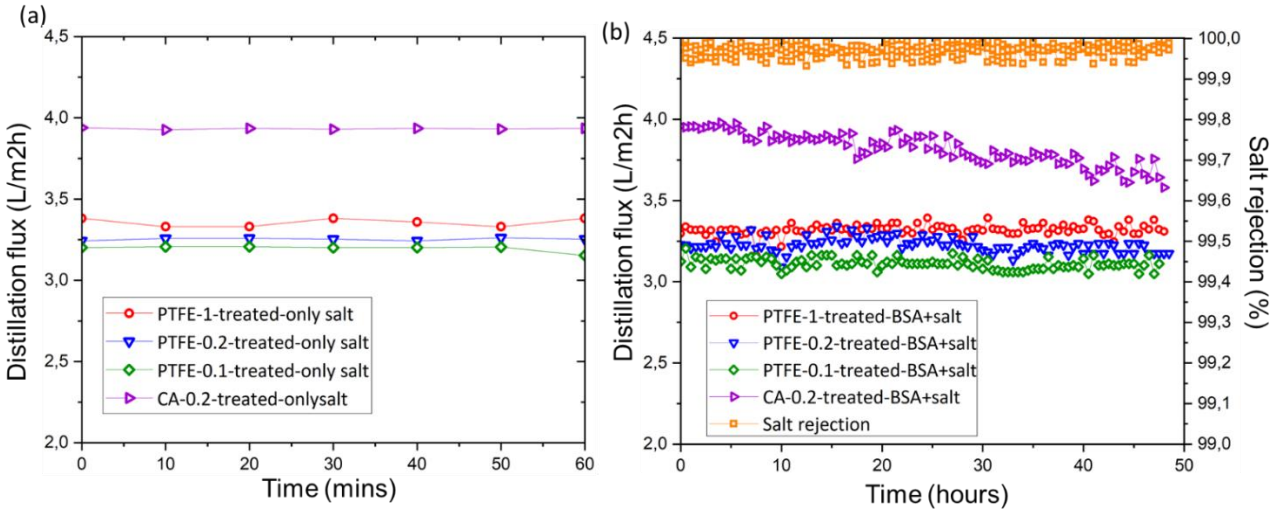

Figure 54: (a) AGMD distillation flux as a function of time for plasma-treated PTFE 0.1, 0.2, 1 µm, and CA 0.2 membranes using only salt in the feed solution. (b) AGMD distillation flux as a function of time for plasma-treated PTFE 0.1, 0.2, 1 µm, and CA 0.2 membranes using BSA and salt in feed solution at T_f of 53 ^oC and T_c of 15 ^oC.

For examining the biofilm formation, we did SEM for the samples after AGMD. It was observed that in the case of untreated PTFE-0.1, there is an additional layer of BSA forming on the membrane surface covering the pores hence explaining the decline in flux during MD (Figure 55 a,b). On the contrary for treated PTFE-0.1, we observe crystals of salt depositions on the membrane surface which is observed only when BSA combines with salt during MD (Figure 55 c,d). These crystals cover the membrane surface leaving a place in between, so flux decline is not as severe as in the case of untreated PTFE 0.1.

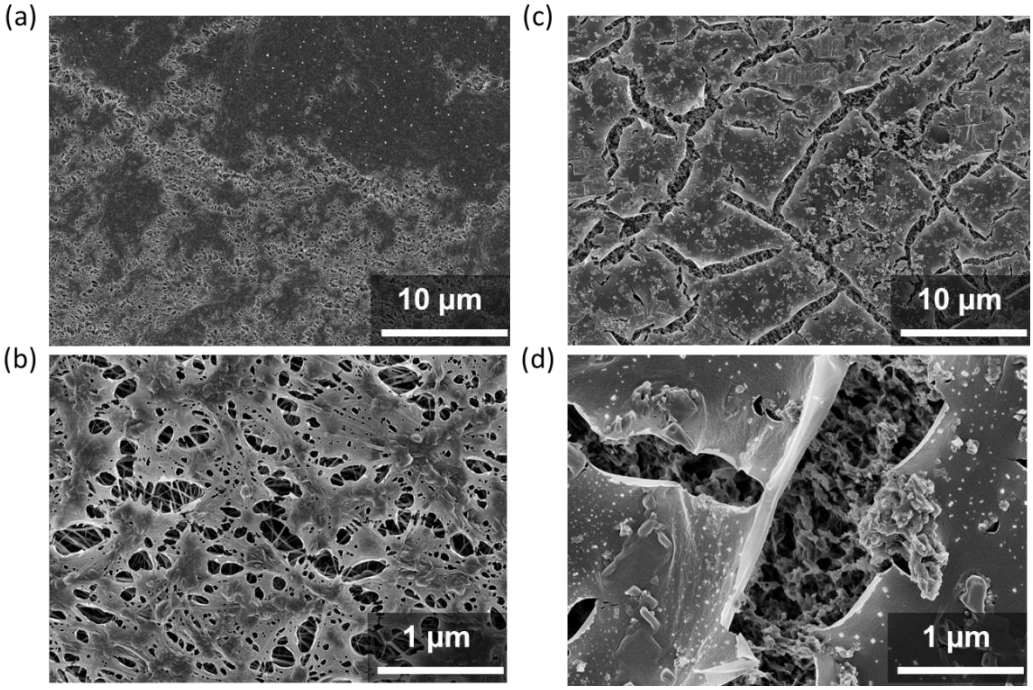

Figure 55: SEM images for (a, b) Untreated PTFE-0.1 (c,d) Treated PTFE-0.1 after AGMD with BSA and salt for 48 hours.

Also for treated CA-0.2 membranes after AGMD, we observed similar morphology of salt crystals and BSA depositions on the membrane surface (Figure 56 c,d)

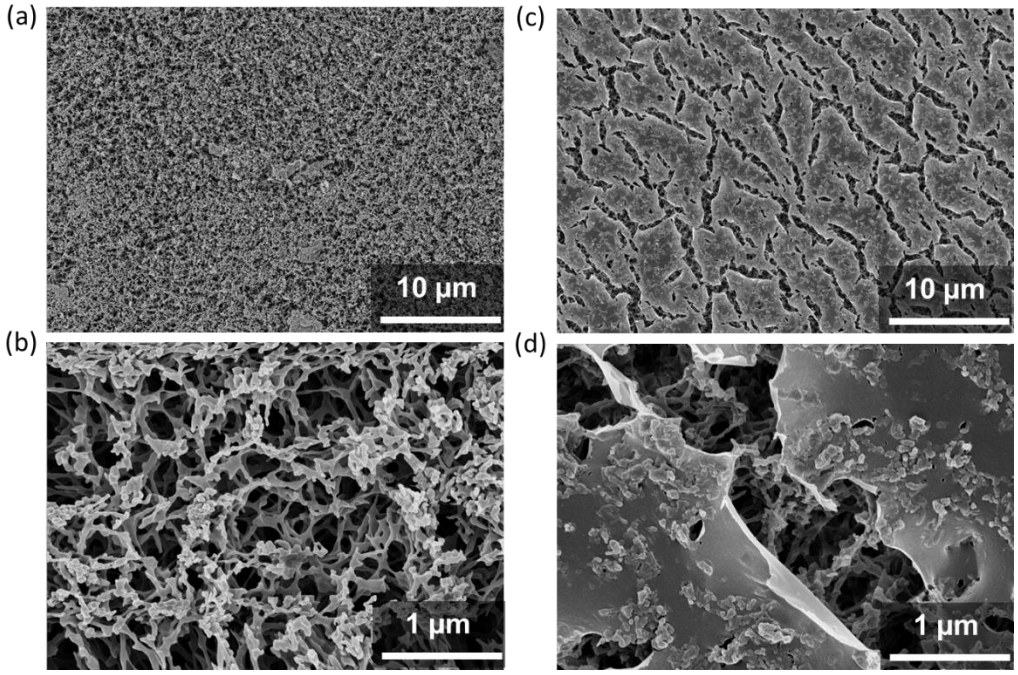

Figure 56: SEM images for (a,b) Untreated CA-0.2 before AGMD (c,d) Treated CA-0.2 after AGMD with BSA and salt for 48 hours.

5.1.4 SDS fouling – Plasma treated membranes

For investigating the anti-wetting properties of the membranes during AGMD, in presence of low surface tension surfactants in the feed solution we used 0.01 mM of SDS with 0.59 M NaCl. The surface tension of this combination is ~ 55 mN/m. The temperatures used here are T_f: 65°C and T_c: 15°C. The feed and distillate volumes were 1 L/min and 2 L/min respectively. All the AGMD experiments were carried out over 48 hours to test the durability for long-term operation.

Figure 57 shows SDS fouling results for PTFE-0.1 membranes untreated and treated ones provided by Demokritos. The range of distillation flux for both membranes was similar for 48 hours experiment, although untreated PTFE-0.1 showed partial wetting as the conductivity of water produced increased to ~ 300 µS/cm in 15 hours and then stays constant over 48 hours experiment. Conversely, for treated PTFE-0.1 membranes, the conductivity of distillate produced lies in the distilled water range for the complete 48 hours experiment.

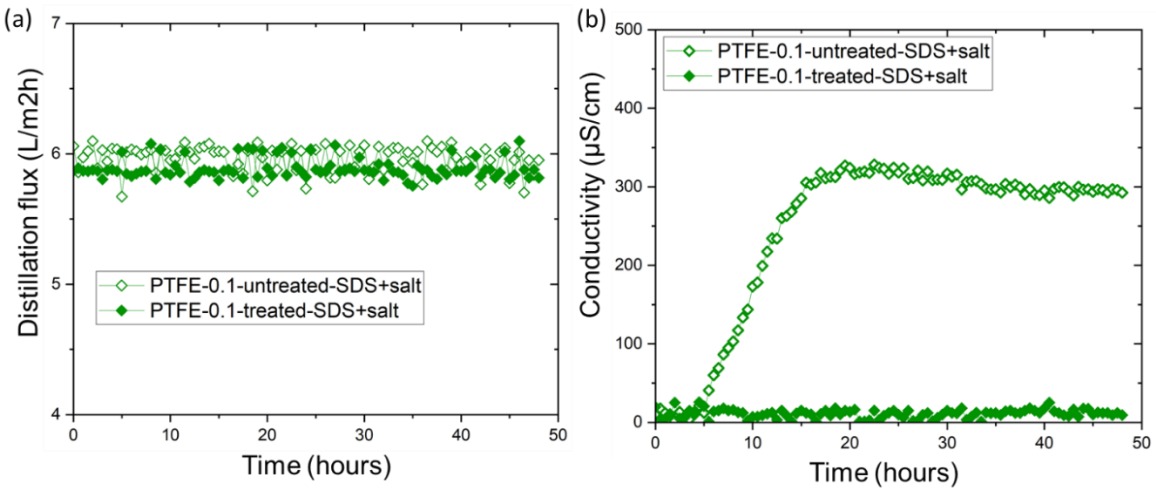

Figure 57: (a) AGMD distillation flux as a function of time (b) Change in distillate conductivity as a function of time for untreated and treated PTFE-0.1 membranes during AGMD with salt and SDS in feed solution at T_f of 65 °C and T_c of 15 °C.

5.2 MOFs coated membranes

Metal-organic frameworks (MOFs) are nanomaterials that exhibit hierarchical structures with multi-level roughness. In combination with suitable surface chemistry, they can be used to create superhydrophobic surfaces. Along with NF-coated and plasma-treated membranes, we have also tested of Nylon-0.22 membranes with a pore size of 0.22 µm & 1.2 µm, which were coated with MOFs by our UCL partners. All samples are coated with MOFs (UIO-66-OH) via layer by layer technique and then MOFs were post-functionalized with long alkyl chains (octadecyl silane) to alter the wettability.

5.2.1 SEM images-MOFs-coated membranes

MOFs treated Nylon membranes show a characteristic increase in surface roughness with highly organized and regular surface morphology (Figure 58).

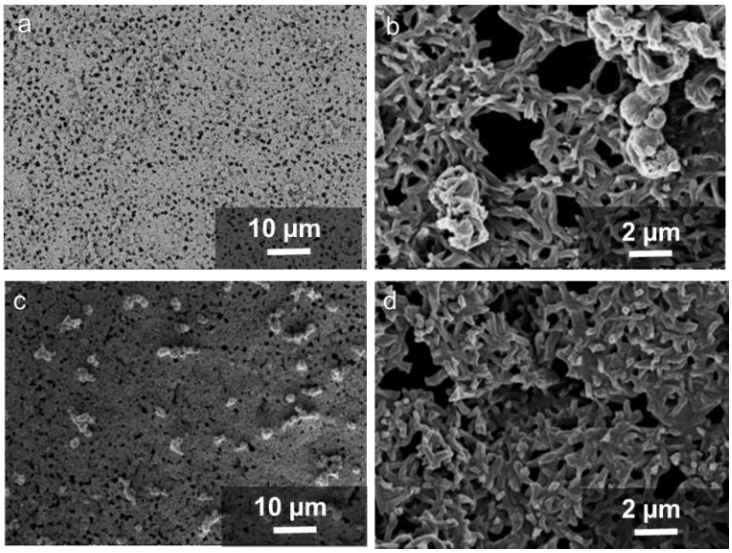

Figure 58: SEM images of (a, b) original Nylon membranes with pore size of 0.22 µm and (c, d) MOFs coated Nylon-0.22 membrane. Images b and d are magnified versions of a, and c respectively.

5.2.2 Liquid entry pressure of MOFs-coated membranes

The hydrophobic surface chemistry of the MOFs in combination with their rough structure is expected to improve the liquid repellency of the membranes. We found a liquid entry pressure of 4.3 bar for MOFs treated Nylon 0.22 membrane, which indicates good wetting resistance and is high enough to conduct the MD experiments (threshold pressure of 1.5 bar). However, for a larger pore size of 1.2 µm, MOFs treated membrane show an LEP value of ~2 bar which is very close to the threshold value and hence easy to wet during MD experiments Table 5.

Table 5: LEP values for MOFs coated membranes

Membrane	LEP (bar)
Nylon 0.22	4.3 ± 0.6
Nylon 1.2	2.1 ± 0.1

5.2.3 Gas permeability tests

Figure 59 shows the measured gas permeation flux as a function of the transmembrane pressure for original and MOFs coated nylon membranes. MOFs coated membranes show 55% lower permeation flux at 70 mbar in comparison to the original Nylon-0.22 membrane. Although for MOFs treated Nylon 1.2 membranes, there is ~56 to 70 % decrease in gas permeation flux compared to the original membrane.

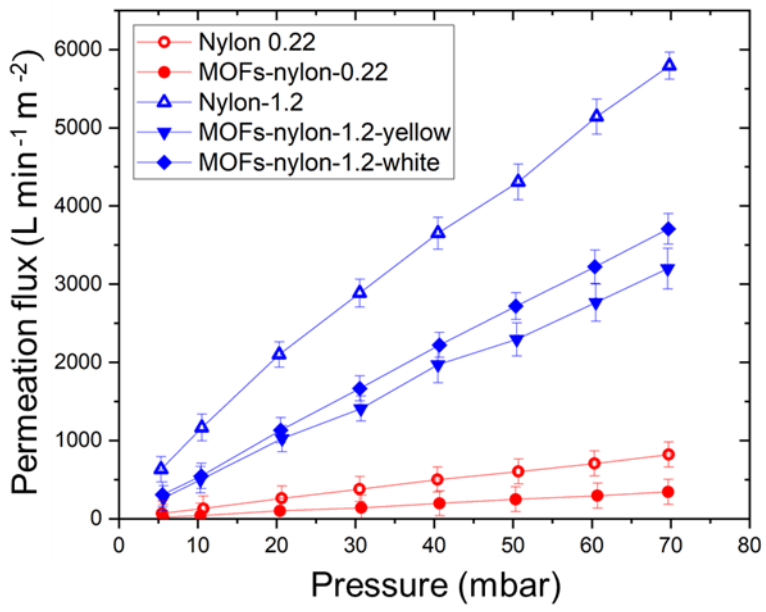

Figure 59: Gas permeability tests of MOF-coated Nylon 0.22 µm membranes.

5.2.4 Standard desalination – MOF-coated nylon membranes

MOF-coated membranes were tested using the custom-made AGMD setup in MPIP. All the MD experiments were carried out over 48 hours to test the membrane's durability for long-term operation.

Figure 60 presents the MD flux and conductivity for permeate versus time for two MOF-coated Nylon 0.22 membranes. In the case of MOFs-1 nylon 0.22 the first sample, MD flux is stable at ~8.2 L/m^{2}h for 48 hours experiment and the conductivity of permeate lies in the distilled water range for the initial 15 hours of the experiment and later gradually increases and reaches ~200 µS/cm at the end of the experiment which is still in the range of drinking water (< 500 µS/cm). The reason for the fluctuations in the distillation flux is because of setup errors during the experiment. For MOFs-2 nylon 0.22 the second sample, MD flux is steady for initial 30 hours at ~7 L/m^{2}h. After 30 hours the membrane completely gives up and the conductivity increases to ~6000 µS/cm, even the flux increases and goes above 8 L/m^{2}h which later decreases can be due to blockage of the pores.

For MOFs treated nylon 1.2, we had 2 samples white and yellow from UCL. In the case of a white sample the flux was stable at ~8.6 L/m^{2}h, and conductivity continuously increases over time from ~150 µS/cm to ~650 µS/cm over 48 hours of the experiment. On the contrary, the yellow sample also shows a stable flux of ~8.5 L/m^{2}h, and the conductivity of distillate stays in the distilled water range for initial 25 hours and later increases to ~200 µS/cm.

The addition of MOFs to the membrane with 0.2 µm pore size increases the resistance to vapor diffusion and results in lower flux. This is also observed from the results obtained in gas permeability data (Figure 59).

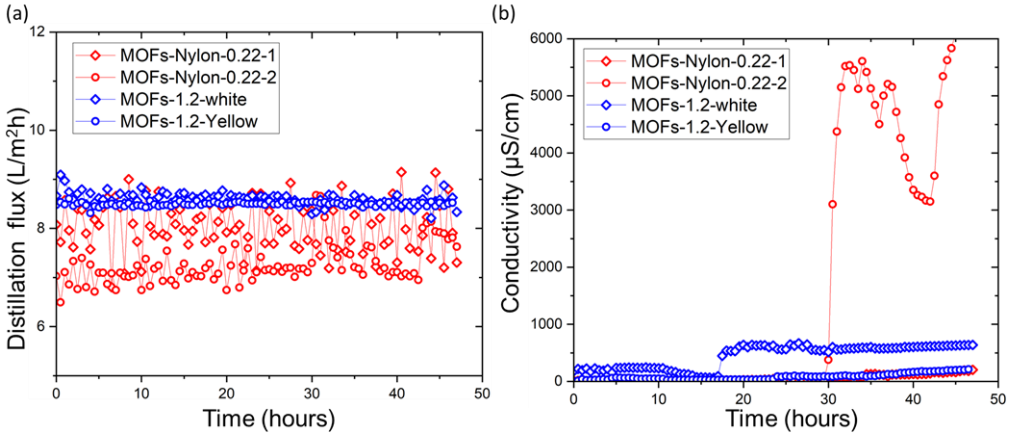

Figure 60: (a) Experimental distillation flux as a function of time. (b) Change in distillate conductivity as a function of time.

We can therefore conclude that MOFs-coating of nylon membranes increases their wetting resistance far enough to allow their use for membrane distillation. However, the wetting resistance is not as reliable as needed for longer-term operation. Therefore, we did not continue with the use of MOF-coated membranes but rather focused on the NF-coated PES membranes and plasma-treated PTFE membranes, which showed clearly better performance.

6 Summary and Outlook

6.1 Summary

Global desalination capacity has grown dramatically in recent decades to fight water shortage in areas where water availability and demand differ. Currently, the desalination sector is virtually entirely based on non-sustainable, industrial-scale methods, with no answer to the genuine water scarcity in rural regions. As a result, one of the primary problems in overcoming water constraint is the development of small-scale, self-sufficient, and ecologically acceptable desalination technologies. Thermally powered membrane distillation has been recognized as a viable decentralized desalination technique. However, MD has yet to be commercialized, necessitating further scientific study into material, module, and system development. The adaptation of membrane module design to unique project needs has a high potential for improvement.

Membrane distillation has been demonstrated to be a viable separation method not only for water purification applications in industrial process water production, but also for recovering valuable by-products and eliminating contaminants from wastewater effluents. In accordance with the study presented in the first chapter of the thesis, we offered a quick summary of some of the existing desalination technologies on the market, with a focus on membrane distillation. The major objective of the thesis was to analyze important barriers affecting the performance of MD systems, hence a complete literature study for membrane distillation was covered. The first obstacle is lower distillation flux, as well as possible membrane fouling and wetting issues.

We were able to create a coating technique for superhydrophobic composite membranes with enhanced desalination performance. These membranes are based on commercial membranes with larger pore diameters than are typically used in membrane distillation. These newly constructed composite membranes displayed remarkable endurance of super liquid-repellency throughout a prolonged water immersion test without the need of any fluorine-containing chemicals. Our NF-coated membranes demonstrated better liquid entry pressure (>11.5 bar) and high distillation flux in AGMD and DCMD tests over a 7-day period due to their unique multi-scale porous structures. In standard desalination, it can be

demonstrated that NF-coated membranes outperform commercial MD membranes currently available (e.g., PE and PTFE).

In order to clearly summarize membrane performance for water desalination, we compared the specific distillation flux of the NF-PES membrane with previous studies of AGMD and DCMD, as shown in Figure 61. Here, the specific distillation flux is defined as the ratio of distillation flux to the vapor pressure difference across the membrane. Due to the insufficient reported data in the literature, we compared the salt rejection of the membranes in AGMD tests and the LEP of the membranes in DCMD tests. As indicated in Figure 61 a, the NF-PES membrane demonstrates top-tier performance in both specific distillation flux and salt rejection, which were not achieved simultaneously in previous reports of AGMD tests. Figure 61 b shows a similar result that the NF-PES membrane effectively enhances the specific distillation flux of the DCMD without compromising the LEP. The multi-scale porous structure apparently strikes a better balance between rapid desalination and high salt rejection, which is necessary for commercial MD installation.

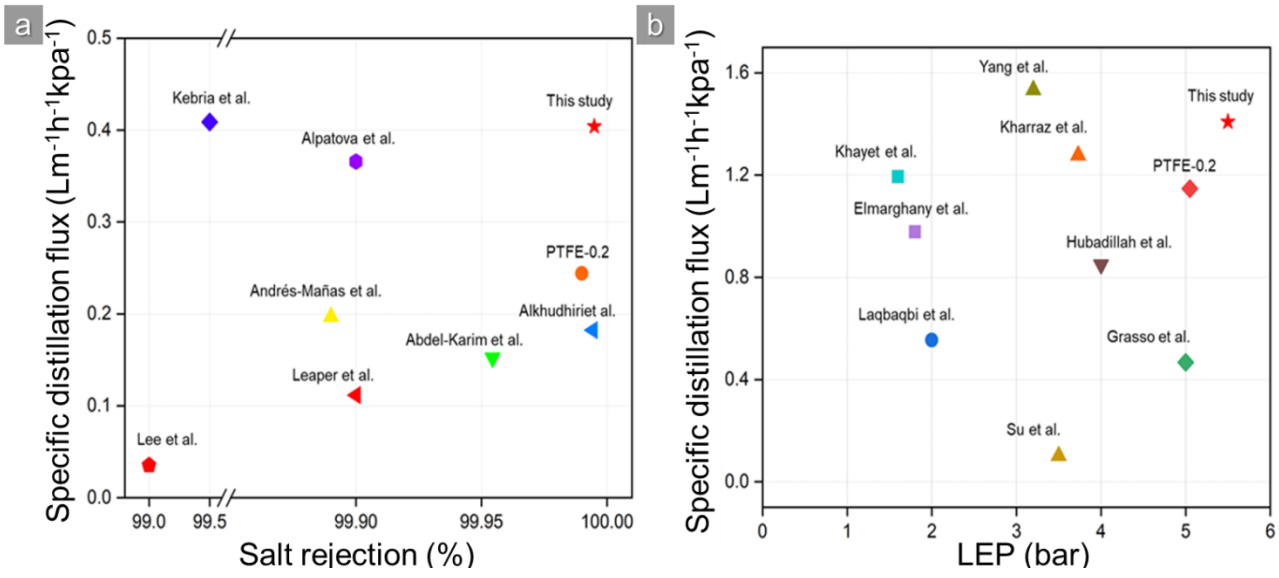

Figure 61: Comparison of the (A) AGMD and (B) DCMD performances of the nanofilament-coated membrane (this study) with various previous reports. For the AGMD test, the NF-PES membrane can simultaneously achieve high specific distillation flux and high salt rejection. Similarly, the NF-PES membrane effectively enhanced the distillation flux in the DCMD test without compromising the liquid entry pressure (LEP) [14, 21, 43, 90, 137-145].

Aside from determining the performance feasibility of an MD system for small-scale drinking water production, a complete study of scaling and organic fouling development in MD

operation is required. Membrane fouling has emerged as one of the most significant issues confronting the RO system as a hydraulically stressed membrane process. The absence of hydraulic pressure in MD, on the other hand, is advantageous for loose fouling deposition. The existence of temperature conditions in MD, on the other hand, contributes to a complicated scaling development. A number of research have been conducted to study the relationship between scaling development and MD thermal operations. As a result, the inquiry in this study focused on analyzing fouling resistance using model pollutants.

As a model substance for organic contaminants, we used BSA. The surfactant SDS was employed to study the effect of contaminants that reduce surface tension. Fouling and wetting resistance of all our membranes was found to be at least on par and in most cases exceeding the antifouling properties of the commercial PTFE membranes. This was evident from adsorption and wetting tests such as FTIR spectroscopy, contact angle measurements after immersion tests, and confocal laser scanning microscopy imaging. Most important were of course the performance tests in membrane distillation themselves. Here excellent anti-fouling properties of NF-coated PES membranes during AGMD were found in presence of BSA, exhibiting increased and stable distillate flux and minimized BSA protein deposition on the membrane surface, exceeding the performance of commercial PTFE membranes. The anti-wetting properties of the membranes were also tested using surfactant SDS, and our fabricated NF-coated membranes showed almost 17% higher water distillate flux in presence of SDS while having at least the same wetting resistance as the PTFE-0.2 membrane.

6.2 Outlook

The MD method has mostly been utilized for desalination; nevertheless, water recovery from wastewater streams from industries is one of the most potential future uses of MD. While it is capable of treating a wide range of wastes and brines, its potential to compete with existing technologies such as RO and thermal-based water treatment technologies is still restricted owing to a lack of pilot-scale experimental data and particular membranes and modules. Finding new and viable applications for the MD process, on the other hand, appears to be one of the greatest hurdles to its commercial adoption.

Furthermore, there is another significant barrier to MD being used for wastewater treatment. Wastewater streams often contain a wide range of compounds that can cause membrane

surface fouling and membrane pore wetting. This is because the deposition of these contaminants on the membrane surface may make the membrane less hydrophobic, resulting in pore wetting and a decrease in flux. This is why few studies on wastewater treatment with MD are compared to desalination. As a result, one of the attractive future prospects is the fabrication of specialized membranes for MD use in wastewater processing. Other resource recovery applications for membrane distillation include brine concentration, the concentration of fruit juices, radioactive solutions, acids, and volatile organic compounds, removal of heavy metals and colors, wastewater treatment, and so on.

The implementation of these hierarchical porous membranes will expand the spectrum of water treatment applications. As demonstrated in this work, NF-coated membranes were evaluated for wetting capabilities with low surface tension liquids as well as after immersion in 18% HCl. NF-coated PES membranes appear to be the best choice even in such extreme environments with low surface tension liquids. However, for strong acids, NF-PVDF and NF-PTFE appear to be better choices, and when pore diameters are greater, such as NF-PTFE-1, they can even provide higher flux with less fouling. For future work, we intend to first scale up the NF-coated membrane to A4 size by using a similar technology then also on rolls of membranes to undertake a speedier roll-to-roll procedure with the assistance of SuperClean project collaborators.

References

1. Arun Subramani and Joseph Jacangelo, Emerging desalination technologies for water treatment: A critical review. Water research, 2015. **75**: p. 164-187.

2. Anshul Yadav, Pawan Labhasetwar and Vinod Shahi, Membrane distillation using low-grade energy for desalination: A review. Journal of Environmental Chemical Engineering, 2021. **9**: p. 105818.

3. Natasha Darre and Gurpal Toor, Desalination of Water: a Review. Current pollution reports, 2018. **4**: p. 101-111.

4. Domenico Curto, Vincenzo Franzitta and Andrea Guercio, A Review of the Water Desalination Technologies. Applied sciences, 2021. **11**: p. 670.

5. Pratiksha Dongare, Alessandro Alabastri, Seth Pedersen, Katherine Zodrow, Nathaniel Hogan, Oara Neumann, Jinjian Wud, Tianxiao Wang, Akshay Deshmukh, Menachem Elimelech, Qilin Li, Peter Nordlander and Naomi Halas, Nanophotonics-enabled solar membrane distillation for off-grid water purification. PNAS, 2017. **114**: p. 27.

6. Younes Ghalavand, Mohammad Hatamipour and Amir Rahimi, A review on energy consumption of desalination processes. Desalination and Water Treatment, 2014: p. 1944-3994.

7. Ioannis Karagiannis and Petros Soldatos, Water desalination cost literature: review and assessment. Desalination, 2008. **223**: p. 448-456.

8. Dongwei Lu, Qianliang Liu, Yumeng Zhao, Huiling Liu and Jun Ma, Treatment and energy utilization of oily water via integrated ultrafiltration forward osmosis–membrane distillation (UF-FO-MD) system. Journal of Membrane Science, 2018. **548**: p. 275-287.

9. Enrico Drioli, Aamer Ali and Francesca Macedonio, Membrane distillation: Recent developments and perspectives. Desalination, 2015. **356**: p. 56-84.

10. Akshay Deshmukh, Chanhee Boo, Vasiliki Karanikola, Shihong Lin, Anthony Straub, Tiezheng Tong, David Warsinger and Menachem Elimelech, Membrane distillation at the water-energy nexus: limits, opportunities, and challenges. Energy & Environmental Science, 2018. **11**(1177).

11. Edward Summers, Hassan Arafat and John Lienhard, Energy efficiency comparison of single-stage membrane distillation (MD) desalination cycles in different configurations. Desalination, 2012. **290**: p. 54-66.

12. Parisa Biniaz, Niloofar Ardekani, Mohammad Makarem and Mohammad Rahimpour, Water and Wastewater Treatment Systems by Novel Integrated Membrane Distillation (MD). Chemengineering, 2019. **3**: p. 8.

13. Melfreya Findley, Vaporization through membrane pores. Industrial & Engineering Chemistry Process Design and Development, 1967. **6(2)**: p. 226-230.

14. Abdullah Alkhudhiri, Naif Darwish and Nidal Hilal, Membrane distillation: A comprehensive review. Desalination, 2012. **287**: p. 2-18.

15. Enrico Drioli, Aamer Ali and Francesca Macedonio, Membrane distillation: Recent developments and perspectives. Desalination, 2015. **356**: p. 56-84.

16. Mohamed Shalouf, El-Bourawi, Zhongwei Ding, Runyu Ma and Mohamed Khayet, A framework for better understanding membrane distillation separation process. Journal of Membrane Science, 2006. **285**: p. 4-29.

17. Kevin Lawson and Douglas Lloyd, Membrane distillation. Journal of membrane science, 1997. **124**: p. 1-25.

18. Mohamed Khayet and Takeshi Matsuura, Pervaporation and Vacuum Membrane Distillation Processes: Modeling and Experiments. AIChE Journal, 2004. **50(8)**: p. 1697-1712.

19. Sen Hsu, Kung Cheng and Jenq Chiou, Seawater desalination by direct contact membrane distillation. Desalination, 2002. **143**: p. 279-287.

20. Lucy Camacho, Ludovic Dumée, Jianhua Zhang, Jun-De Li, Mikel Duke and Juan Gomez, Advances in Membrane Distillation for Water Desalination and Purification Applications. Water Purification/Harvesting, 2013. **5**: p. 94-196.

21. Mohamed Khayet, Membranes and theoretical modeling of membrane distillation: A review. Advances in Colloid and Interface Science, 2011. **164**: p. 56-88.

22. Heru Susanto, Towards practical implementations of membrane distillation. Chemical Engineering and Processing: Process Intensification, 2011. **50**: p. 139-150.

23. Navya Thomas, Musthafa Mavukkandy, Savvina Loutatidou and Hassan Arafat, Membrane distillation research & implementation: Lessons from the past five decades. Separation and Purification Technology, 2017. **189**: p. 108-127.

24. Quist-Jensen, Cejna Anna, Francesca Macedonio, Carmela Conidi, Alfredo Cassano, Saad Aljlil, Omar Alharbi and Enrico Drioli, Direct contact membrane distillation for the concentration of clarified orange juice. Journal of Food Engineering, 2016. **187**: p. 37-43.

25. Maria Tomaszewska, Marek Gryta and Antoni Morawski, Recovery of hydrochloric acid from metal pickling solutions by membrane distillation. Separation and Purification Technology, 2001. **22-23**: p. 591-600.

26. Xuan Feng, Lan Jiang and Yang Song, Titanium white sulfuric acid concentration by direct contact membrane distillation. Chemical Engineering Journal, 2016. **285**: p. 101-111.

27. Daniel Woldemariam, Alaa Kullab, Ershad Khan and Andrew Martin, Recovery of ethanol from scrubber-water by district heat-driven membrane distillation: Industrial-scale technoeconomic study. Renewable Energy, 2018. **128**: p. 484-494.

28. Ershad Khan and Andrew Martin, Water purification of arsenic contaminated drinking water via air gap membrane distillation (AGMD). Periodica Polytechnica Mechanical Engineering, 2013. **58(1)**: p. 47-53.

29. Hung Duong, Paul Cooper, Bart Nelemans, Tzahi Cath and Long Nghiem, Evaluating energy consumption of air gap membrane distillation for seawater desalination at pilot scale level. Separation and Purification Technology, 2016. **166**: p. 55-62.

30. Abu-Zeid, Mostafa Rady, Yaqin Zhang, Hang Dong, Lin Zhang, Huan Chen and Lian Hou, A comprehensive review of vacuum membrane distillation technique. Desalination, 2015. **356**: p. 1-14.

31. Jiao Shi, Zhi Zhao and Chun Zhu, Studies on simulation and experiments of ethanol–water mixture separation by VMD using a PTFE flat membrane module. Separation and Purification Technology, 2014. **123**: p. 53-63.

32. Jingwen Chen, Yaqin Zhang, Yafei Wang, Xiaosheng Ji, Lin Zhang, Xigeng Mi and He Huang, Removal of inhibitors from lignocellulosic hydrolyzates by vacuum membrane distillation. Bioresource Technology, 2013. **144**: p. 680-683.

33. Rosalam Sarbatly and Chel Chiam, Evaluation of geothermal energy in desalination by vacuum membrane distillation. Applied Energy, 2013. **112**: p. 737-746.

34. El Bourawi, Mohamed Khayet, Runyu Ma, Zhongwei Ding, Zhaoman Lia and Xinmiao Zhang, Application of vacuum membrane distillation for ammonia removal. Journal of Membrane Science, 2007. **301**: p. 200-209.

35. Luca Basini, Gabriele Angelo, Marco Gobbi, Giulio Sarti and Carlo Gostoli, A desalination process through sweeping gas membrane distillation. Desalination, 1987. **64**: p. 245-257.

36. Mohamed Khayet, Paz Godino and Juan Mengual, Theory and experiments on sweeping gas membrane distillation. Journal of Membrane Science, 2000. **165**: p. 261-272.

37. Lies Eykens, Ivaylo Hitsov, Kristien Sitter, Chris Dotremont, Luc Pinoy and Bart Bruggen, Direct contact and air gap membrane distillation: Differences and similarities between lab and pilot scale. Desalination, 2017. **422**: p. 91-100.

38. Lies Eykens, Tim Reyns, Kristien Sitter, Chris Dotremont, Luc Pinoy and Bart Bruggen, How to select a membrane distillation configuration? Process conditions and membrane influence unraveled. Desalination, 2016. **399**: p. 105-115.

39. Jian Zuo, Tai Chung, Gregory O'brien and Walter Kosar, Hydrophobic/hydrophilic PVDF/Ultem® dual-layer hollow fiber membranes with enhanced mechanical properties for vacuum membrane distillation. Journal of Membrane Science, 2017. **523**: p. 103-110.

40. Hyunho Kim, Taekgeun Yun, Seungkwan Hong and Seockheon Lee, Experimental and theoretical investigation of a high performance PTFE membrane for vacuum-membrane distillation. Journal of Membrane Science, 2020. **617**: p. 118524.

41. Alicia An, Jiaxin Guo, Eui Lee, Sanghyun Jeong, Yanhua Zhao, Zuankai Wang and Torove Leiknes, PDMS/PVDF hybrid electrospun membrane with superhydrophobic property and drop impact dynamics for dyeing wastewater treatment using membrane distillation. Journal of Membrane Science, 2017. **525**: p. 57-67.

42. Anish Tuteja, Wonjae Choi, Minglin Ma, Joseph Mabry, Sarah Mazzella, Gregory Rutledge, Gareth Mckinley and Robert Cohen, Designing Superoleophobic Surfaces. SCIENCE, 2007. **318**(1618).

43. Chi Yang, Xue Li, Jack Gilron, Ding Kong, Yong Yin, Yoram Oren, Charles Linder and Tao He, CF_4 plasma-modified superhydrophobic PVDF membranes for direct contact membrane distillation. Journal of Membrane Science, 2014. **456**: p. 155-161.

44. Gábor Rácz, Steffen Kerker, Zoltán Kovács, Gyula Vatai, Mehrdad Ebrahimi and Peter Czermak, Theoretical and Experimental Approaches of Liquid Entry Pressure Determination in Membrane Distillation Processes. Periodica Polytechnica Chemical Engineering 2014. **58(2)**: p. 81-91.

45. Sara Claramunt, Florian Völker, Uta Gerhards, Manfred Kraut and Roland Dittmeyer, Membranes for the Gas/Liquid Phase Separation at Elevated Temperatures: Characterization of the Liquid Entry Pressure. Membranes, 2021. **11**: p. 907.

46. Allyson Mcgaughey, Prathamesh Karandikar, Malancha Gupta, and Amy Childress, Hydrophobicity versus Pore Size: Polymer Coatings to Improve Membrane Wetting Resistance for Membrane Distillation. ACS Appl. Polym. Mater, 2020. **2**: p. 1256-1267.

47. Jirachote Phattaranawik, Ratana Jiraratananon and Tony Fane, Effect of pore size distribution and air flux on mass transport in direct contact membrane distillation. Journal of Membrane Science, 2003. **215**: p. 75-85.

48. Jason Woods, John Pellegrino and Jay Burch, Generalized guidance for considering pore-size distribution in membrane distillation. Journal of Membrane Science, 2011. **368**: p. 124-133.

49. Marek Gryta, Influence of polypropylene membrane surface porosity on the performance of membrane distillation process. Journal of Membrane Science, 2007. **287**: p. 67-78.

50. Woo-Ju Kim, Osvaldo Campanella and Dennis Heldman, Predicting the performance of direct contact membrane distillation (DCMD): Mathematical determination of appropriate tortuosity based on porosity. Journal of Food Engineering, 2021. **294**: p. 110400.

51. Ingrid Curcino, Costa Júnior, Cárdenas Gómez, Peñaranda Chenche, J. Lima, Naveira-Cotta and Renato Cotta, Analysis of effective thermal conductivity and tortuosity modeling in membrane distillation simulation. Micro and Nano Engineering, 2022. **17**: p. 100165.

52. Lies Eykens, Ivaylo Hitsov, Kristien Sitter, Chris Dotremont, Luc Pinoy and Bart Bruggen, Influence of membrane thickness and process conditions on direct contact membrane distillation at different salinities. Journal of Membrane Science, 2016. **498**: p. 353-364.

53. Lourdes Martinez and Rodriguez-Maroto, Membrane thickness reduction effects on direct contact membrane distillation performance. Journal of Membrane Science, 2008. **312**: p. 143-156.

54. Marek Gryta and Marta Barancewicz, Influence of morphology of PVDF capillary membranes on the performance of direct contact membrane distillation. Journal of Membrane Science, 2010. **358**: p. 158-167.

55. Ho Wu, Rong Wang and Robert Field, Direct contact membrane distillation: An experimental and analytical investigation of the effect of membrane thickness upon transmembrane flux. Journal of Membrane Science, 2014. **470**: p. 257-265.

56. Efrem Curcio and Enrico Drioli, Membrane Distillation and Related Operations—A Review. Separation and Purification Reviews, 2005. **34**: p. 35-86.

57. Lies Eykens, Kristien Sitter, Chris Dotremont, Luc Pinoy and Bart Bruggen, Membrane synthesis for membrane distillation: A review. Separation and Purification Technology, 2017. **182**: p. 36-51.

58. Yuan Liao, Guangtai Zheng, Jinhui Huang, Miao Tian and Rong Wang, Development of robust and superhydrophobic membranes to mitigate membrane scaling and fouling in membrane distillation. Journal of Membrane Science, 2020. **601**: p. 117962.

59. Ali Boubakria, Amor Hafianea and Salah Bouguecha, Nitrate removal from aqueous solution by direct contact membrane distillation using two different commercial membranes. Desalination and Water Treatment, 2014: p. 1-8.

60. Lourdes Martinez and Isabel Gonzàlez, Temperature and concentration polarization in membrane distillation of aqueous salt solutions. Journal of Membrane Science, 1999. **156**: p. 265-273.

61. Jirachote Phattaranawik, Ratana Jiraratananon and Tony Fane, Heat transport and membrane distillation coefficients in direct contact membrane distillation. Journal of Membrane Science, 2003. **212**: p. 177-193.

62. Lijo Francis, Noreddine Ghaffour, Ahmad Alsaadi and Gary Amy, Material gap membrane distillation: A new design for water vapor flux enhancement. Journal ofMembraneScience, 2013. **448**: p. 240-247.

63. Marek Gryta, Maria Tomaszewska and Krzysztof Karakulski, Wastewater treatment by membrane distillation. Desalination, 2006. **198**: p. 67-73.

64. Lourdes Martinez, Comparison of membrane distillation performance using different feeds. Desalination, 2004. **168**: p. 359-365.

65. Lourdes Martinez and Florido-Diaz, Theoretical and experimental studies on desalination using membrane distillation. Desalination, 2001. **139**: p. 373-379.

66. Amira Alkhatib, Mohamed Ayari and Alaa Hawari, Fouling mitigation strategies for different foulants in membrane distillation. Chemical Engineering and Processing - Process Intensification, 2021. **167**(108517).

67. David Warsinger, Jaichander Swaminathan, Elena Burrieza, Hassan Arafat and John Lienhard, Scaling and fouling in membrane distillation for desalination applications: A review. Desalination, 2015. **356**: p. 294-313.

68. Marek Gryta, Fouling in direct contact membrane distillation process. Journal of Membrane Science, 2008. **325**: p. 383-394.

69. Mahbuboor Choudhury, Nawrin Anwar, David Jassby and Md Rahaman, Fouling and wetting in the membrane distillation driven wastewater reclamation process – A review. Advances in Colloid and Interface Science, 2019. **269**: p. 370-399.

70. Mohamed Khayet and Juan Mengual, Effect of salt concentration during the treatment of humic acid solutions by membrane distillation. Desalination, 2004. **168**: p. 373-381.

71. Gayathri Naidu, Sanghyun Jeong, Sung Kim, In Kim and Saravanamuthu Vigneswaran, Organic fouling behavior in direct contact membrane distillation. Desalination, 2014. **347**: p. 230-239.

72. Gayathri Naidu, Sanghyun Jeong, Saravanamuthu Vigneswaran, Tae Hwang, Yong Choi and Seung Kim, A review on fouling of membrane distillation. Desalination and Water Treatment, 2015: p. 1-25.

73. Leonard Tijing, Yun Woo, June Choi, Sangho Lee, Seung Kim and Ho Shon, Fouling and its control in membrane distillation—A review. Journal of MembraneScience, 2015. **475**: p. 215-244.

74. Shengying Yang, Saade Jasim, Dmitry Bokov, Supat Chupradit, Ali Nakhjiri and El-Shafay, Membrane distillation technology for molecular separation: A review on the fouling, wetting and transport phenomena. Journal of Molecular Liquids, 2022. **349**: p. 118115.

75. Thomas Horseman, Yiming Yin, Kofi Christie, Zhangxin Wang, Tiezheng Tong and Shihong Lin, Wetting, Scaling, and Fouling in Membrane Distillation: State-of the-Art Insights on Fundamental Mechanisms and Mitigation Strategies. ACS EST Engineering, 2021. **1**: p. 117-140.

76. David Warsinger, Amelia Servi, Sarah Belleghem, Jocelyn Gonzalez, Jaichander Swaminathan, Jehad Kharraz, Hyung Chung, Hassan Arafat, Karen Gleason and John Lienhard, Combining air recharging and membrane superhydrophobicity for fouling prevention in membrane distillation. Journal ofMembraneScience, 2016. **505**: p. 241-252.

77. Wenwei Zhong, Jingwei Hou, Hao Yang and Vicki Chen, Superhydrophobic membranes via facile bio-inspired mineralization for vacuum membrane distillation. Journal of Membrane Science, 2017. **540**: p. 98-107.

78. Zhe Dong, Xiao Ma, Zhen Xu and Zhi Gu, Superhydrophobic modification of PVDF–SiO_2 electrospun nanofiber membranes for vacuum membrane distillation. RSC advances, 2015. **5**: p. 67962.

79. Kevin Lawson and Douglas Lloyd, Review Membrane distillation. Journal of Membrane Science, 1997. **124**: p. 1-25.

80. Pei Goh, Woei Lau, Mohd Othman and Ahmad Ismail, Membrane fouling in desalination and its mitigation strategies. Desalination, 2018. **425**: p. 130-155.

81. Marek Gryta, Concentration of saline wastewater from the production of heparin. Desalination, 2000. **129**: p. 35-44.

82. Krzysztof Karakulski and Marek Gryta, Water demineralisation by NF/MD integrated processes. Desalination, 2005. **177**: p. 109-119.

83. Le Han, Yong Tan, Tanmay Netke, Anthony Fane and Jia Chew, Understanding oily wastewater treatment via membrane distillation. Journal of Membrane Science, 2017. **539**: p. 284-294.

84. Leihong Zhao, Liguo Shen, Yiming He, Huachang Hong and Hongjun Lin, Influence of membrane surface roughness on interfacial interactions with sludge flocs in a submerged membrane bioreactor. Journal of Colloid and Interface Science, 2015. **446**: p. 84-90.

85. Marek Gryta, Effect of iron oxides scaling on the MD process performance. Desalination, 2007. **216**: p. 88-102.

86. Mohammad Rezaei, David Warsinger, John Lienhard and Wolfgang Samhaber, Wetting prevention in membrane distillation through superhydrophobicity and recharging an air layer on the membrane surface. Journal of Membrane Science, 2017. **530**: p. 42-52.

87. Long Nghiem and Tzahi Cath, A scaling mitigation approach during direct contact membrane distillation. Separation and Purification Technology, 2011. **80**: p. 315-322.

88. Marek Gryta, Alkaline scaling in the membrane distillation process. Desalination, 2008. **228**: p. 128-134.

89. Geun Lee, Leonard Tijing, Bock Pak, Byung Baek and Young Cho, Use of catalytic materials for the mitigation of mineral fouling. International Communications in Heat and Mass Transfer, 2006. **33**: p. 14-23.

90. Guillermo Zaragoza, Andrés-Mañas and Ruiz-Aguirre, Commercial scale membrane distillation for solar desalination. Clean water, 2018. **1**: p. 20.

91. Douglas Rice, Shahrouz Ghadimi, Ana Barrios, Skyler Henry, Shane Walker, Qilin Li and François Perreault, Scaling Resistance in Nanophotonics-Enabled Solar Membrane Distillation. Environ. Sci. Technol, 2020. **54**: p. 2548-2555.

92. Marek Gryta, Calcium sulphate scaling in membrane distillation process. Chemical papers, 2009. **63 (2)**: p. 146-151.

93. Elena Burrieza, Alba Aguirre, Guillermo Zaragoza and Hassan Arafat, Membrane fouling and cleaning in long term plant-scale membrane distillation operations. Journal ofMembraneScience, 2014. **468**: p. 360-372.

94. Wenli Qin, Jianhua Zhang, Zongli Xie, Derick Ng, Ying Ye, Stephen Gray and Ming Xie, Synergistic effect of combined colloidal and organic fouling in membrane distillation: Measurements and mechanisms. Environmental Science Water Research & Technology, 2017. **3**(119).

95. Wenli Qin, Zongli Xie, Derrick Ng, Ying Ye, Xiaosheng Ji, Stephen Gray and Jianhua Zhang, Comparison of colloidal silica involved fouling behavior in three membrane distillation configurations using PTFE membrane. Water Research, 2018. **130**: p. 343-352.

96. Jack Gilron, Yitzhak Ladizansky and Eli Korin, Silica Fouling in Direct Contact Membrane Distillation. I&EC research, 2013. **52**: p. 10521-10529.

97. Deyin Hou, Lijuan Zhang, Changwei Zhao, Hua Fan, Jun Wang and Hongjing Huang, Ultrasonic irradiation control of silica fouling during membrane distillation process. Desalination, 2016. **386**: p. 48-57.

98. Omkar Lokare, Sakineh Tavakkoli, Shardul Wadekar, Vikas Khanna and Radisav Vidic, Fouling in direct contact membrane distillation of produced water from unconventional gas extraction. Journal of Membrane Science, 2017. **524**: p. 493-501.

99. Ahmed Al-Amoudi, Factors affecting natural organic matter (NOM) and scaling fouling in NF membranes: A review. Desalination, 2010. **259**: p. 1-10.

100. Linhua Fan, John Harris, Felicity Roddick and Nic Booker, Influence of the characteristics of natural organic matter on the fouling of microfiltration membranes Water research, 2001. **35**: p. 18.

101. Marek Gryta, Maria Tomaszewska, Joanna Grzechulska and Antoni Morawski, Membrane distillation of NaCl solution containing natural organic matter. Journal of Membrane Science, 2001. **181**: p. 279-287.

102. Mourad Laqbaqbi, Julio Sanmartino, Mohamed Khayet, Carmen Payo and Mehdi Chaouch, Fouling in Membrane Distillation, Osmotic Distillation and Osmotic Membrane Distillation. Applied sciences, 2017. **7**: p. 334.

103. Mohamed Khayet, Armando Velázquez and Juan Mengual, Direct contact membrane distillation of humic acid solutions. Journal of Membrane Science, 2004. **240**: p. 123-128.

104. Agata Zarebska, Ángel Amor, Klaudia Ciurkot, Henrik Karring, Ole Thygesen, Thomas Andersen, May Hägg, Knud Christensen and Birgir Norddahl, Fouling mitigation in membrane

distillation processes during ammonia stripping from pig manure. Journal of Membrane Science, 2015. **2015**: p. 119-132.

105. M. Krivorot, Ariel Kushmaro, Yoram Oren and Jack Gilron, Factors affecting biofilm formation and biofouling in membrane distillation of seawater. Journal of Membrane Science, 2011. **376**: p. 15-24.

106. Shuwen Goh, Qiaoyun Zhang, Jinsong Zhang, Diane Mcdougald, William Krantz, Yu Liu and Anthony Fane, Impact of a biofouling layer on the vapor pressure driving force and performance of a membrane distillation process. Journal of Membrane Science, 2013. **438**: p. 140-152.

107. Tshepiso Mpala, Anita Etale, Heidi Richards and Lebea Nthunya, Biofouling phenomena in membrane distillation: mechanisms and mitigation strategies. Environmental Science Advances, 2023. **2**: p. 39.

108. Marek Gryta, The assessment of microorganism growth in the membrane distillation system. Desalination, 2002. **142**: p. 79-88.

109. Hua Zhang, Richard Lam and Jenny Lewis, Engineering nanoscale roughness on hydrophobic surface—preliminary assessment of fouling behaviour. Science and Technology of Advanced Materials, 2005. **6**: p. 236-239.

110. Flávia Costa, Bárbara Ricci, Bárbara Teodoro, Konrad Koch, Jörg Drewes and Míriam Amaral, Biofouling in membrane distillation applications - a review. Desalination, 2021. **516**: p. 115241.

111. El-Abbassi, Abdellatif Hafidi, Mohamed Khayet and García-Payo, Integrated direct contact membrane distillation for olive mill wastewater treatment. Desalination, 2013. **323**: p. 31-38.

112. Anne Bogler, Shihong Lin and Edo Zeev, Biofouling of membrane distillation, forward osmosis and pressure retarded osmosis: Principles, impacts and future directions. Journal of Membrane Science, 2017. **542**: p. 378-398.

113. Thomas Young, An essay on the cohesion of fluids. Phil. Trans. Roy. Soc. Lond. 95, 65e87. https://doi.org/10.1098/rstl.1805.0005., 1805.

114. Mohammad Shirazi and Ali Kargari, A Review on Applications of Membrane Distillation (MD) Process for Wastewater Treatment. Journal of membrane science and research, 2015. **1**: p. 101-112.

115. Mohammad Rezaei, David Warsinger, John Lienhard, Mikel Duke, Takeshi Matsuura and Wolfgang Samhaber, Wetting phenomena in membrane distillation: Mechanisms, reversal, and prevention. Water Research, 2018. **139**: p. 329-352.

116. Jesús García, Noel Dow, Nicholas Milne, Jianhua Zhang, Leslie Naidoo, Stephen Gray and Mikel Duke, Membrane Distillation Trial on Textile Wastewater Containing Surfactants Using Hydrophobic and Hydrophilic-Coated Polytetrafluoroethylene (PTFE) Membranes. Membranes, 2018. **8**: p. 31.

117. Marek Gryta, Long-term performance of membrane distillation process. Journal of Membrane Science, 2005. **265**: p. 153-159.

118. Dejun Feng, Yuanmiaoliang Chen, Zhangxin Wang, and Shihong Lin, Janus Membrane with a Dense Hydrophilic Surface Layer for Robust Fouling and Wetting Resistance in Membrane

Distillation: New Insights into Wetting Resistance. Environmental Science & Technology, 2021. **55**: p. 14156-14164.

119. Bomin Kim, Yongjun Choi, Jihyeok Choi, Yonghyun Shin, and Sangho Lee, Effect of surfactant on wetting due to fouling in membrane distillation membrane: Application of response surface methodology (RSM) and artificial neural networks (ANN). REVIEW PAPER, 2020. **37**: p. 1-20.

120. Po Lin, Ming Yang, Yu Li and Jun Chen, Prevention of surfactant wetting with agarose hydrogel layer for direct contact membrane distillation used in dyeing wastewater treatment. Journal of MembraneScience, 2015. **475**: p. 511-520.

121. Yuanmiaoliang Chen, Kang Lu, Wenxiao Gai and Tai Chung, Nanofiltration-Inspired Janus Membranes with Simultaneous Wetting and Fouling Resistance for Membrane Distillation. Environmental Science & Technology, 2021. **55**(11): p. 7654-7664.

122. Lies Eykens, Kristien Sitter, Chris Dotremont, Wim Schepper, Luc Pinoy and Bart Bruggen, Wetting Resistance of Commercial Membrane Distillation Membranes in Waste Streams Containing Surfactants and Oil. Applied sciences, 2017. **7**(118).

123. Zhangxin Wang and Shihong Lin, Membrane fouling and wetting in membrane distillation and their mitigation by novel membranes with special wettability. Water Research, 2017. **112**: p. 38-47.

124. Liang Chen, Allen Huang, Yi Chen, Chien Chen, Che Hsu, Feng Tsai and Kuo Tung, Omniphobic membranes for direct contact membrane distillation: Effective deposition of zinc oxide nanoparticles. Desalination, 2018. **428**: p. 255-263.

125. Chanhee Boo, Jongho Lee and Menachem Elimelech, Omniphobic Polyvinylidene Fluoride (PVDF) Membrane for Desalination of Shale Gas Produced Water by Membrane Distillation. Environmental Science & Technology, 2016. **50**: p. 12275-12282.

126. Junping Zhang and Stefan Seeger, Polyester Materials with Superwetting Silicone Nanofilaments for Oil/Water Separation and Selective Oil Absorption. Advance funtional materials, 2011. **21**: p. 4699-4704.

127. Junping Zhang and Stefan Seeger, Superoleophobic Coatings with Ultralow Sliding Angles Based on Silicone Nanofilaments. Angew. Chem. Int. Ed, 2011. **50**: p. 6652-6656.

128. Florian Geyer, Clarissa Schönecker, Hans-Jürgen Butt, and Doris Vollmer, Enhancing CO2 Capture using Robust Superomniphobic Membranes. Adv. Mater., 2017. **29**(1603524).

129. Mohamed Khayet and Takeshi Matsuura, Preparation and Characterization of Polyvinylidene Fluoride Membranes for Membrane Distillation. Ind. Eng. Chem. Res., 2001. **40**: p. 5710-5718.

130. Fei Guo, Amelia Servi, Andong Liu, Karen Gleason, and Gregory Rutledge, Desalination by Membrane Distillation using Electrospun Polyamide Fiber Membranes with Surface Fluorination by Chemical Vapor Deposition. ACS Appl. Mater. Interfaces, 2015. **7**: p. 8225-8232.

131. Mélanie Gardette, Anthony Perthue, Jean Gardette, Tünde Janecska, Eniko Földes, Béla Pukánszky and Sandrine Therias, Photo- and thermal-oxidation of polyethylene: Comparison of mechanisms and influence of unsaturation content. Polymer Degradation and Stability, 2013. **98**: p. 2383-2390.

132. Marek Gryta, Joanna Damszel, Agata Markowska and Krzysztof Karakulski, The influence of polypropylene degradation on the membrane wettability during membrane distillation. Journal of Membrane Science, 2009. **326**: p. 493-502.

133. Dipak Rana, G. Neale and Vladimir Hornof, Surface tension of mixed surfactant systems: lignosulfonate and sodium dodecyl sulfate. Colloid Polym Sci, 2002. **280**: p. 775-778.

134. Francisco Hernainz and Antonio Caro, Variation of surface tension in aqueous solutions of sodium dodecyl sulfate in the flotation bath. Colloids and Surfaces A: Physicochemical and Engineering Aspects, Elsevier, 2002. **196**: p. 19-24.

135. Deyin Hou, Dichu Lin, Changwei Zhao, Jun Wang and Chaochen Fu, Control of protein (BSA) fouling by ultrasonic irradiation during membrane distillation process. Separation and Purification Technology, 2017. **175**: p. 287-297.

136. Yong Tan, Hou Wang, Le Han, Melike Kanbur, Mehta Pranav and Jia Chew, Photothermal-enhanced and fouling-resistant membrane for solar-assisted membrane distillation. Journal of Membrane Science, 2018. **565**: p. 254-26.

137. Sebastian Leaper, Ahmed Karim, Tarek Allah and Patricia Gorgojo, Air-gap membrane distillation as a one-step process for textile wastewater treatment. Chemical Engineering Journal, 2018. **360**: p. 1330-1340.

138. Siti Hubadillah, Mohd Othman, Takeshi Matsuura, Mukhlis Rahman, Juhana Jaafar, Ahmad Ismail and Siti Amin, Green silica-based ceramic hollow fiber membrane for seawater desalination via direct contact membrane distillation. Separation and Purification Technology, 2018. **205**: p. 22-31.

139. Mourad Laqbaqbi, García-Payo, Mohamed Khayet, Jauad Kharraz and Mehdi Chaouch, Application of direct contact membrane distillation for textile wastewater treatment and fouling study. Separation and Purification Technology, 2019. **209**: p. 815-825.

140. Mohamed Elmarghany, Ahmed Shazly, Mohamed Salem, Mohamed Sabry and Norhan Nady, Thermal analysis evaluation of direct contact membrane distillation system. Case Studies in Thermal Engineering, 2019. **13**: p. 100377.

141. Noreddine Ghaffoura, Sofiane Soukane, Junggil Lee, Youngjin Kim and A. Alpatova, Membrane distillation hybrids for water production and energy efficiency enhancement: A critical review. Applied Energy, 2019. **254**: p. 113698.

142. Youngkwon Choi, Gayathri Naidu, Long Nghiem, Sangho Lee and Saravanamuthu Vigneswaran, Membrane distillation crystallization for brine mining and zero liquid discharge: opportunities, challenges, and recent progress. Environmental Science Water Research & Technology, 2019. **5**: p. 1202.

143. Giuseppe Grasso, Francesco Galiano, M. Yoo, R. Mancuso, Hobum Park, Bartolo Gabriele, A. Figoli and Enrico Drioli, Development of graphene-PVDF composite membranes for membrane distillation. Journal of Membrane Science, 2020. **604**: p. 118017.

144. Ahmed Karim, Sebastian Leaper, Clara Skuse, Guillermo Zaragoza, Marek Gryta and Patricia Gorgojo, Membrane cleaning and pretreatments in membrane distillation – a review. Chemical Engineering Journal, 2021. **422**: p. 129696.

145. Chunlei Su, Thomas Horseman, Hongbin Cao, Kofi Christie, Yuping Li and Shihong Lin, Robust Superhydrophobic Membrane for Membrane Distillation with Excellent Scaling Resistance. Environ. Sci. Technol, 2019. **53**: p. 11801-11809.